Title
DNA-cell conjugates and cellular biophysical studies using AFM

Author
Hsiao, Shih-Chia

Publication Date
2011

Peer reviewed|Thesis/dissertation

DNA-cell conjugates and cellular biophysical studies using AFM

by

Shih-Chia Hsiao

A dissertation submitted in partial satisfaction of the

requirements for the degree of

Doctor of Philosophy

in

Chemistry

in the

GRADUATE DIVISION

of the

UNIVERSITY OF CALIFORNIA, BERKELEY

Committee in charge:

Professor Carolyn R. Bertozzi, Co-Chair

Professor Matthew B. Francis, Co-Chair

Professor Daniel A. Fletcher

Fall 2011

DNA-cell conjugates and cellular biophysical studies using AFM

Abstract

DNA-cell conjugates and cellular biophysical studies using AFM

by

Shih-Chia Hsiao

Doctor of Philosophy in Chemistry

University of California, Berkeley

Professor Carolyn R. Bertozzi, Co-Chair

Professor Matthew B. Francis, Co-Chair

During my graduate years in Berkeley, I focused on the development of a new tool that can be used to attach DNA to live cells, and the subsequent use of the DNA modified live cells for different applications, including cell patterning, single cell analysis, and cell targeting. Chapter 1 focuses on a new and efficient bioconjugation method to attach single-stranded DNA to live cells. Chapter 2 describes the adaptation of this strategy into a highly-efficient system for multiplex cell patterning, capable of achieving single-cell resolution. Chapter 3 shows the application of this technique for the electrochemical analysis of individual live cells. Single cell metabolism is measured with the integrated device. Chapter 4 focuses on the attachment of DNA-modified cells to an AFM cantilever for direct live cell patterning and the measurement of cell adhesion force. Chapter 5 describes the measurement of the anchoring force of cell membrane protein receptor using AFM technique.

This dissertation is dedicated to my family,
whose love and support has made this work
possible and worthwhile.

DNA-cell conjugates and cellular biophysical studies using AFM

Table of Contents

Acknowledgements

First, I would like to express my deep and sincere appreciation to my advisors, Matt Francis and Carolyn Bertozzi. Thank you for letting me be a joint student between your labs. Thank you for giving me the space to run with many different ideas. You have been tremendously supportive and have taught me the way to be a scientist. Your counsel and examples have shaped my career and my idea of the professional that I want to become. I am very proud to be a lab member in both the Francis group and the Bertozzi group.

During my graduate career in Berkeley, I was privileged to work with some amazing colleagues whose passion for research was inspiring. First, I was very lucky to work with Ailey Crow, Wilbur Lam and Professor Dan Fletcher. One of my first research projects was to collaborate with this amazing crew to make the first direct live cell pattering happen using atomic force microscopy. I was learning a lot of things in doing research in my first year, and my English expression was not very accurate during that time. I sincerely thank you for being understanding and willing to give me all the support so that we can get the project done quickly.

Then I would like to express my appreciation to my two colleagues in the Mathies lab, Erik Douglas and Hiro Onoe. I'm so glad to have you intertwined with my memories of graduate research. Working with you will be the standard by which I compare future collaborations. We honed each other's ideas, challenged each other, and created a positive working environment based on mutual support rather than competition. I fear, though, that I asked more of you in terms of scheduling patience over these past years than you did of me. Thank you for never complaining. Finishing this work would not have been possible without you. But more than all the results we obtained in lab, I am most grateful for your friendship.

Before I joined the lab, Ravi Chandra and Zev Gartner had already laid down the ground of these research projects. Ravi and Erik were the first ones to discover DNA-mediated cell adhesion and Zev was the first one to apply the technology to cell-cell binding. I am very grateful that I could learn the technology from them and also learn how to conduct research correctly and smartly from them. To the younger students poised to continue this work, particularly Amy Twite and Jelly Netirojjanakul, thank you for what you've already taught me. I was always afraid that I did not do well as a senior student to lead you in the beginning of the research projects. However, I see that you already are very productive and have already gained plenty of knowledge. Thank you for willing to share all your knowledge with me and answer my variety of questions. I can't wait to see where you'll take your own work in the years ahead.

I owe a special thank you to Betty Shum, the undergraduate student who worked with me for two years during my time here. I saw a lot of myself in you when we first began our work together, and I hope that you emerged from the experience with new skills and a greater confidence in your abilities. You made a significant contribution to the research contained in this thesis. I am very grateful for your

friendship, and I believe you'll do very well in medical school at Tufts and have a great future.

I appreciate all the lab mates and collaborators who took time out for me. Among these many students and postdocs, thank you to Nick Toriello, Andy Hsieh, Nick Stephanopoulos, and Gary Tong. To other friends outside of graduate school, a hearty thanks to each of you. It is a privilege to call each of you my friend.

Finally, and most importantly, thank you to my family. I love all of you very much. Your support, sacrifice, and patience have supported me throughout these years in Berkeley and oversea studying. To Mom and Dad, you shaped me into the person that I am. You cultivated in me a love for science when I was young and convinced me that I could succeed in anything. You both model unconditional love and generosity in inspiring ways, and I can only hope to give a fraction of what you have given me to my children one day.

Thesis overview

As integrated cellular devices become more complex, the demands placed on technologies for engineering cell adhesion will increase. Applications will likely require many different kinds of cells to be patterned at once within multi-component devices. Approaches for patterning cells will need to be precise and efficient, while providing minimal perturbation to cellular physiology. Current methods for engineered cell adhesion do not satisfy all of these criteria, and thus new strategies are needed. Previously in the Bertozzi and Francis lab, Ravi Chandra had reported a method for the attachment of living cells to surfaces through the hybridization of synthetic DNA strands attached to their plasma membranes. The oligonucleotides were introduced using metabolic carbohydrate engineering, which allowed reactive tailoring of the cell surface glycans for chemoselective bioconjugation.

I describe here a significant improvement of this technique that allows the direct modification of cell surfaces with NHS-DNA conjugates. This method is rapid and efficient, allowing virtually any mammalian cell to be patterned on surfaces bearing complementary DNA in under one hour. We demonstrate this technique using several types of cells that are generally incompatible with integrin-targeting techniques, including red blood cells, primary T-cells, and myoblasts. The availability of this new protocol greatly expands the applicability of the DNA-based attachment strategy for the generation of artificial tissues and the incorporation of living cells into device settings. In addition, we can also adapt this new NHS-DNA method to modify live cells with DNA aptamers to allow them to be targeted to specific biomolecules or other cells.

This thesis describes the creation and development of a novel strategy to attach DNA to live cell surfaces. It then explores the integration of cells into analytical devices, such as AFMs and electrodes, and also allows multiple cells to be patterned precisely on 2-D surfaces. I also describe here a method to attach a DNA apatmer to live cell surfaces as a targeting group for potential cell therapeutics.

Chapter 1 focuses on the experimental validation of the new cell modification method. Reactions were developed for functionalizing cells with ssDNA of any sequence. Cells coated with ssDNA were shown to bind to ssDNA on surfaces in a sequence-specific manner. Work with both primary cells and cultured cells suggested that the linkage strategy was compatible with a number of experimental platforms, and could establish patterns of cells for long-term culture.

Chapter 2 presents the use of DNA-programmed cell adhesion to prepare self-assembled cellular patterns. Precise multiplex DNA patterns were formed quickly by using this photolithography method. In addition, patterns containing multiple types of cells were self-assembled in a single step, and cultured for extended periods.

Interrogation of bound cells with exogenous reagents established that bound cells retain of physiological properties similar to unbound cells.

Chapter 3 describes a microdevice developed for DNA-barcode directed capture of single cells on an array of pH-sensitive microelectrodes for metabolic analysis. Cells are modified with membrane-bound single-stranded DNA, and specific single-cell capture is directed by the complementary strand bound in the sensor area of the iridium oxide pH microelectrodes within a microfluidic channel. This bifunctional microelectrode array is used to demonstrate pH monitoring and differentiation of primary T cells and Jurkat T lymphoma cells.

Chapter 4 describes the development of an AFM system to facilitate direct live cell patterning and allows cell-matrix interaction force to be measured. Methods are described for displaying DNA on AFM cantilever. Importantly, cells are shown to bind to the DNA coated cantilever. Detailed biophysical characterization of this platform is also described, so that system properties may be adjusted as applications require.

Chapter 5 presents a method to express azide groups on a specific receptor present on live cell surfaces. The azide can form a covalent bond with alkyne modified AFM tips. The force measurement can then be applied to quantify the anchoring force of a receptor on live cell surfaces.

Chapter 1: Direct modification of membrane proteins for the capture of living cells

INTRODUCTION

The ability to pattern cells on surfaces provides new platforms for the study of cell biology,[1-4] the control of stem cell differentiation,[5] and the engineering of new tissues.[6] Typically, cell-containing arrays are formed by printing surfaces of interest with "RGD" sequences that are designed to bind to integrins on the cell surface.[7] While this approach has been widely adopted for the immobilization of many cell types, it cannot be used to capture non-adherent cell lines (such as leukocytes). It also can cause undesired changes in cell differentiation or behavior because it engages the very surface receptors that are involved in controlling these processes.[8,9] As an alternative method that can circumvent these limitations, we have reported the capture of live cells through the hybridization of synthetic DNA strands introduced on their plasma membranes to surfaces printed with complementary sequences.[10] In addition to allowing multiple cell types to be patterned on a single substrate, this method offers the important advantages of substrate reuse and tunability. Most importantly, we have used this approach to capture non-adherent cells in addition to adherent ones, and we have shown that the cells experience minimal changes in behavior as a result of immobilization through this receptor-independent process. In previous reports, we have shown the utility of this method for the formation of complex cell patterns,[11] the capture of single cells for RT-PCR analysis,[12] and the attachment of living cells to AFM tips for force measurement.[13]

The DNA strands used in these studies were installed into cell surface glycans through a two-step process. First, the cells were fed with an azide-containing mannose derivative for 1-3 days, which was converted by the cell's metabolic machinery into azido-sialic acid groups on the cell membranes.[14] The DNA was then introduced by using a Staudinger ligation to target the azide groups.[10] While effective, this protocol is most appropriate for cultured mammalian cell lines, as it requires multiple days of exposure to install a sufficient number of azide groups. To expand the generality of this DNA-based adhesion method, this chapter describes a significantly improved method for the direct installation of DNA strands on virtually any cell surface. This procedure can be carried out in less than 1 hour, and leads to equivalent levels of cell surface functionalization with any oligonucleotide sequence of interest. In this report, we demonstrate the use of this new labeling method for the capture of red blood cells, primary T-cells, and myoblasts, which are all types of cells that are difficult to pattern using other methods. This new technique greatly expands the scope of the DNA-based adhesion strategy and is sufficiently straightforward to be used in labs that do not specialize in organic synthesis.

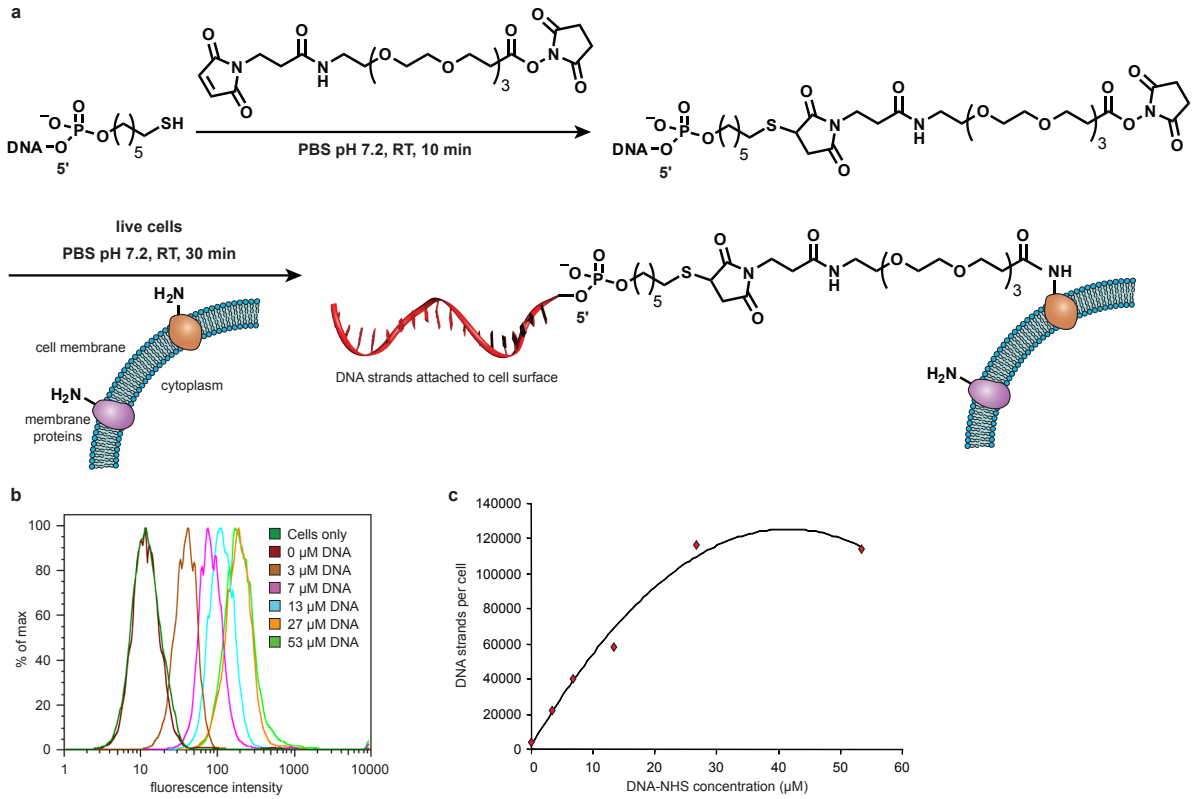

Figure 1. Covalent attachment of ssDNA to cell surfaces. (a) Thiolated single-stranded DNA was first reacted with NHS-PEG-maleimide in PBS at room temperature to form the NHS-DNA conjugate. This solution was then incubated with suspensions of live cells in PBS at room temperature for 30 min. After attachment of the DNA strands, the cells were returned to the culture media. (b,c) Jurkat cells were exposed to NHS-DNA solutions of varying concentrations as described in (a). The fluorescent strand complement was then added, and the level of cell modification was quantified using flow cytometry. Up to 120,000 DNA strands could be installed on each cell.

RESULTS

Approaches for live cell surface modification with NHS-DNA

Our general strategy for the direct modification of cell surfaces with DNA strands targeted amino groups present on membrane proteins (Figure 1a). To prepare an appropriately reactive DNA conjugate, commercially available 5'-thiol modified DNA was conjugated to an NHS-PEG-maleimide crosslinker at pH 7.2 for 10 min, yielding an NHS-DNA conjugate. This reagent was immediately incubated with live cells in PBS at room temperature for 30 min, and the cells were then applied to patterned surfaces for study. The NHS-DNA conjugates were characterized using MALDI-TOF MS, and model studies were conducted by exposing the conjugate to a small molecule amine confirmed the formation of the expected amide product (Figure 2). Based on the mass spectrometry results, there was no thiol-substituted DNA remaining in the final product. The concentration of the NHS-DNA product was determined using UV absorption.

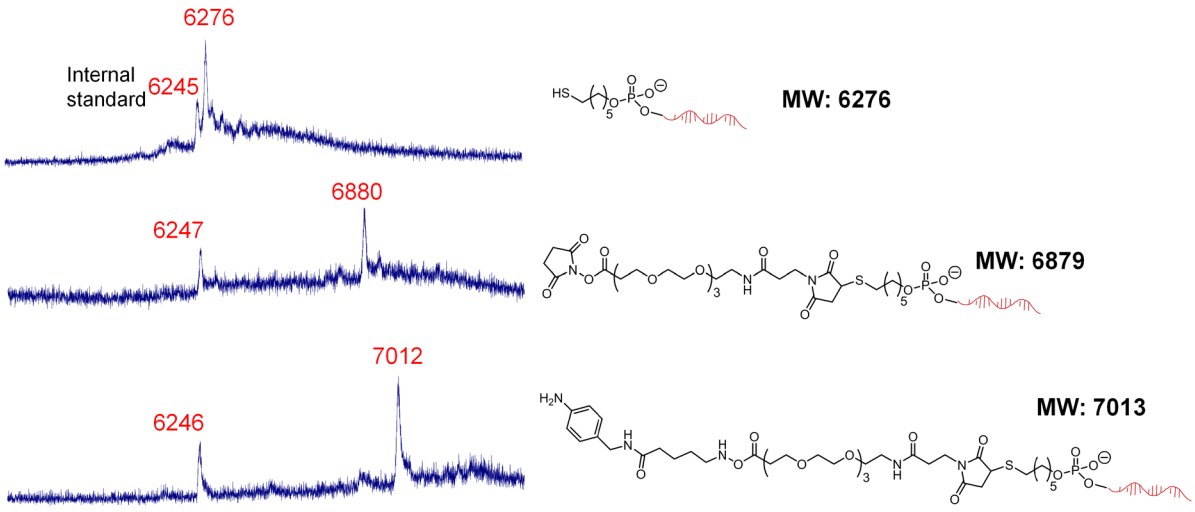

Figure 2. Matrix-assisted laser desorption ionization-time of flight (MALDI-TOF) mass spectrometry of DNA oligonucleotide modification. MALDI-TOF spectra for each oligonucleotide species as indicated. These data show that NHS-DNA was successfully synthesized and was competent to react with an amine functional group.

To verify the ability of the DNA-NHS conjugates to react with lysines on the cell surfaces, human T-cell lymphocytes (Jurkat cell line) were used as a model because they are non-adherent and thus any observed binding could only be attributed to DNA hybridization. Jurkat cells were first washed with PBS buffer to remove any serum proteins left in the media. The cells were then reacted with the NHS-DNA conjugates for 30 min at room temperature to conjugate ssDNA to amino groups on proteins extending from the cell surfaces. In order to quantify the amount of DNA on their surfaces, the modified Jurkat cells were incubated with complementary ssDNA strands labeled with FITC. Flow cytometry was then used to quantify the number of DNA molecules by comparing the signal to that obtained with fluorescent beads of known fluorophore density (Bangs Laboratories, Inc., Fishers, IN).[15] By varying the concentration of the NHS-ssDNA conjugate from 3 μM to 54 μM, up to 120,000 DNA strands could be introduced on each cell (Figure 1b,c). Control experiments conducted with unmodified cells and cells modified with a mismatched DNA sequence showed the same fluorescence intensity as native Jurkat cells with no added fluorophore.

Capture of adherent cells and nonadherent cells using NHS-DNA

Glass slides were prepared for cell adhesion studies as previously described.[11] Upon exposure to Jurkat cells labeled with NHS-DNA, rapid cell capture was observed. The capture efficiency was comparable to that observed in previous studies, with close-packed arrays forming in as little as three minutes. No cells adhered to regions of the slide that lacked DNA or to spots prepared with the incorrect sequence (Figure 3a).

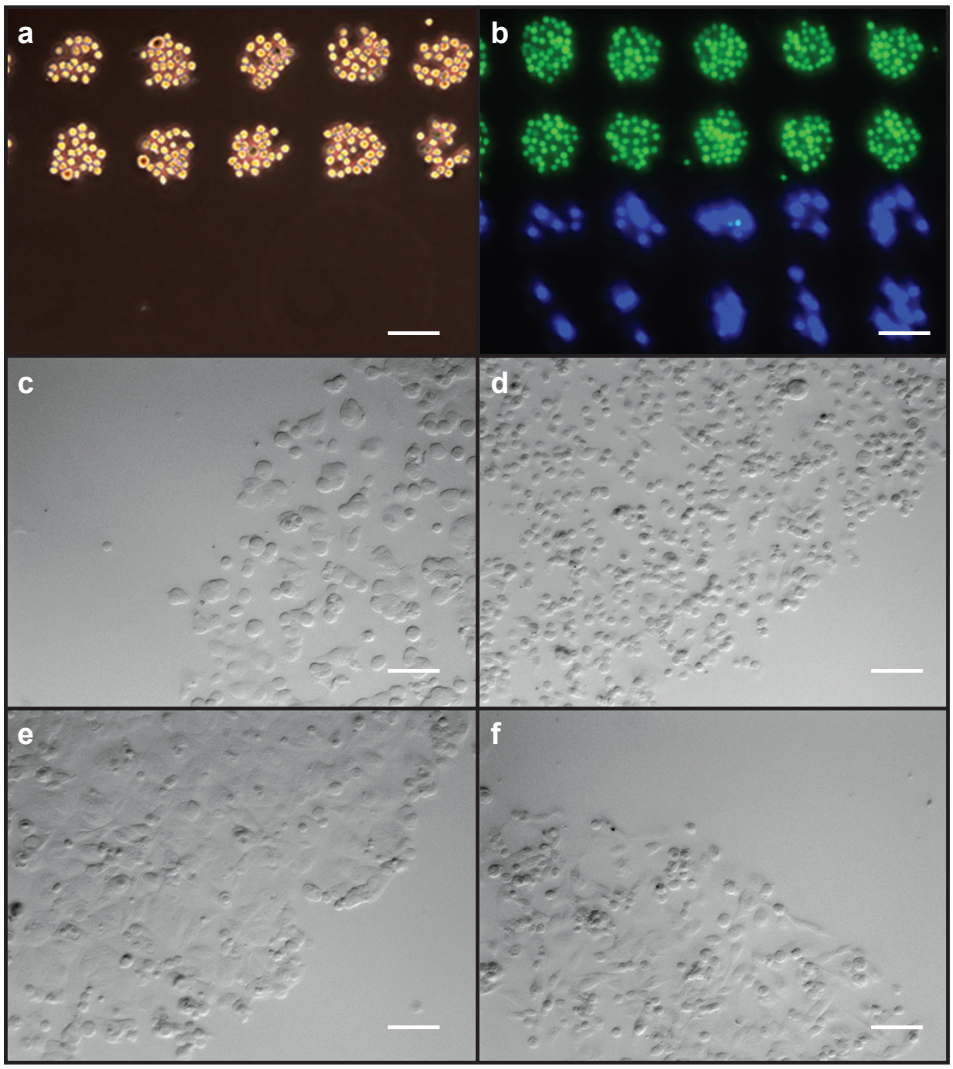

Figure 3. Immobilization of cells in a DNA sequence-specific manner. (a) Cells bearing DNA sequence C2 bound to complementary (sequence M2) spots on a DNA microarray (spot size = 60 μm). Neighboring spots with non-complementary sequence M1 (in the area below) remained unoccupied. (b) The same microarray substrate was exposed to a mixed suspension of Jurkat and MDA cells bearing sequences C2 and C1, respectively. Jurkat cells were stained with Cell-Tracker Green, and MDA cells were stained with Cell-tracker Blue. (c) MCF-7 and (d) MDA cells also bound to DNA coated surfaces in a rapid, stable, and sequence-specific manner. A clear delineation between the DNA-coated and uncoated regions was observed. Phase contrast images are shown after 2 h of incubation. (e) MCF-7 and (f) MDA cells had spread and proliferated after 36 h, but were still confined to the DNA-printed area.

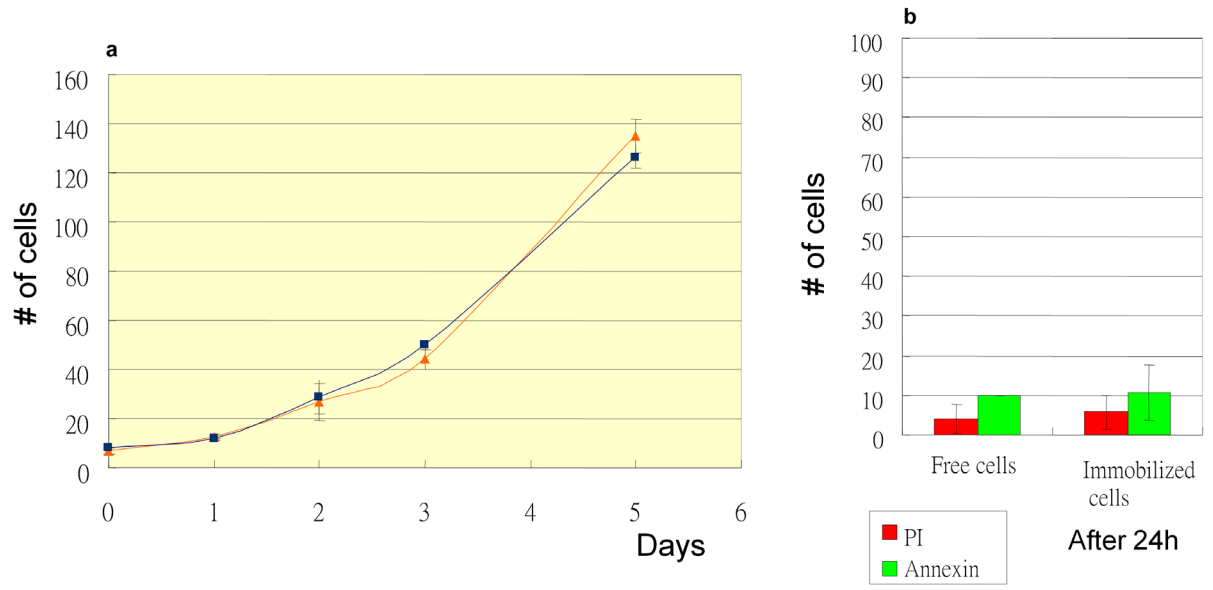

Figure 4. Viability tests for Jurkat cells. a) A solution of DNA coated cells was combined with the complementary DNA strands. At various time points, the total number of cells was counted. The control sample was unmodified Jurkat cells grown in the absence of DNA molecules. b) To evaluate cell viability of immobilized cells, cells were immobilized on DNA coated aldehyde slides. After immobilization for 24 h and 48 h, the cells was incubated with a solution of annexin V-FITC (green bars) and PI (red bars). The cells were evaluated in 1 h by fluorescence microscopy. Free cells were control samples not bound to the surfaces.

The effects of the synthetic DNA molecules on cell viability were assessed using two different methods. First, suspensions of DNA-coated cells were supplemented with the complementary DNA sequence and the growth curves were monitored over a three day period (Figure 4a). No changes in cell growth were observed relative to unmodified cells. In a second assay, the viability of DNA-bound cells was determined after 24 hours using FITC-labeled annexin V and propidium iodide solutions.[13] For the DNA-immobilized cells, the low percentages of apoptotic and necrotic cells were similar to those obtained for unmodified cells maintained in the same culture media (Figure 4b).

To test the compatibility of the platform with adherent cells, two breast cancer cell lines (MCF-7 and MDA-MB-231) were investigated. Cultured MCF-7 and MDA cells were first treated with EDTA to detach them from the culture plate surface, and they were then modified with NHS-DNA as described above. Trypsin was not used to detach them because it was found to prevent DNA conjugation by reducing the number of available amino groups on the cell surfaces. The DNA-modified MCF-7 and MDA cells were then applied to glass slides spotted with complementary sequences, and the cells were returned to culture conditions (growth media at 37 °C with an atmosphere of 5% CO_2). Phase contrast images were acquired 2 hours and 36 hours after washing (Figure 3c-f). At early time points (2 h), the MCF-7 and MDA cells appear morphologically identical to Jurkat cells. However, after 36 h, the MCF-7

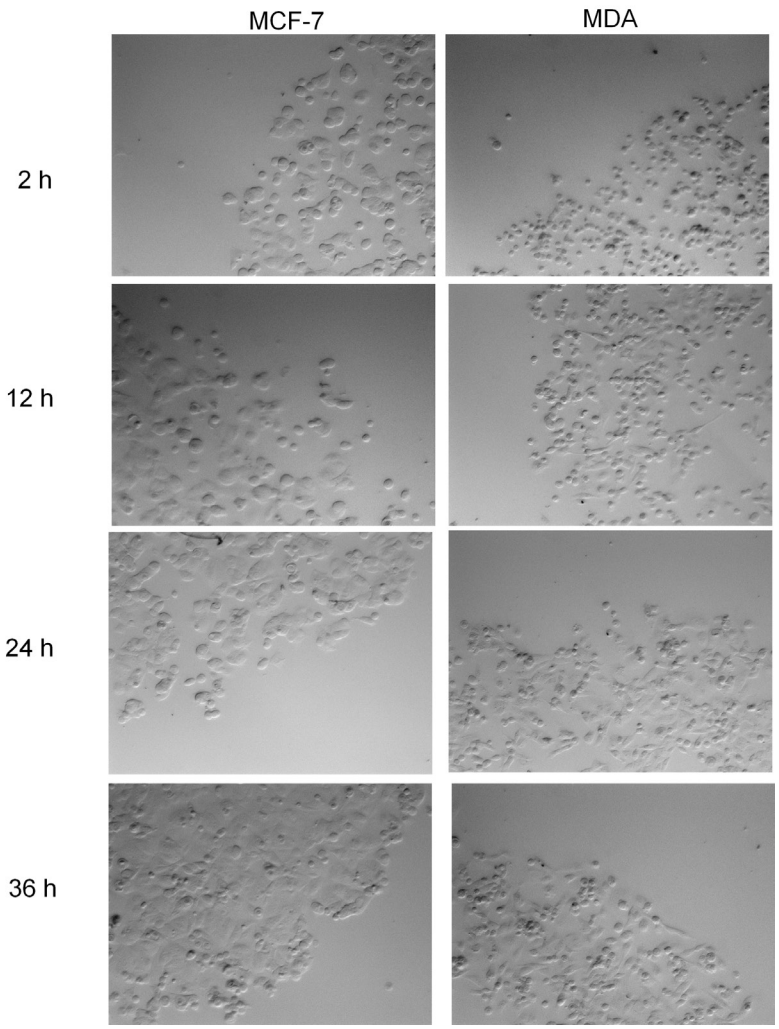

Figure 5. Immobilized MCF-7 and MDA cells were imaged at 2, 12, 24, 36 hours.

and MDA cells had adhered and spread at the site of their initial binding. Their shapes and morphologies were identical to the native cells cultured on Petri dishes. The initial cellular patterns remained, validating both the utility of this system for adherent cells and the ability to interrogate such cell populations over sustained periods. Cell proliferation was observed, confirming viability of the adhered cells (Figure 5).

With the successful DNA-programmed capture of both Jurkat and breast cancer cells, we sought to demonstrate the parallel self-assembly of patterns of these cells from a mixed population. To this end, a spotted microarray of DNA was produced with alternating sequences **M1** and **M2**. MDA and Jurkat cells were then labeled with complementary sequences **C1** and **C2**, respectively. The labeled cells were mixed in equal proportions, and the mixture was incubated with the array for 30 min. The array was then rinsed and visualized, revealing the ordered multi-cell type array shown in Figure 3b. Visual inspection of all cells suggested that bound cells were still

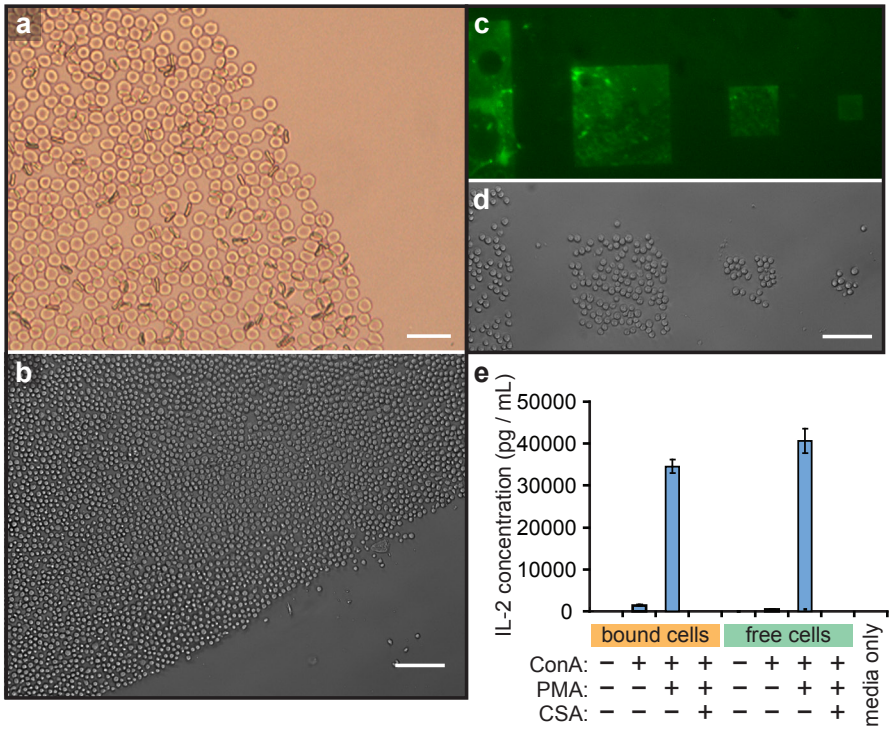

Figure 6. Direct DNA modification and capture of primary cells. (a) Human red blood cells were bound in the same manner as Jurkat cells on a DNA spot, and appeared to be morphologically identical immediately after binding. Trypan blue staining indicated that the membranes remained intact. (b) DNA-coated mouse CD4+ helper T cells were bound by spots coated with complementary DNA. After 3 minutes of exposure, a clear boundary could be seen between the printed and unprinted regions of the slide. (c) Microscale DNA patterns made by photolithography and microfabrication. Fluorescein-conjugated ssDNA strands were patterned on the substrate to allow visualization. (d) Mouse primary T cells were captured on the same DNA patterns. (e) IL-2 production of DNA-immobilized T cells and free T cells, as determined by ELISA. ConA = concanavalin A. PMA = phorbol meristyl acetate. CSA = cyclosporin A.

viable.

We then applied this method for the capture of primary cells taken directly from a living organism. These cells are often difficult to culture for long periods, and thus are incompatible with many surface patterning techniques. As the first example, this technique was applied to capture red blood cells obtained from a healthy human. DNA strands were introduced on the cell surfaces as described above, and then the cells were immobilized on complementary DNA spots (Figure 6a). Although red blood cells are anuclear and cannot divide, assays using annexin-V and trypan blue indicated that the cell membranes remained intact after surface binding.[16]

As a second target, primary $CD4^+$ T-cells were harvested from mice and grown

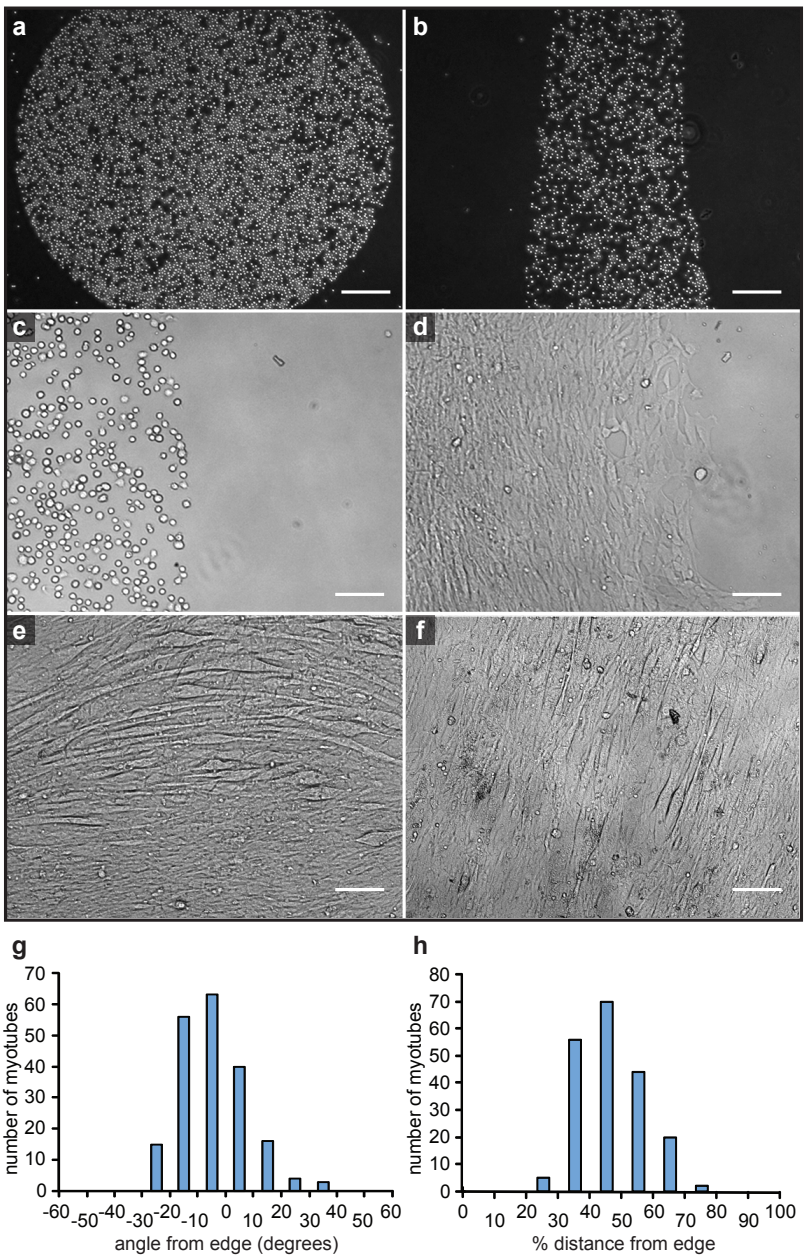

Figure 7. Capture and differentiation of primary myoblast cells. (a,b) DNA patterns on glass slides dictate the areas in which cells are bound. (c) Myoblast cells show no signs of differentiation immediately after capture (shown), or after 1 day when kept in growth media. (d) Myotubes form upon addition of differentiation media. The photo was taken five days after the switch was made. (e) After 6 days of incubation in differentiation media, circularly patterned myoblasts formed arced myotubes that were aligned with the edge. (f) After 6 days, myocytes in rectangular arrangements formed myotubes that were aligned with the long axis of the patterns. For the linear patterns, the majority of the myocytes (g) aligned to within 20° of the pattern boundary angles and (h) were found half way between the edges.

using literature protocols.[17] After surface modification with NHS-DNA, the cells were successfully immobilized on glass surfaces bearing patterns of complementary DNA generated using photolithography (Figure 6b,c). Successful cell capture was observed for a variety of different patterns (Figure 6d). Both the DNA-immobilized T cells and free T cells were then cultured in normal growth media for 20 hours, and the Interlukin-2 (IL-2) production levels of the cell samples were examined using ELISA. Both DNA-bound T cells and free T cells produced a very low level of IL-2 in normal media, indicating that the adhesion process did not activate T-cell signaling pathways. When both populations were treated with phorbol 12-myristate 13-acetate (PMA) and concanavalin A (ConA) to costimulate IL-2 production, similar increases in IL-2 production were observed. This increase could be suppressed by adding cyclosporin (CSA) in both cases.[18]

Approaches of studying patterned myoblasts behaviors

Finally, we have used the same NHS-DNA method to pattern primary myoblast cells on DNA-coated surfaces (Figure 7a,b). After adhesion the cells remained undifferentiated for a period of 1 day. At this point the media was switched, and differentiation into skeletal and heart muscle cells occurred. After incubation for 5 days, myotube formation could be observed in some areas (Figure 7c-f), and after 5 to 7 days the myotubes began to contract spontaneously. Similar myoblast growth and myotube formation was observed on collagen coated surfaces,[17] but with less control over the patterns that were formed.

By patterning myoblasts in different topologies, we were able to study the influence of cell patterns on myotube formation. Myoblasts were first patterned in strips or in circular shapes as shown in Figure 7g-h. After differentiation, myotube alignments were analyzed using ImageJ (A software from NIH). The majority of the myotubes were found in the middle of the patterned areas, and they were predominantly aligned to within 20° of the edge angles.

DISCUSSION

The most significant finding of these studies is the fact that NHS-DNA can modify a wide range of different cells in under 1 hour. The required reagents can be prepared from commercially available materials in two steps with minimal purification, and are therefore accessible to almost any biological lab. Unlike our previous labeling method, which required the modification of azido sugars on the cell surface, this new technique does not require prolonged cell culture and is thus more suitable for modifying primary cells. It is also compatible with metabolically inactive cells, such as erythrocytes, which would be expected to show little-to-no incorporation of artificial functional groups into the surface glycans. As morphological changes in red blood cells are associated with sickle-cell anemia and spherocytosis,[19] the ability to immobilize them into arrays could facilitate diagnosis and render them compatible with lab-on-a-chip technologies. While it has been previously shown that red blood cells can be immobilized using phytohemagglutinin,[20] our DNA-based method leads

to more densely packed arrays in significantly less time, and could potentially be used to isolate single cells.

The results of the IL-2 production assay indicate that DNA-bound T-cells are not activated by virtue of surface attachment, a result that is difficult to achieve using lectins or antibody-based methods.[21-23] However, upon the proper addition of ConA and PMA, robust activation was observed with similar levels of IL-2 production to that of free cells in solution. In combination with previous studies of cell viability after DNA-based adhesion,[13] we take these results to indicate that minimal perturbation of the cells occurs during the DNA attachment process. While any adhesion method would be expected to have some influence on cellular behavior, this method stands as the most mild method available for the anchoring of cells on surfaces, and it is readily compatible with DNA printing methodologies.

The ability to create defined patterns comprising multiple types of cells could provide a powerful tool for the study of cell-to-cell communication and the engineering of new tissues. In the latter context, initial experiments have begun to pattern cells that exhibit collective behavior, with the long-term goal of learning how spatial arrangements influence differentiation and growth. We chose myoblasts for this purpose, as they have the ability to differentiate into cardiac muscle cells or into skeletal muscle cells.[24-26] Using the NHS-DNA modification technique we found that these cells can be patterned on surfaces with similarly high efficiency. Upon addition of differentiation media, many of the cells formed myotubes that were capable of spontaneous contraction.

Our preliminary observations in these experiments have shown that the underlying pattern can influence myotube formation and alignment significantly. The highest density of myotube formation was observed in the center of the patterned regions (Figure 4f), indicating that some mechanism is allowing them to sense the edges. The lack of myotube formation near the pattern edges may result because cells having fewer neighbors in these areas. Similar considerations are likely to govern the alignment of the formed myotubes, which are generally found to be within 20° of the pattern edges. The mechanism of myoblast differentiation and myotube formation on the DNA patterns is currently under examination, as the ability to grow contractile fibers with controlled alignment is likely to be highly useful for tissue engineering applications.

CONCLUSION

We have developed an efficient new method that allows the direct modification of the cell surface with DNA strands using NHS-DNA conjugates. The NHS-DNA conjugates react with lysine residues of cell surface proteins to conjugate single-stranded DNA to the cell surface. This method allows us to capture many new types of cells, including primary cells, on specified locations on surfaces in a sequence-dependent fashion. This strategy allows complex networks of living cells to be created

through self-assembly, and in combination with lab-on-a-chip RT-PCR analysis,[12] it provides a valuable tool for the study of cell behavior and differentiation mechanisms. Currently we are using this method to understand the effects of spatial patterning on the behavior of myocytes in more detail. Subsequent chapters in this thesis describe the combination of this technique with microfabrication techniques to integrate living cells with sensing and stimulatory electrodes.

MATERIALS AND METHODS

General Experimental Procedures.

All cell culture reagents were obtained from Gibco/Invitrogen Corp (Carlsbad, CA) unless otherwise noted. Cell culture was conducted using standard techniques. Jurkat cells were grown in T-25 culture flasks (Corning, USA) in RPMI Medium 1640 supplemented with 10% (v/v) fetal bovine serum (FBS, HyClone) and 1% penicillin/streptomycin (P/S, Sigma). MCF-7 cells were grown in DMEM supplemented with 1% non-essential amino acids and 10% fetal bovine serum, plus 1% penicillin/streptomycin. MDA-MB-231 cells were grown under the same conditions as the MCF-7 cells, but without non-essential amino acids.

Fluorescence micrographs were acquired using an Axiovert 200M inverted microscope (ZEISS) with fluorescence filter sets for DAPI/Hoechst, fluoroscein/fluo-3, and rhodamine. Ultraviolet absorption of the different oligonucleotides was determined at 260 nm on a UVIKON 933 double beam UV/vis spectrophotometer (Kontron Instruments, United Kingdom).

Synthesis of NHS-DNA conjugates.

For cell adhesion studies, three complementary oligonucleotide pairs were designed such that they were identical in overall composition and differed only in sequence. Each sequence pair was also calculated to possess comparable melting temperatures (55 °C) and minimal secondary structures. The sequence identities were as follows:

C1: 5'-GTA ACG ATC CAG CTG TCA CT-3'
M1: 5'-AGT GAC AGC TGG ATC GTT AC-3'
C2: 5'-TCA TAC GAC TCA CTC TAG GG-3'
M2: 5'-CCC TAG AGT GAG TCG TAT GA-3'
C3: 5'-ACT GAC TGA CTG ACT GAC TG-3'
M3: 5'-CAG TCA GTC AGT CAG TCA GT-3'

The oligonucleotides were obtained from Integrated DNA Technologies (Coralville, IA) with thiol groups installed at the 5'-end. Samples (2 mg in 80 μL) were combined with 320 μL of 10 mM TCEP and 400 μL of 1X TE buffer (pH 7) and stored frozen at -20 °C until use.

NHS-PEO_6-Maleimide (succinimidyl-[(*N*-maleimidopropionamido)-hexaethyleneglycol] ester) was purchased from Pierce. A stock solution was prepared by dissolving 5 mg of NHS-PEO_6-maleimide in 1 mL of DMSO (Sigma). Aliquots of this solution (20 μL each) were stored at -20 °C until use.

DNA modification was achieved by passing a thawed solution of 5'-thiol ssDNA (30 μL, 0.39 mM)through a NAP-5 size-exclusion column (GE Healthcare). The eluent was then exposed to 20 μL of the NHS-PEO_6-Maleimide solution at room temperature for 10 minutes. The reaction was then purified by passing it through a second NAP-5 column that was pre-equilibrated with PBS solution (pH 7.2). The concentration of DNA in the column eluent was verified using UV-vis spectroscopy. The resulting solution was then applied to samples of live cells (see below).

To confirm the nature of the modification chemistry, models of the oligonucleotide conjugates were prepared and characterized. To do this, 0.5 mL of DMF was saturated with 6-amino-*N*-(4-aminophenethyl)hexanamide and added to 1 mL of the reaction solution obtained after NAP-5 purification. After 30 min of incubation at room temperature, the oligonucleotide conjugates were analyzed using MALDI-TOF. Observed masses were within 0.090% of expected values.

Modification of live cells and quantification of attached DNA molecules.

Immediately prior to modification, a sample of $5x10^6$ Jurkat cells was washed with PBS buffer three times to remove any proteins from the culture medium. The cells were then exposed to solutions of NHS-DNA (C3 strand, 3 μM to 54 μM final concentrations) for 30 minutes at room temperature. After isolation via centrifugation, the cells were returned to the culture medium, or labeled with fluorescent DNA complements as described in the next paragraph.

In order to quantify the number of surface DNA molecules, portions of the modified cells were incubated with 10 μL solutions of FITC-labeled complementary DNA strands at 0 °C for 30 minutes. The cells were then washed with PBS solution and resuspended in 1% FBS/PBS culture media. The cells were then analyzed by flow cytometry. Fluorescence measurements were calibrated using fluorescent beads of known fluorophore density. Relevant control conditions were performed to confirm the NHS-DNA-dependence of fluorophore binding.

General protocol for the attachment of DNA strands to cells and for their immobilization onto DNA-printed surfaces.

Immediately prior to modification, a sample of $5x10^6$ Jurkat cells was washed with PBS buffer three times to remove any proteins from the culture medium. After the final rinse, additional PBS was added to bring the volume to 5 mL ($1x10^6$ cell/mL). The cell suspension was then reacted with 1 mL of NHS-DNA (11.7 μM) solution

synthesized and purified from 30 μL of 5'-thiol ssDNA (C2 sequence). The mixture was allowed to react at room temperature for 30 minutes, and was then washed three times with PBS containing 1% FBS. The cells were then resuspended in 0.5 mL of PBS containing 1% FBS.

To print the glass surfaces, a 20 μM solution of 5' amine functionalized ssDNA in 3X saline sodium citrate buffer (SSC: 45 mM sodium citrate, 450 mM NaCl, pH 7.0) was used for sample preparation. DNA solutions were deposited onto aldehyde-functionalized glass slides (SCHOTT Nexterion, Louisville, KY) using pipettors or a robotic microarray printing system at the UC Berkeley Functional Genomic Laboratory. Spotted DNA was immobilized and the slides were passivated according to the manufacturer's protocol. After printing, the slides were dried under a stream of N_2 and stored under dry and dark conditions. Patterned slides were used within one month. Micropatterning of the glass slides was achieved using photolithography in conjunction with an aluminum lift-off technique.[28]

For studies with one cell type, all cells were labeled with the C2 sequence. Slides were patterned with complementary DNA sequence, M2 unless otherwise noted. Solutions of DNA-modified cells were introduced onto each surface and incubated for 3-5 minutes without agitation. The devices were then washed twice with PBS containing 1% FBS. Replicate data sets were collected by selecting three device regions at random before washing. Each location was photographed, washed, and then visualized again.

Evaluation of cell viability.

Jurkat cells coated with the C2 strand were seeded in a 1 mL Petri dish with normal growth media, and M2 strand DNA was added into the solution to a concentration of 2 μM. The unmodified Jurkat cells were cultured under same conditions as a control. The number of cells was counted in each of the four samples using a hemocytometer after 24, 48, and 72 hours. Cell viability was monitored by adding Trypan Blue.

For evaluation of bound cells, an annexin V-FITC/propidium iodide apoptosis detection kit was obtained from BD Biosciences. After immobilization on the slides by DNA, the cells were incubated in normal media at 37 °C for 24 hours. A sample of unbound Jurkat cells (lacking surface DNA strands) was grown under the same conditions as a control. A solution consisting of 900 μL of 1X binding buffer, 30 μL of the annexin V-FITC stock solution, and 30 μL of the PI stock solution was prepared. After 24 hours, 100 μL of this solution was applied to the slides for 15 min at room temperature. The cells were imaged using a fluorescence microscope and counted within 1 hour.

Immobilization of adherent cell lines on patterned surfaces.

Two breast cancer cell lines, MCF-7 and MDA, were obtained from ATCC. The cells were detached from culture plates with 1 mM EDTA without any trypsin, and the cell solutions were washed with PBS three times. A 5 mL portion of the cell solution ($1x10^6$ cell/mL) was reacted with 1 mL of NHS-DNA solution synthesized and purified from 30 μL of 5'-thiol ssDNA (C2 sequence). The mixture was allowed to react at room temperature for 30 minutes, and was then washed three times with PBS containing 1% FBS. The cells were then resuspended in 0.5 mL of PBS containing 1% FBS. The cell solution was introduced onto glass slides patterned with complementary DNA sequence M2, and the samples were incubated for 5 minutes. The slides were then washed two times with PBS containing 1% FBS. After immobilization on to slides via DNA hybridization, the cells were incubated in their normal media and observed for 36 hours. Replicate data sets were collected by photographing three different surface regions at 12 hour intervals.

Confirmation of the sequence-specificity of cell immobilization.

DNA-modified Jurkat cells and MDA cells were prepared by incubating each cell population with NHS-DNA (sequence C2 or C1, respectively) in PBS for 30 minutes as described above. To facilitate visual differentiation of the cells, each population was also cytosol-labeled with either CellTracker Blue™ or CellTracker Green™ dye. After rinsing, equal amounts of each population were mixed, introduced onto microspotted DNA microarrays bearing either sequence M2 or M1 (constructed as above), and incubated for 5 minutes. The microarray was then washed twice with PBS containing 1% FBS and observed under a fluorescence microscope.

Immobilization of human red blood cells.

Fresh samples of red blood cells were obtained from a blood sample of a healthy human and stored in 1% citric acid solution at room temperature. The cells were used within 1 hour. The cell solution was washed three times with PBS and was then incubated in the NHS-ssDNA solution for 30 minutes to allow modification of cell surfaces. The cell suspension was then washed three times with 1% FBS/PBS solution before being applied to glass slides bearing the complementary ssDNA strands. After cell attachment, the glass slides were washed with 1% FBS/PBS to remove any unbound cells and viewed under an optical microscope. Cells were incubated in 1% FBS/PBS after immobilization, and their viability was examined after 3 hours using annexin-V and trypan blue staining.

Patterning of primary $CD4^+$ T cells and IL-2 Production Assay

Primary $CD4^+$ T cells (obtained in collaboration with Jay T. Groves' lab, UC Berkeley) were harvested from mice and grown under reported conditions[29] before use. The primary T cells were then modified using the NHS-DNA protocol and exposed to different DNA patterns printed by spotting or by using photolithography, as described above. The glass slides with DNA-immobilized cells were washed with 1% FBS/PBS to

remove any unbound cells and viewed under a microscope.

The IL-2 production of primary T cells immobilized with DNA duplexes was examined using ELISA. A population of $2x10^5$ primary T cells was modified with DNA strands and immobilized on a series of slides (1 cm^2) bearing the complementary sequence. These samples were then divided into three portions. The first sample was incubated in normal T cell growth media without any additional reagents. The second sample was treated with PHA (1 μg/mL) and PMA (50 ng/mL). The third sample was treated with ConA (1 μg/mL), PMA (50 ng/mL) and CSA (μg/mL). Analogous samples of free T cells with no surface DNA were prepared as controls. All the cell samples were incubated at 37 °C for 20 h and then centrifuged. Portions of the culture media (1 mL) were withdrawn from each population of cells and tested for IL-2 production using a Mouse Interlukin-2 ELISA test kit (Thermo Scientific).

Patterning of primary myoblasts

Primary myoblasts (obtained in collaboration with Dr. Randall Lee's lab, UCSF) were harvested from mice and purified according to a published protocol.[17] Normal cell growth was achieved in Ham's F-10 media (Invitrogen) with 10% (v/v) fetal bovine serum (FBS, HyClone), 1% bGF (Invitrogen), and 1% penicillin/streptomycin (P/S, Sigma). Immediately before surface modification, the cells were detached with 1 mM EDTA without any trypsin. The resulting cell suspensions were rinsed with PBS three times. A 5 mL portion of the cell solution ($1x10^6$ cell/mL) was reacted with 1 mL of NHS-DNA solution synthesized and purified from 30 μL of 5'-thiol ssDNA. The mixture was allowed to react at room temperature for 30 minutes, and the cells were then washed three times with PBS containing 1% FBS. Surfaces were patterned with the complementary DNA sequence through spotting or photolithography, and incubated with PBS containing 1% FBS at room temperature for 1 h. The cell solution was introduced onto the slides and incubated for 5 minutes. The devices were then washed three times with PBS containing 1% FBS. After immobilization, the cells were incubated in growth media or fusion media DMEM (Invitrogen) containing 5% horse serum, and 1% penicillin/streptomycin (P/S, Sigma)) at 37 °C for 14 days. The unbound myoblasts were cultured under identical conditions as a control. Images and movies of all cell samples were recorded every 24 hours.

REFERENCES

1. Falconnet, D., Csucs, G., Grandin, H. M., and Textor, M. (2006) Biomaterials 27(16), 3044-3063.

2. Lee, H., Purdon, A. M., and Westervelt, R. M. (2004) Applied Physics Letters 85(6), 1063-1065.

3. Li, Y., Yuan, B., Ji, H., Han, D., Chen, S. Q., Tian, F., and Jiang, X. Y. (2007) Angewandte Chemie-International Edition 46(7), 1094-1096.

4. Liu, V. A., and Bhatia, S. N. (2002) Biomedical Microdevices 4(4), 257-266.

5. Rosenthal, A., Macdonald, A., and Voldman, J. (2007) Biomaterials 28(21), 3208-3216

6. Khademhosseini, A., Langer, R., Borenstein, J., and Vacanti, J. P. (2006) Proc. Natl. Acad. Sci. U. S. A. 103(8), 2480-2487

7. Roberts, C., Chen, C. S., Mrksich, M., Martichonok, V., Ingber, D. E., and Whitesides, G. M. (1998) J. Am. Chem. Soc. 120(26), 6548-6555

8. Du, X. P., Plow, E. F., Frelinger, A. L., Otoole, T. E., Loftus, J. C., and Ginsberg, M. H. (1991) Cell 65(3), 409-416

9. Xiong, J. P., Stehle, T., Zhang, R. G., Joachimiak, A., Frech, M., Goodman, S. L., and Aranout, M. A. (2002) Science 296(5565), 151-155

10. Chandra, R. A., Douglas, E. S., Mathies, R. A., Bertozzi, C. R., and Francis, M. B. (2006) Angewandte Chemie-International Edition 45(6), 896-901

11. Douglas, E. S., Chandra, R. A., Bertozzi, C. R., Mathies, R. A., and Francis, M. B. (2007) Lab on a Chip 7(11), 1442-1448

12. Toriello, N. M., Douglas, E. S., Thaitrong N., Hsiao, S. C., Francis, M. B., Bertozzi, C. R., Mathies, R. A. (2008) Proc. Natl. Acad. Sci. U. S. A. accepted

13. Hsiao, S. C., Crow, A. K., Lam, W. A., Bertozzi, C. R., Fletcher, D. A., Francis, M. B. (2008) Angewandte Chemie-International Edition 120(44), 8601-8605

14. Saxon, E., and Bertozzi, C. R. (2000) Science 287(5460), 2007-2010

15. Vogt, R. F., Cross, G. D., Henderson, L. O., and Phillips, D. L. (1989) Cytometry 10(3), 294-302

16. Kuypers, F. A., Lewis, R. A., Hua, M., Schott, M. A., Discher, D., Ernst, J. D., and Lubin, B. H. (1996) Blood 87(3), 1179-1187

17. Huang, N. F., Patel, S., Thakar, R. G., Wu, J., Hsiao, B. S., Chu, B., Lee, R. J., and Li, S. (2006) Nano Lett. 6(3), 537-542

18. Elliott, J. F., Lin, Y. A., Mizel, S. B., Bleackley, R. C., Harnish, D. G., and Paetkau, V. (1984) Science 226(4681), 1439-1441

19. Konoteya.Fi. (1974) Arch. Intern. Med. 133(4), 611-619

20. Shinozuka, T., Takei, S., Yanagida, J., Watanabe, H., and Ohkuma, S. (1988) Blut 57(3), 117-123

21. Barten, M. J., Tarnok, A., Garbade, J., Bittner, H. B., Dhein, S., Mohr, F. W.,

and Gummert, J. F. (2007) Cell Prolif. 40(1), 50-63

22. Roosnek, E. E., Brouwer, M. C., and Aarden, L. A. (1985) Eur. J. Immunol. 15(7), 652-656

23. Stohl, W., Hofman, F. M., and Gray, J. D. (1990) J. Immunol. 145(4), 1078-1087

24. Jankowski, R. J., Deasy, B. M., and Huard, J. (2002) Gene Ther. 9(10), 642-647

25. Partridge, T. A. (1991) Muscle Nerve 14(3), 197-212

26. Wollert, K. C., and Drexler, H. (2005) Circ.Res. 96(2), 151-163

27. Jackson, B. L., and Groves, J. T. (2007) Langmuir 23(4), 2052-2057

28. DeMond, A. L., Mossman, K. D., Starr, T., Dustin, M. L., and Groves, J. T. (2008) Biophys. J. 94(8), 3286-3292

Chapter 2: Heterogeneous self-assembly of cells on DNA micro-patterns

INTRODUCTION

The micropatterning of cells on a chip surface is an essential technique for cell biology and bioengineering because it facilitates single cell experiments in microfluidic devices, the observation of cell communications and cell differentiation, the engineering of artificial tissues, and cell-based chemical sensor applications.[1] Several techniques have been used for the micro-scale arrangement of cells, such as the chemical pattering of surfaces,[2] physical trapping in microscale wells,[3] dielectrophoretic (DEP) capture,[4, 5] and hydrodynamic cell trapping in microchannels.[6, 7] However, it is still challenging to arrange multiple heterogeneous cells on the microscale in a user defined pattern. Although some research groups have reported the patterning of multiple cells on a chip,[5, 7, 8] the design flexibility of the patterns and number of the cell types are limited. Patterning of more than two different cells with designed patterns has not been achieved, but is highly desirable because it would enable the formation of complex heterotypic structures characteristic of tissues and organs.

The previous chapter describes a new a cell patterning method, in which proteins extending from their plasma membranes of cells are directly derivatized with single-stranded deoxyribonucleic acid (DNA) molecules, and the modified cells are captured on complementary sequences on a substrate via DNA hybridization.[9-14] We have used this method to pattern multiple cells on spotted DNA arrays,[10] to facilitate single cell manipulation with atomic force microscope,[11] for the observation of myotube formation,[12] for single cell gene and metabolic analyses,[13] and for building three-dimensional cellular microstructures.[14] This DNA-assisted cell patterning method also has quite favorable features for creating heterogeneous cellular patterns: (i) DNA barcode delivery exhibits high selectivity for capturing multiple cells, (ii) this method has widespread applicability to both non-adherent and adherent cells, and also to primary cells, and (iii) DNA barcode capture appears to exhibit no influence on main vital activities and functions of cells.[12] Consequently, by executing this technique with multiple different micro-scale DNA patterns on a substrate, it should be possible to arrange heterogeneous cells in arbitrary complex two-dimensional and ultimately three-dimensional micropatterns.

Here we describe a patterning technique for laying down multiple heterogeneous cells in any desirable pattern on a substrate. The surface of cells was directly modified with ssDNA molecular barcodes using a NHS-DNA conjugate method that we described in chapter 1 (Figure 1a).[12] The micropatterns of multiple DNA sequences on the substrate were defined using photolithography, and the DNA-modified cells were assembled on the patterns via hybridization (Figure 1b). To investigate the feasibility of performing complex functional assays with these assemblies, we embedded the DNA-anchored cells in an agarose hydrogel, and

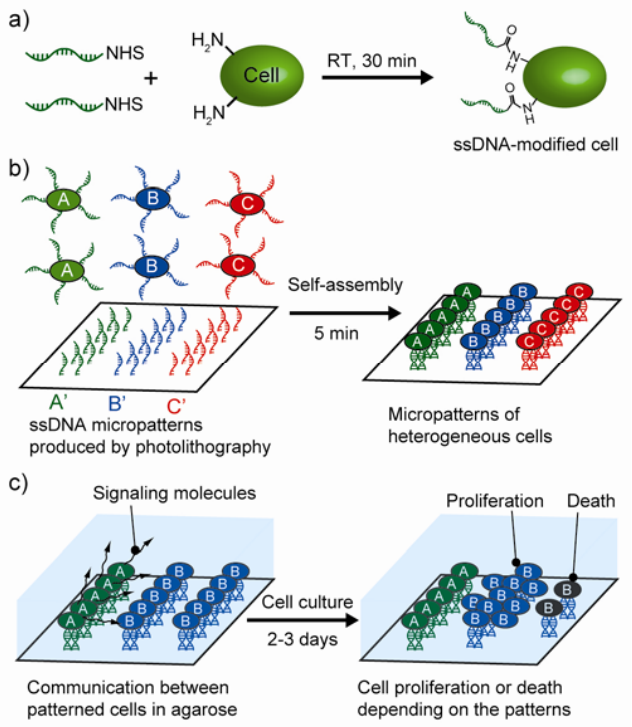

Figure 1. Self-assembly of heterogeneous cells on micro-scale patterns via DNA hybridization. a) Cell surfaces are modified with single-stranded DNA (ssDNA, 20 bp) with an *N*-hydroxysucinimidyl (NHS) ester at the 5' end. The NHS-DNA modifies primary amino groups on the cell surface. b) Multiple types of cells, which are modified with different DNA barcode sequences, self-assemble on the complementary ssDNA micropatterns on a substrate. The DNA micropatterns are made by photolithography, and the dimensions of the patterns varied from single cell resolution (~10 μm) to whole wafer scale (typically 4-8 inches). c) This technique can be used to prepare complex heterotypic cellular arrays that can be used to perform functional experiments depending on cell-cell communication or juxtaposition.

observed diffusion-based signal communication between them (Figure 1c).

RESULTS AND DISCUSSION

Patterning DNA with photolithography

A key challenge for patterning heterogeneous cells on the micro-scale in desirable patterns is the fabrication of the DNA micropatterns. To do this, we used standard photolithography methods in combination with of an aluminum liftoff technique[15] and DNA protection with a poly(methyl meta-acrylate) (PMMA) layer (Figure 2). Unlike other DNA patterning methods such as dip-pen nanolithography (DPN),[16] micro contact printing (μCP),[17] and DNA microarray synthesis with photolithography[18, 19] or a robotic spotter,[20] our method has several advantages for heterogeneous cell patterning: (i) photolithography allows the formation of arbitrary two-dimensional patterns of ssDNA at single cell resolution (~10 mm) over a wafer-scale area (typically 4-8 inch in diameter) with precise alignment (< 1 mm); (ii) multiple DNA sequences can be patterned; (iii) pre-prepared DNA samples can be

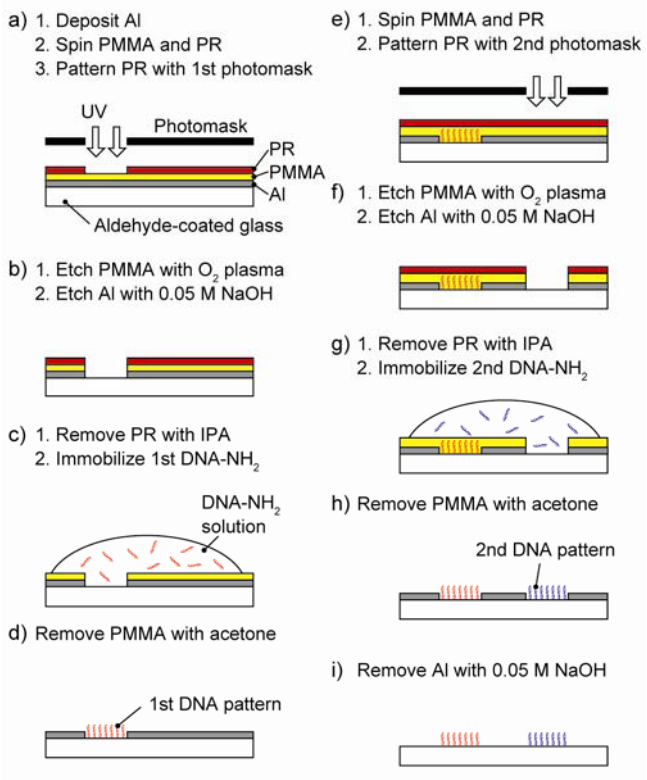

Figure 2. Fabrication steps to form ssDNA micropatterns on a substrate. a) A 100 nm aluminum layer is deposited on an aldehyde-coated glass substrate by vacuum evaporation. Poly(methyl methacrylate) (PMMA) and S-1818 photoresist (PR) are then spin-coated onto the substrate, and the PR layer is photolithographically patterned with a first photomask. b) The PR pattern is transferred to the PMMA and aluminum layers with oxygen plasma etching and 0.05 M NaOH wet etching, respectively. c) After removing the PR with isopropanol (IPA), the first amino-ssDNA (DNA-NH2) is immobilized on the aldehyde-glass surface using reductive amination. d) Unwanted DNA-NH2 on the PMMA surface is washed away together with the PMMA layer by acetone rinse. e)-h) A second DNA pattern is made using the same process as that for the first DNA pattern, except with a second photomask at step e and a second DNA-NH2 at step g. Steps e-h can be repeated for patterning more than two different DNA sequences. i) The remaining aluminum layer is finally removed with 0.05 M NaOH.

used for the patterns, instead of direct synthesis of nucleotide bases on a substrates;[18] (iv) a photoresist and its developer solution do not directly contact immobilized DNA molecules, preventing DNA degradation; and (v) all processes in the fabrication are commonly used techniques.

We use a three-layer system consisiting of aluminum, PMMA and photoresist (PR), for patterning DNA sequences on a glass substrate (Figure 2a). These layers were deposited on an aldehyde-coated glass slide, and patterned using standard microfabrication techniques(Figure 2b). Single-stranded amine-DNA (DNA-NH_2, 20 bp) was then immobilized on the exposed aldehyde glass surface with reductive amination prtotocol described in chapter 1(Figure 2c). An acetone rinse removed the PMMA layer together with unanchored DNA-NH_2 molecules in order to pattern the first DNA sequences (Figure 2d). Through these steps, the aluminum layer protected the aldehyde groups on the glass from the etching process. After making

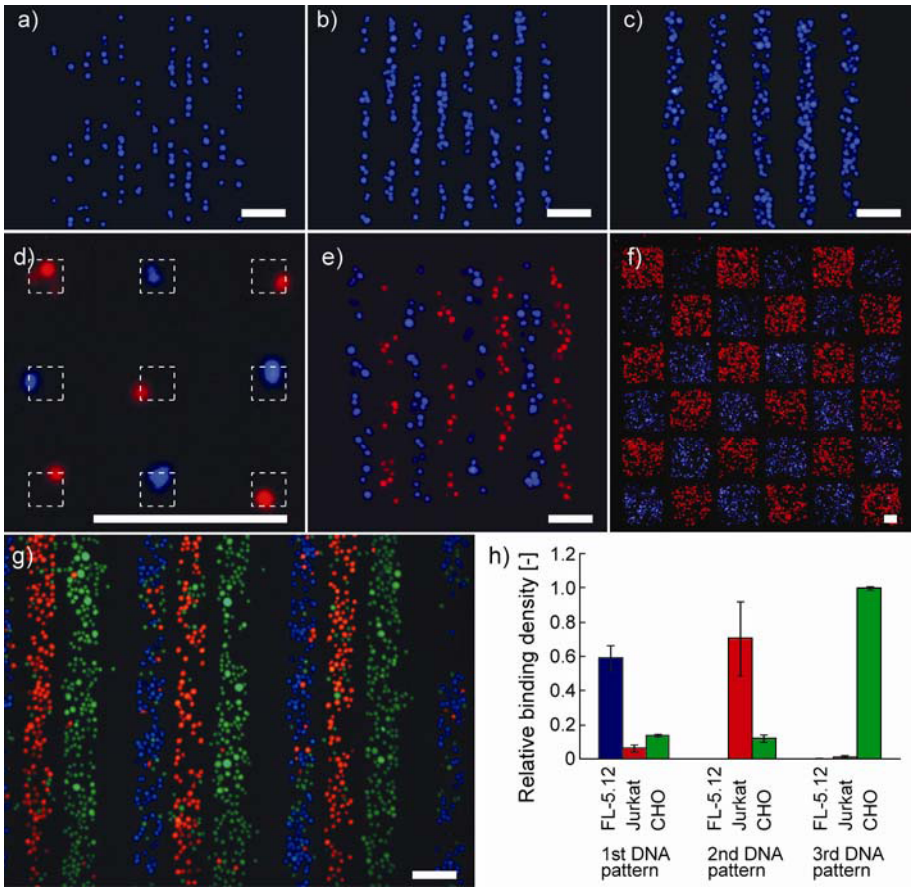

Figure 3. Capture of DNA-modified cells on DNA micropatterns. All scale bars indicate 100 µm. a-c) Jurkat cells modified with strand C1 were captured on M1 micropatterns. Line to space dimensions of the patterns are 10 µm/30 µm, 20 µm/40 µm and 40 µm/60 µm for a, b and c, respectively. d-f) Two types of Jurkat cells, which were modified with either C1 (blue) or C2 (red), were captured on single cell sized array patterns (d), or in stripes and checker board patterns (e, f). g) Three different types of cells, FL-5.12 (modified with C1, blue), Jurkat (C2, red) and CHO (C3, green), were assembled on stripe micropatterns. h). The patterned cells shown in (g) were counted for evaluating the relative binding densities. The error bars represent the standard deviation for three sets of the stripes.

the first DNA pattern, a second sequence was successively patterned in the same manner (Figure 2e-h). A key step in this process was the use of a PMMA layer that was directly spun on the first DNA (Figure 2e). Since commonly-used photoresists damage DNA, a method was needed to keep photoresist from contacting DNA molecules directly. We found that the DNA/PMMA/PR structure can successfully protect the DNA from the photoresist, thereby maintaining the DNA integrity for cell capture after PR and PMMA layer removal. To pattern more than two different DNA sequences on the substrate, steps e-h can be simply repeated. This feature makes it possible in principle to pattern a large number of different DNA sequences on a single substrate, enabling capture of several different cells on the patterns via hybridization. As a final step, the remaining aluminum layer was removed with 0.05 M sodium hydroxide (NaOH) without damaging the patterned DNA sequences (Figure 2i). The

DNA-patterned substrate was immersed in phosphate buffer saline (PBS) containing 1% fetal bovine serum (FBS) for 0.5 h to 1 h to eliminate the non-specific binding of cells to the glass surface.

Pattern multiple types of live cells on DNA patterns

Cell capture was first performed on simple patterns(Figure 3). Using the NHS-DNA conjugate obtained in chapter 1,[12] the surface of the cells was directly modified with 20 bp single-stranded DNA molecules that were complementary to the patterned sequences on the substrate. At the same time, the cells were stained with CellTracker Blue, Green, or Orange (Invitrogen) for fluorescent observation. The DNA-modified cells were then dispersed on the substrate in PBS, and incubated for 5 min to complete hybridization. After that, unbound cells were rinsed away with PBS.

Jurkat T lymphoma cells, which were modified with sequence A, were precisely assembled on micropatterns of sequence A' (Figure 3) without any non-specific capture in the background areas. We could clearly observe the difference ine pattern widths varing from the single cell level (width (*w*): 10 mm, gap (*g*): 30 mm, in Figure 3a) to several cells (*w*: 20 mm, *g*: 40 mm in Figure 3b, and *w*: 40 mm, *g*: 60 mm in Figure 3c, respectively). Also, two types of Jurkat cells, which were modified with A (blue) or B (red) sequences, were captured on square array patterns (square: 20 x 20 mm, gap: 40 mm, sequence A' and B') that were sized such that only one cell was captured per pad (Figure 3d). The fluorescent images show that the majority of pads retained the single cell after washing. Stripes (width: 40 mm, gap: 20 mm) and checker board patterns (square: 300 x 300 mm, gap: 50 mm) were also demonstrated with high

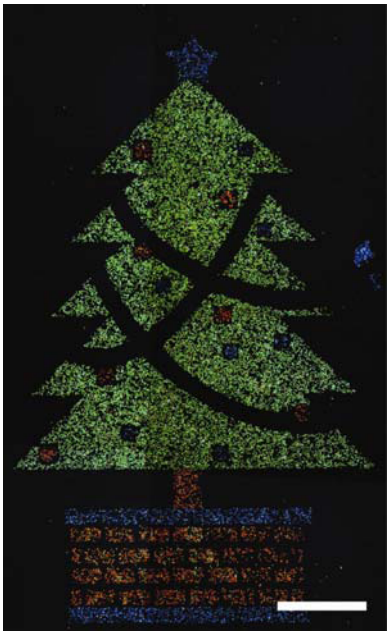

Figure 4. Demonstration of a Christmas tree cell pattern. CHO (C1, green), Jurkat (C2, red), andFL-5.12 (C3, green) cells were captured. The scale bar indicates 1 mm.

binding selectivity (Figure 3e-f). Three different cell lines, FL-5.12 hematopoietic progenitor (sequence A, blue), Jurkat (sequence B, red), and Chinese hamster ovary (CHO) (sequence C, green), were patterned on the substrate with line patterns of three different DNA sequences (width: 80 mm, gap: 20 mm, sequences: A', B', and C'). Efficient adhesion was observed regardless of the types of the cells, i.e., non-adherent cells (Jurkat, FL-5.12) and adherent cells (CHO) (Figure 3g) a feat thatother pattering methods have not achieved. The relative binding density of these captured cells showed that ~75 % (on the first DNA pattern) to ~ 99 % (on the third DNA patterns) of cells were selectively retained by their complementary strands on the substrate.

Photolithographic patterning of DNA allows us to design any arbitrary pattern. To illustrate this, Christmas tree cell pattern (width: 5 mm, height: 7 mm) was preparedwith CHO (sequence A, green), Jurkat (sequence B, red), and FL-5.12 (sequence D, blue) cells providing the decorations (Figure 4).

Cell-cell interaction studies

To examine the applicability of the DNA-based adhesion technique for performing functional assays of cellular networks, we designed a cell communication experiment using heterogeneous cells (Figure 5). FL-5.12 cells are interleukin-3 (IL-3)-dependent cells, as they can live and proliferate only in the presence of IL-3 molecules. They undergo apoptosis without IL-3 molecules in ~36 h.[21] We also prepared gene-transfected CHO cells (CHO IL-3 cells) that can produce IL-3 molecules and express green fluorescent protein (GFP).[14] If FL-5.12 cells and CHO IL-3 cells were co-cultured in the same medium, the FL-5.12 cells would be expected to proliferate when they receive IL-3 molecules from the CHO IL-3 cells. In contrast, when FL-5.12 cells are co-cultured with CHO cells, which only express GFP but do not produce IL-3, the FL-5.12 should go through apoptosis in ~36 h. We used the DNA-based technique to assemble designed patterns of FL-5.12 cells and CHO IL-3 cells, and observed the difference in their behavior depending on the two-dimensional spatial patterns.

To perform this experiment, we fabricated concentric ring patterns of FL-5.12 cells surrounding a central region of patterned CHO cells (Figure 5b left). Fifteen ring patterns were formed (R1-R15, width: 50 mm), where the distance from the center varied from 350 um to 8800 um. The patterned FL-5.12 and CHO IL-3 cells were embedded in 1 % agarose hydrogels, which prevented the cells from moving during cell culture (Figure 5b right) and inhibited convective flow. The IL-3 molecules that were produced by the CHO IL-3 cells at the center gradually diffused in the agarose towards the surrounding FL-5.12 cells. The CHO IL-3 cells were distinguished from the FL-5.12 cells by fluorescence of GFP (Figure 5c) even after their proliferation. The cells were incubated at 37 °C in a 5% CO_2 environment for 72 h to observe the behavior of the FL-5.12 cells.

Distance-dependent cell proliferation was observed after 72 h of culture (Figure 6a and b). We counted the number of the FL-5.12 cells every 24 h, and then calculated the growth ratio, R_{growth}, which was defined as (number of cells after culture

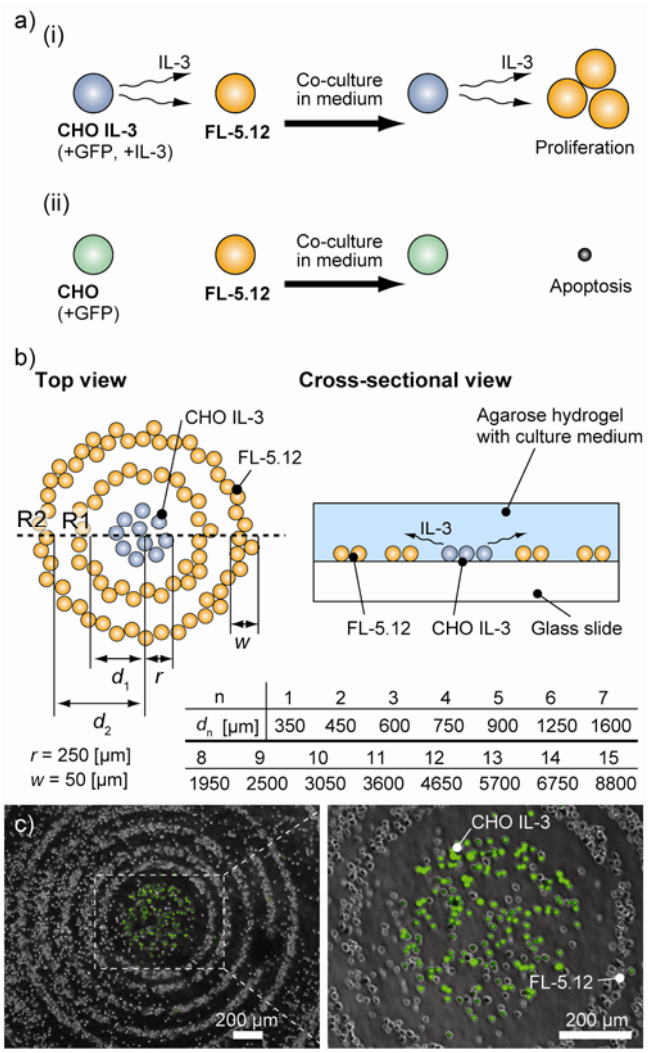

Figure 5. CDesign of a distance-based cell communication experiment using DNA-captured cells. a) An interleukin-3 (IL-3) dependent cell line, FL-5.12, proliferates by receiving IL-3 molecules from gene-transfected CHO cells (+IL-3, +GFP) that are co-cultured with the FL-5.12. However, FL-5.12 cells undergo apoptosis after 36-72 h when they are co-cultured with CHO (+GFP) cells that do not produce IL-3. b) For surface experiments, CHO IL-3 cells were patterned at the center of a ring pattern in which FL-5.12 cells are presented in surrounding rings. Fifteen FL-5.12 ring patterns (R1-R15), which varied from 350 μm to 8800 μm in radius (d1-d15), were used (bottom). The patterned CHO IL-3 and FL-5.12 cells were embedded in a 1% agarose gel layer containing culture medium (right). IL-3 molecules generated by CHO IL-3 diffused to the patterned FL-5.12 cells. c) Images of the patterned CHO IL-3 and FL-5.12 cells after they were embedded in the agarose gel. Green fluorescence indicates the CHO IL-3 cells.

for a time of interest, *t*)/(number of cells before culture), for each ring pattern (Figure 6d). The FL-5.12 cells on R1-R8, which were close to the CHO IL-3 cells (*d*: 350-1950 um), proliferated and reached confluence (R_{growth}: >9 at 72 h). The growth ratio of the FL-5.12 cells on R9-R13, however, decreased as the distance increased from the CHO IL-3 cells, and no proliferation occurred on R14 and R15 (R_{growth}: <1.0). We also performed a cell viability test using calcein AM and ethidium homodimer-1 after 72 h of culture (Fluorescent images in Figure 6c). The fraction of live cells also

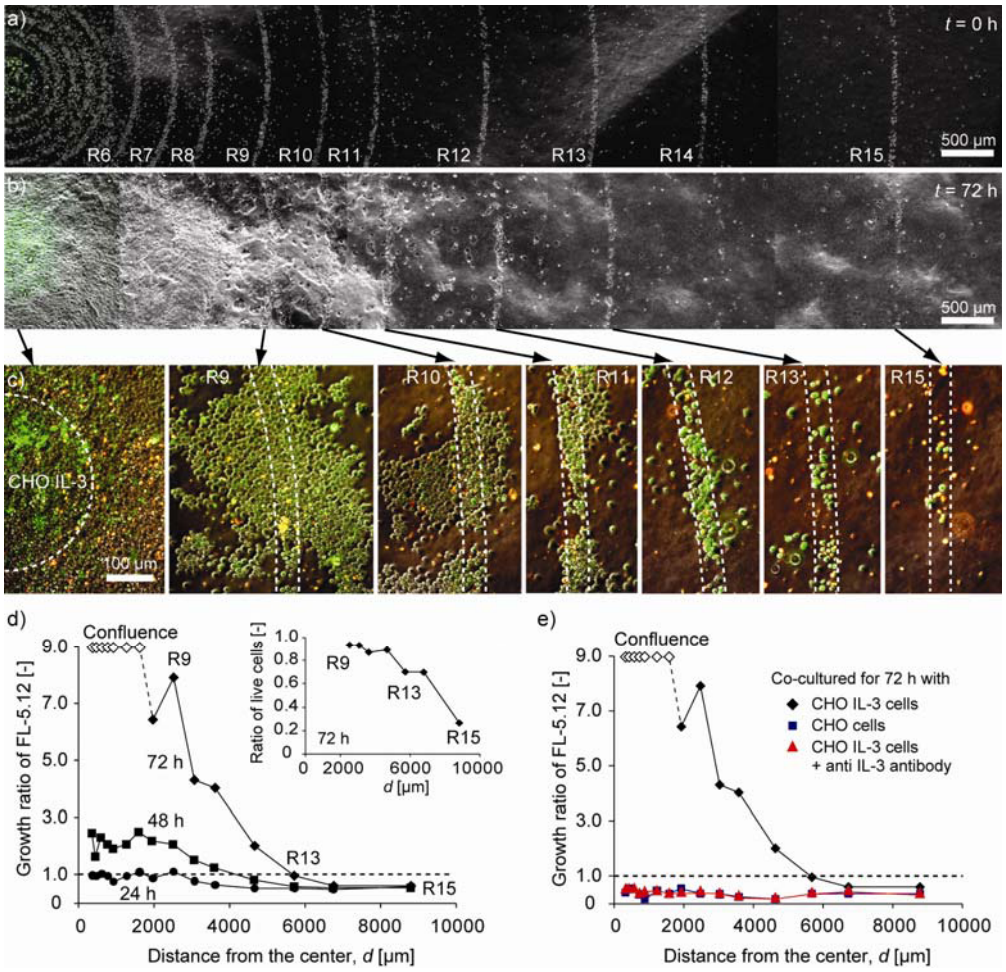

Figure 6. Proliferation of FL-5.12 cells as a function of their distance from the CHO IL-3 center. a)Image of the patterned CHO IL-3 and FL 5.12 cells before cell culture (t = 0 h). b) Image of the CHO IL-3 and FL-5.12 cell patterns after 72 h of culturing at 37 ° C in a 5% CO_2 environment. FL-5.12 cells on R1-R7, which were close to the CHO IL-3 core, proliferated and reached confluence. The proliferation rate decreased as the distance from the CHO IL-3 cells became larger (R9-R12), and almost no proliferation occurred in the outer rings (R13-R15). c) Magnified images of FL-5.12 cells shown in B after applying calcein AM and ethidium homodimer-1. Green fluorescence indicates live cells and red fluorescence indicates dead cells. d) The growth of the FL-5.12 cells depended on their distance from CHO IL-3 cells that are patterned at the center. The growth ratio was defined as (number of FL-5.12 cells after culture) / (number of FL-5.12 cells before culture). (inset) The ratio of live cells, which was defined as (number of live cells) / (total number of cells), also decreasesed at R9-R15. e) Comparison of the growth ratios of FL-5.12 cells that were co-cultured with (i) CHO IL-3 cells, (ii) CHO cells that did not produce IL-3, and (iii) CHO IL-3 cells with anti IL-3 antibodies in the medium.

decreased as the distance increased following the growth ratio.

As control experiments, we co-cultured (i) FL-5.12 cells with CHO cells, that did not produce IL-3 (but still express GFP), and (ii) FL-5.12 cells and CHO IL-3 cells with 0.5 mg/ml anti-IL-3 antibodies in the agarose. After 72 h of culture, no proliferation was observed on any ring patterns in both control experiments (Figure 6e). This result indicated that the proliferation of the DNA-captured FL-5.12 cells clearly depended on the presence of IL-3 molecules in the agarose.

The distance-dependent proliferation of the FL-5.12 cells observed here indicated that there was a concentration gradient of the IL-3 molecules produced by the CHO IL-3 cells in the center. The diffusion speed of an an IL-3 molecule in 1 % agarose gel was calculated to be ~1.5 mm/h. Thus, the IL-3 molecules diffused from the center to the outmost ring pattern (d_{15} = 8800 um) in ~6 h. The average rate of IL-3 production from a single CHO IL-3 cell we used was 3.9 x 10^{-6} pg·s^{-1}, which was determined via enzyme-linked immunosorbent assay (ELISA) (Mouse IL-3 ELISA kit, BD Biosciences). Using this value, the concentration gradient of the IL-3 molecules over the ring patterns could be estimated as a function of time and spatial location. The results of these calculations showed that (i) there was a ~6 h time lag between the appearance of the IL-3 concentration increase at the R1 (the innermost) and R15 (the outtermost) patterns, and (ii) the inner ring patterns always had a higher IL-3 concentration than outer patterns, e.g., the IL-3 concentration at R1 is ~260 times higher than that at R15 after 24, respectively. In addition to this, (iii) the FL-5.12 cells on the inner patterns might consume the IL-3 molecules, and (iv) the FL-5.12 cells also might block the IL-3 diffusion physically, which could slow the diffusion speed. We think that a combination of these aspects cause the IL-3 gradient to form between the inner and outer patterns and generate the proliferation difference observed between the inner and outer rings.

CONCLUSION

In summary, we have developed an aluminum lift off micropattern method that provides the ability to capture heterogeneous cells on any desirable microscale pattern at single cell resolution. The patterned cells can be embedded in agarose hydrogel while maintaining their viability and activity. This ability allows us to observe diffusion-based cell communication as defined by two-dimensional spatial patterns. We believe that this ability to build 2-D heterogeneous cell patterns will be a powerful platform for examining the differentiation and communication of cells, and it will potentially be expandable to create 3-D cell structures, which enable the formation of artificial tissue where chemical and physical interactions are paramount to complex function.

MATERIALS AND METHODS

Oligonucleotide sequences.

Twenty base-pair sequences were designed for the modification of cell surfaces (A-D) and substrates (A'-D'). The sequences A-D and A'-D' have thiol groups and amino groups at the ends, respectively. All oligonucleotides were obtained from Integrated DNA Technologies (Coralville, IA). The sequences were as follows:

A: HS-C_6-5'-GTA ACG ATC CAG CTG TCA CT-3',

A': H_2N-C_6-5'-AGT GAC AGC TGG ATC GTT AC-3',

B: HS-C_6-5'-TCA TAC GAC TCA CTC TAG GG-3',

B': H_2N-C_6-5'-CCC TAG AGT GAG TCG TAT GA-3',

C: 5'-ACT GAC TGA CTG ACT GAC TG-3'-C_6-SH,

C': 5'-CAG TCA GTC AGT CAG TCA GT-3'- C_6-NH_2,

D: HS-C_6-5'-ACT GAT GGT AAT CTG CAC CT-3',

D': H_2N-C_6-5'-AGG TGC AGA TTA CCA TCA GT-3'.

General cell culture conditions.

Jurkat cells were cultured in RPMI-1640 medium (Gibco/Invitrogen) supplemented with 10% (v/v) fetal bovine serum (FBS, HyClone) and 1% penicillin/streptomycin (P/S, Sigma). FL-5.12 cells were grown in RPMI-1640 medium with 10% FBS, 1% P/S, 50 μM β-mecaptoethanol (Sigma), and 3.5 ng/ml murine recombinant IL-3 (Sigma). CHO cells were kept in F-12 (HAM) medium (Gibco) with 10% FBS and 1% P/S. For the cell communication experiment, the murine IL-3 gene was introduced to CHO cells by retroviral infection, and the gene encoding GFP was inserted into the vector pCDNA 3.1 and introduced into the CHO cells by transient transfection.[14] All cell lines were maintained at 37 °C in a 5 % CO_2 environment.

Aluminum/PMMA micro patterns on glass slides.

The starting substrate was an aldehyde-functionalized glass slide (SCHOTT Nexterion, Lousiville, KY) with a 100 nm aluminum (Al) layer deposited by a vacuum evaporator (401 vacuum system, Vecco). PMMA (M_W: ~996,000, Aldrich), which was dissolved in acetone (3.2 % w/w), was spun on the slide at 2500 rpm for 30 s, followed by S1818 photoresist (PR) (Shipley) spincoated at 500 rpm for 10 sec, and 2500 rpm for 30 s. The slide was then baked at 120 °C for 2 min to evaporate solvent. The PR was exposed by UV light through a photomask, and patterned with a 1:1 mixture solution of MicroDev developer and deionized (DI) water. The pattern was then transferred to the PMMA layer using oxygen plasma etching (Plasma-Therm PK-12 RIE, 150 W, 100 sccm O_2). The Al layer was also etched with aluminum etchant (Air Products). To protect the aldehyde-glass surface from the aluminum etchant, the etching was stopped before the Al layer was completely removed (typical etching time: ~1 min). The remaining Al layer was removed with 0.05 M sodium hydroxide (NaOH). Finally, the PR layer on the PMMA was rinsed away with isopropanol (IPA).

DNA-NH_2 prinitng on the slides.

The attachment of DNA-NH_2 on the aldehyde groups on the glass slide is based on the protocol in our previous work.[10, 11] After fabricating the aluminum/PMMA

micro patterns described above, chemical vapor deposition of trimethoxysilylpropanal (PSX1050-KG, UCT Specialties LLC) was performed on the glass slide at 60 °C for 1 h to improve the the number of aldehydes group on the exposed glass surface. Then, 80 μM DNA-NH_2 (sequence A-D) in phosphate buffer saline (PBS(-), Gibco) was placed on the pattern and incubated at room temperature (RT) for 15 min, followed by heating at 100 °C for 1 h to promote amine-aldehyde condensation. After that, the slide was rinsed with 0.4 % sodium dodecyl sulfate (SDS) and DI water, and immersed in 65 mM sodium borohydride ($NaBH_4$, Sigma) in a mixture of ethanol and PBS at a ratio of 1:3 to conduct reductive amination. Finally, the unbound DNA-NH_2 was washed using 0.4 % SDS and in DI water, and the PMMA layer was removed with acetone. When patterning more than one type of DNA sequence, the PMMA patterning and DNA immobilization steps were repeated in the same manner. The DNA-patterned slide was stored dry at RT and used within two weeks.

DNA modification of live cells.

The detailed protocol and characterization were reported in our previous work.[12] Briefly, 60 ml of 0.39 mM DNA with a thiol at the 5' end (sequence A'-D') was reacted with 0.2 mg succinimidyl-[(*N*-maleimidopropionamido)-hexaethyleneglycol] (NHS-PEO_6-Maleimide) (Pierce) in 40 ml of DMSO to obtain 1 ml of 23.4 μM NHS-DNA in PBS. Target cells, which were rinsed twice with PBS, were then incubated with the NHS-DNA solution for 30 min at RT. The cell concentration was 5 x 10^6 cells/ml. Either CellTracker Blue, Green, or Orange (Invitrogen) was added together with the NHS-DNA if fluorescent labeling was needed. After that, the cells were washed twice with PBS containing 1 % FBS, and re-suspended in the 1 % FBS in PBS at a concentration of 1 x 10^7 cells/ml. The cells were used for cell capture within 2 hours.

Cell capture by DNA hybridization.

The aluminum layer on the DNA-patterned glass slide was removed with 0.05 M NaOH. After a DI water rinse, the slide was immersed in PBS containing 1 % FBS for 1-2 h to block the glass area with proteins in the serum, which significantly reduced unwanted background cell capture. Then the slide was placed in PBS solution in a Petri dish. The DNA-modified cells were dispersed on the slide using a micro pipette, and incubated for 5 min to capture them via DNA hybridization. Unbound cells were gently washed away in the Petri dish. In the case of patterning two or three different types of cells, the dispersing and washing steps were sequentially repeated for each type of cells. The captured cells were observed with a fluorescent microscope (Nikon, ECLIPSE E800).

Culture of the patterned cells in agarose.

For the cell communication experiment, the patterned FL-5.12 and CHO IL-3 cells were immersed in an agarose hydrogel containing culture medium. Preparation

of the agarose hydrogel was as follows: Ultra-low gelling point agarose (Type IX-A, A2576, Sigma) was dissolved in PBS (2% (w/w)), and sterilized. The agarose solution was mixed with RPMI 1640 medium containing 12 % FBS and 1 % P/S at a 1:1 ratio, and warmed to 37 °C. The glass slide with the patterned cells was then carefully immersed in 6 ml of the agarose/medium mixture in a 60 x 15 mm Petri dish, and cooled to 4 °C for 30 min to form the gel. After that, the cells were incubated at 37 °C in a 5 % CO_2 environment for 72 h. For the control experiments in Figure 6e, CHO (+GFP) cells were used instead of CHO IL-3 cells, or 0.5 mg/ml of mouse anti IL-3 antibody was added to the agarose.

Observation of FL-5.12 proliferation.

We took optical images of the patterned FL-5.12 and CHO IL-3 cells were collected every 24 h with an inverted fluorescent microscope (IX71, Olympus), the number of the FL-5.12 cells on the micro patterns were counted. For the cell viability assay, 1.5 ml of 4 mM calcein AM and 10 ml of 2 mM ethidium homodimer-1 (LIVE/DEAD Vialibity/Cytotoxicity Kit for mammalian cells, Invitrogen) in 500 ml of PBS were applied to the 6 ml agarose gel with the patterned cells, followed by incubation at 37 °C for 1 h.

REFERENCES

1. D. Di Carlo, L. P. Lee, *Anal. Chem.* **2006**, *78*, 7918; A. Khademhosseini, R. Langer, J. Borenstein, J. P. Vacanti, *Proc. Natl. Acad. Sci. USA.* **2006**, *103*, 2480.

2. R. Singhvi, A. Kumar, G. P. Lopez, G. N. Stephanopoulos, D. I. C. Wang, G. M. Whitesides, D. E. Ingber, *Science* **1994**, *264*, 696; C. S. Chen, M. Mrksich, S. Huang, G. M. Whitesides, D. E. Ingber, *Science* **1997**, *276*, 1425; C. Roberts, C. S. Chen, M. Mrksich, V. Martichonok, D. E. Ingber, G. M. Whitesides, *J. Am. Chem. Soc.* **1998**, *120*, 6548; J. Ziauddin, D. M. Sabatini, *Nature* **2001**, *411*, 107; A. Revzin, P. Rajagopalan, A. W. Tilles, F. O. Berthiaume, M. L. Yarmush, M. Toner, *Langmuir* **2004**, *20*, 2999.

3. J. R. Rettig, A. Folch, *Anal. Chem.* **2005**, *77*, 5628; E. Ostuni, C. S. Chen, D. E. Ingber, G. M. Whitesides, *Langmuir* **2001**, *17*, 2828; A. Revzin, K. Sekine, A. Sin, R. G. Tompkins, M. Toner, *Lab Chip* **2005**, *5*, 30.

4. D. R. Albrecht, G. H. Underhill, T. B. Wassermann, R. L. Sah, S. N. Bhatia, *Nat. Methods* **2006**, *3*, 369; B. M. Taff, J. Voldman, *Anal. Chem.* **2005**, *77*, 7976; N. Mittal, A. Rosenthal, J. Voldman, *Lab Chip* **2007**, *7*, 1146.

5. C. T. Ho, R. Z. Lin, W. Y. Chang, H. Y. Chang, C. H. Liu, *Lab Chip* **2006**, *6*, 724.

6. A. R. Wheeler, W. R. Throndset, R. J. Whelan, A. M. Leach, R. N. Zare, Y. H. Liao, K. Farrell, I. D. Manger, A. Daridon, *Anal. Chem.* **2003**, *75*, 3581;

D. Di Carlo, L. Y. Wu, L. P. Lee, *Lab Chip* **2006**, *6*, 1445; P. J. Lee, P. J. Hung, R. Shaw, L. Jan, L. P. Lee, *Applied Physics Letters* **2005**, *86*.

7. A. M. Skelley, O. Kirak, H. Suh, R. Jaenisch, J. Voldman, *Nat. Methods* **2009**, *6*, 147.

8. E. E. Hui, S. N. Bhatia, *Langmuir* **2007**, *23*, 4103.

9. R. A. Chandra, E. S. Douglas, R. A. Mathies, C. R. Bertozzi, M. B. Francis, *Angewandte Chemie-International Edition* **2006**, *45*, 896.

10. E. S. Douglas, R. A. Chandra, C. R. Bertozzi, R. A. Mathies, M. B. Francis, *Lab Chip* **2007**, *7*, 1442.

11. S. C. Hsiao, A. K. Crow, W. A. Lam, C. R. Bertozzi, D. A. Fletcher, M. B. Francis, *Angewandte Chemie-International Edition* **2008**, *47*, 8473.

12. S. C. Hsiao, B. J. Shum, H. Onoe, E. S. Douglas, Z. J. Garter, R. A. Mathies, C. R. Bertozzi, M. B. Francis, *Langmuir* **2009**, in press.

13. N. M. Teriello, E. S. Douglas, N. Thaitrong, S. C. Hsiao, M. B. Francis, C. R. Bertozzi, R. A. Mathies, *Proc. Natl. Acad. Sci. USA.* **2009**, *105*, 20173; E. S. Douglas, S. C. Hsiao, H. Onoe, C. R. Bertozzi, M. B. Francis, R. A. Mathies, *Lab Chip* **2009**, in press.

14. Z. J. Gartner, C. R. Bertozzi, *Proc. Natl. Acad. Sci. USA.* **2009**, *106*, 4606.

15. B. L. Jackson, J. T. Groves, *Langmuir* **2007**, *23*, 2052.

16. L. M. Demers, D. S. Ginger, S. J. Park, Z. Li, S. W. Chung, C. A. Mirkin, *Science* **2002**, *296*, 1836.

17. C. Xu, P. Taylor, M. Ersoz, P. D. I. Fletcher, V. N. Paunov, *J. Mater. Chem.* **2003**, *13*, 3044; S. A. Lange, V. Benes, D. P. Kern, J. K. H. Horber, A. Bernard, *Anal. Chem.* **2004**, *76*, 1641.

18. R. J. Lipshutz, S. P. A. Fodor, T. R. Gingeras, D. J. Lockhart, *Nature Genet.* **1999**, *21*, 20; A. C. Pease, D. Solas, E. J. Sullivan, M. T. Cronin, C. P. Holmes, S. P. A. Fodor, *Proc. Natl. Acad. Sci. USA.* **1994**, *91*, 5022.

19. L. A. Chrisey, C. E. Oferrall, B. J. Spargo, C. S. Dulcey, J. M. Calvert, *Nucleic Acids Res.* **1996**, *24*, 3040.

20. M. Schena, D. Shalon, R. W. Davis, P. O. Brown, *Science* **1995**, *270*, 467.

21. L. London, J. P. McKearn, *J. Exp. Med.* **1987**, *166*, 1419.

Chapter 3: DNA-barcode directed capture and electrochemical metabolic analysis of single mammalian cells

INTRODUCTION

The controlled capture of single cells in microfluidic devices is essential for the development of integrated microdevices for single cell analysis. With size and volume scales comparable to those of individual cells, microfluidic devices provide a powerful tool for control of the cellular microenvironment.[1] Previously we have demonstrated the use of engineered cell surface DNA (cell adhesion barcodes) for cell capture,[2, 3] and the use of this capture technique to perform single-cell gene expression analysis in a microfluidic chip.[4] Here we describe the use of DNA barcode cell capture to populate an array of pH-sensitive microelectrodes, enabling the rapid, selective and reversible capture of both adherent and non-adherent single cells on the pH sensor surface. This bifunctional system enables accurate real-time monitoring of single cell metabolism because extracellular acidification is proportional to overall energy usage.[5,6] We demonstrate the use of this technology to identify cell metabolism.

Previous work has demonstrated the individual aspects of single cell capture and pH monitoring in microfluidic systems. A variety of methods for arrayed single cell capture have been shown, including physical[7] and energetic traps,[8] and biochemical adhesion.[9, 10] While a simple restrictive capture well or microfluidic trap could be used to isolate cells over a sensor, it has been shown that access to fresh media and the ability to clear waste products are important to normal cell function.[11] Highly precise cell placement is also important for monitoring if subcellular-scale electrodes are to be used.[12]

The use of extracellular acidification is a valuable tool in the quantitative analysis of cell activity.[13] A key example is the Cytosensor Microphysiometer, which has been widely used to measure acidification from bulk cell populations (10^4 – 10^6 cells per 3 ml sample) as a way to quantify metabolism. This system has been used for a number of applications, including the detection of G-protein coupled (chemokine) receptor activation, the activity of neurotrophin, the activation of ligand gated ion channels, and the binding of ligands to tyrosine kinase receptors[5]. It has also been used to identify ligands for orphan receptors.[14] Other devices have also employed pH electrodes to measure cell activity down to the single cell level. Ges *et al.* recently demonstrated a device for on-chip measurement of acidification rates from single cardiac myocytes using physical confinement.[15] In their system, single myocytes were isolated in the sensing volume by closing the ends of a PDMS channel. While this system represented an important step in single cell monitoring, the cell isolation technique does not allow for controlled capture on the sensor electrodes, which is necessary for simultaneous multi-analyte monitoring.

The primary goal of the present work is the direct integration of a versatile DNA-based cell capture technique with sensors that are on the same size scale of

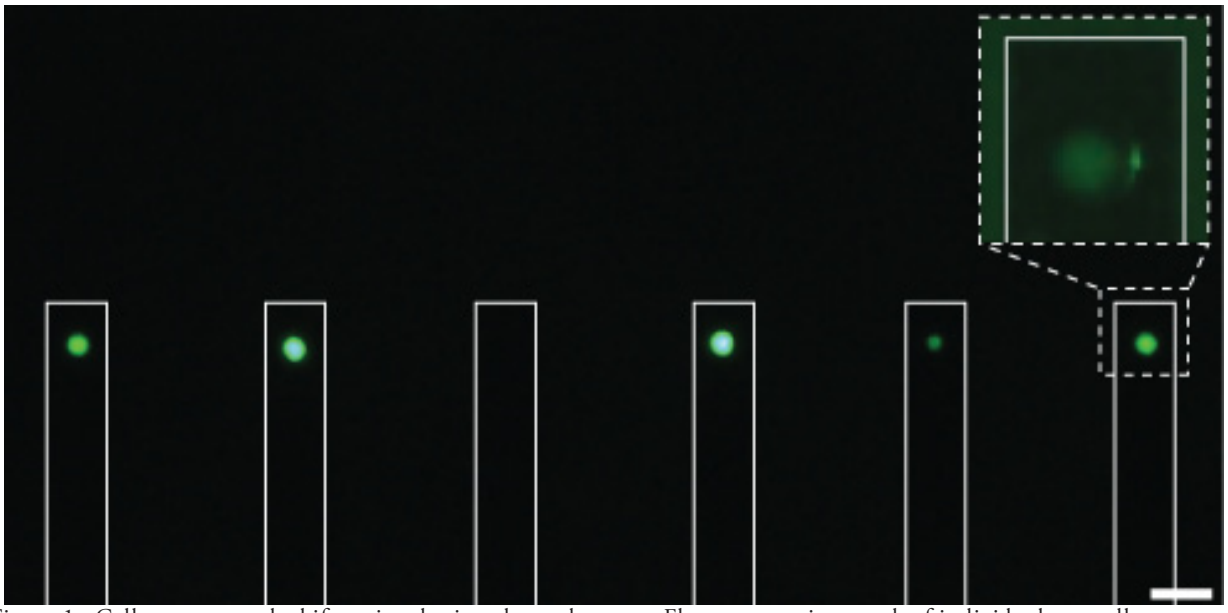

Figure 1. Cell capture on the bifunctional microelectrode array. Fluorescent micrograph of individual non-adherent Jurkat cells with a surface-bound DNA barcode bound to the complementary strand on the sensor electrode. Electrode areas are outlined in white. The scale bar = 40 um. Inset: Magnified view of a single Jurkat cell on an electrode, with additional oblique illumination to reveal the electrode area.

an individual cell, forming a bifunctional electrode system. To do this, an array of lithographically patterned iridium oxide pH microelectrodes was first enclosed within a microfluidic channel. Single stranded DNA was then attached to the iridium oxide surface using a silane linker, giving the sensor the ability to capture cells bearing complementary DNA sequences while retaining its detection sensitivity. Here, we used this system to measure the extracellular acidification resulting from the metabolism of non-adherent T cells, and we demonstrate that the pH sensitivity is sufficient to discriminate between healthy primary T cells and cancerous Jurkat T cells that have a higher metabolism. [9] The novel combination of DNA-directed cell capture and electrochemical monitoring on a bifunctional electrode thus opens many new avenues as a platform for single cell analysis.

RESULTS

The integration of an affinity DNA probe with a pH microelectrode

The integration of an affinity capture DNA probe with the pH microelectrodes on our bifunctional microelectrode array chip provides a platform for the direct monitoring of extracellular acidification for cells that are normally non-adherent. As seen in Figure 1, the size-limiting bifunctional microelectrode enables single cell capture directly on the sensor. The bifunctional microelectrode array was tested by measuring the extracellular acidification of Jurkat and primary T cells. First, Jurkat and primary T cells were captured and monitored separately on the array to establish the sensor functionality and the difference in single-cell acidification between the two cell types. Figure 2a shows single cell acidification data over a 10 min period. Jurkat

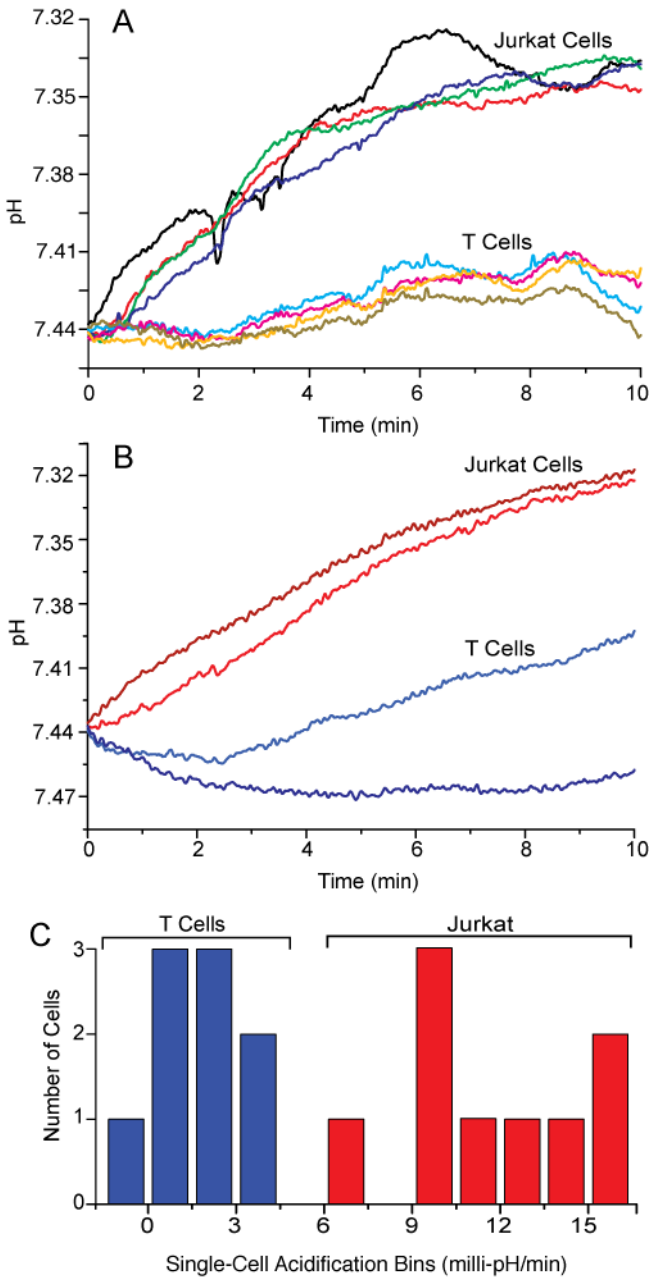

Figure 2. Single cell acidification measured with the bifunctional microelectrode array. (A) Representative composite data of single Jurkat and primary T cell acidification measured in known homogenous samples. (B) Single Jurkat and primary T cells captured from a mixture and monitored simultaneously over a 10 min span on the array. (C) Histogram of individual cell acidification in known-type samples over 10 min. Jurkat cells are seen to have a significantly higher ($P < 0.0002$) rate of acidification than primary T cells in low-buffered media.

cells exhibited an extracellular acidification rate of 11.5±3.3 milli-pH/min, while primary T cells exhibited 1.61±1.5 milli-pH/min (s.d., n=9 each). This difference was also confirmed with bulk cell population acidification measurements (~10^6 cell/ml in low-buffered media at 37 °C).

Single cell pH electrochemical measurement

To demonstrate the ability to distinguish different cells in a mixed population, single cells from a mixture of Jurkat and primary T cells bearing the same cell adhesion barcode were monitored simultaneously on the array. Figure 2b shows acidification data from mixed cells on the array over 10 min. The difference in measured acidification rates followed the same trend as the separate samples, and allowed for discrimination between the two visually similar cells. Jurkat cells had an acidification rate of 10.1±2.3 milli-pH/min, and healthy T cells had 2.41±2.54 milli-pH/min (s.d., n=5 each).

Figure 2c presents a bar graph of the acidification rates over several trials using known cell populations on the array. For Jurkat cells the mean acidification rate was 11.5±3.2 milii-pH/min, while primary T cells exhibited a rate of 1.62±1.31 milli-pH/min. The difference is clearly significant with a T-test value of $P<0.0002$. While the Jurkat cells were slightly larger than the primary T cells (typically 12 mm vs. 10 mm diameter), the size difference is not large enough to account for the difference in acidification.

Measuring single cell response to exogenous stimulation

To demonstrate the ability to measure single cell responses to exogenous stimulation, Jurkat cells were treated with rotenone while captured on the bifunctional microelectrode array (Figure 3). Incubation with rotenone would be expected to interfere with the mitochondrial electron transport chain, causing cells to shift to lactic acid fermentation to complete the glycolytic cycle.[16, 17] The resulting excretion of lactic acid should then increase the rate of acidification in the cellular environment.[18] In the experiment, a sample of captured cells was first incubated under normal conditions to establish a baseline rate of acidification (~8.8 milli-pH/min) under aerobic metabolism. After 13 min, 10 μM rotenone was added to the channel, which resulted in a three-fold increase in the acidification rate (~27.7 milli-pH/min) within 1 minute. Bulk cell controls, in which Jurkat cells were treated with 1 μM rotenone in low-buffered media (~10^6 cells/mL at 37 °C), consistently demonstrated more than twice the acidification over 60 min, compared to identical untreated cells. The observation of this metabolic shift provides an important demonstration of this technique's ability to monitor responses to exogenous agents, such as receptor-ligand binding,[19] at the single cell level.

DISCUSSION

The bifunctional microelectrode array developed here combines the two important functions of selective cell capture and metabolic monitoring of single cells in an array format. In earlier work, Castellarnau *et al.* used dielectrophoresis to localize high concentration suspensions of bacteria near an ISFET pH sensor

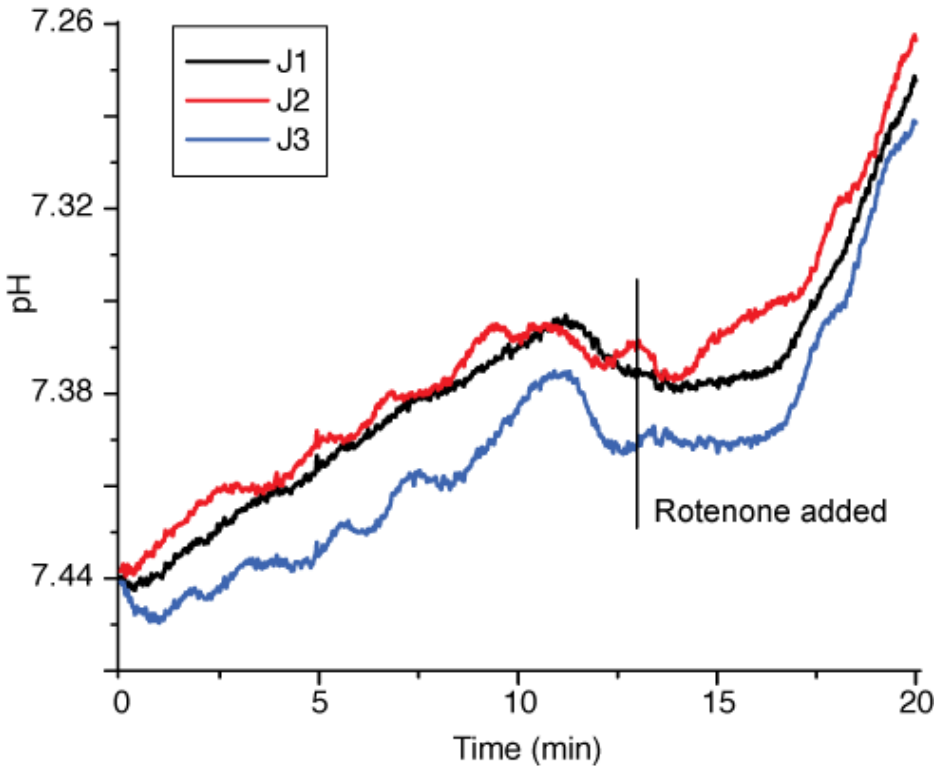

Figure 3. Single cell stimulation measured by the bifunctional microelectrode array. Jurkat cells exhibit normal baseline acidification during the first 13 minutes, then 125 uL of 10 uM rotenone in low-buffered media is added to the channel outlet reservoir where it diffuses into the channel within seconds. Rotenone inhibits the mitochondrial electron transport chain, causing an increased rate of lactic acid excretion, and therefore a higher rate of acidification.

and measured the acidification of the cells in the presence of glucose.[29] While this technique was well suited to measure the bulk response, it lacked the ability to resolve the unique activity of single cells. The single cardiac cell pH system of Ges *et al.*[15] provides the ability to monitor large adherent cells, but the volume displacement caused by sealing the channel makes it difficult to direct the cell attachment. DNA-barcode capture provides the advantage of directed capture of both adherent and naturally non-adherent cells, such as T and B cells. This controlled capture provides a platform for spatially-resolved electrical and/or optical probing and measurement of activity on the cell surface.

The acidification data show that single non-adherent cells continue to behave normally after treatment with capture DNA and attachment to the electrode. While any capture technique is likely to have some effect on the cell, cell adhesion barcodes bypass the natural cell-surface receptors that are often used for integrin or antibody-based capture,[10] and should thus avoid the activation of those known signaling pathways. For both the Jurkat and primary T cells the extracellular acidification rates measured are comparable to the single cell acidification rates reported by Ges *et al.*,[15] but the increased sensitivity of our functionalized microelectrode technique allows discrimination between the two cell types.

Our single-cell results show that the difference between the metabolic activity of primary non-transformed cells and immortalized cancerous T cells can be detected at the single-cell level. This methodology could be used to identify individual circulating tumor cells by their distinctive metabolic activity, going beyond simple antibody-based capture.[9] It could also be used to differentiate between cancerous cells of different metastatic potential.[6] Single-cell monitoring within such a mixture would allow for the detection of differences in drug response based on the cell's state of cancer progression or origin.

The array format with its future extension to include more elements allows the direct comparison of the individual activity of many cells under the same conditions with sufficient power to characterize ensemble variation. We are also pursuing the construction of a nanofabricated electrode array that would produce an electrochemical analysis map of a cell surface with high spatial-resolution. Static cell surface profiling has previously been demonstrated using scanning electrochemical microscopy,[20] but a nanoelectrode array could transform this from a serial to a parallel process and provide temporal resolution as well.

Going forward, we are working to add functionality to our single cell analysis by increasing the number of detected analytes from a single cell and the complexity of the analysis system. The previously mentioned Cytosensor Microphysiometer system for bulk cell monitoring was modified to simultaneously measure glucose, lactate and oxygen levels, in addition to the standard pH measurement capabilities.[21] Glucose and lactate were measured amperometrically using enzyme sensors bearing their respective oxidases. Oxygen was measured amperometrically at a platinum electrode coated with Nafion. Micro- or nanofabricated analyte-selective sensors could also be added to our system for additional analytical depth, including multi-analyte sensing on a single cell. A combination of calcium-sensitive fluorophores and electrical control has been used to monitor calcium flux in single neurons during patch-clamp recording by Thayer *et al.*[22] Our PDMS/glass multilayer device is readily modified to enable such simultaneous fluorescence and electrical measurements. While fluorescent probes often suffer from photobleaching, our technique could be used to track single-cell metabolic activity over hours or days, revealing any changes as the cell progresses through its life cycle. DNA barcode-based capture also provides the ability to engineer attachment between individual cells in a bio-orthogonal fashion. This could allow for the construction and analysis of discrete multi-type cell systems on an electrode. For example, a single neuron could be linked using DNA to a single muscle cell to allow analysis of the single-cell neuromuscular synaptic formation and operation.[23]

Dias et al. demonstrated a four electrode array for sub-cellular resolution detection of catecholamine release from single chromaffin cells, which used the relative strength of the amperometric signal at each electrode to estimate the location of exocytosis.[12] A nanoelectrode array would have the advantage of real-time spatially resolved measurement.

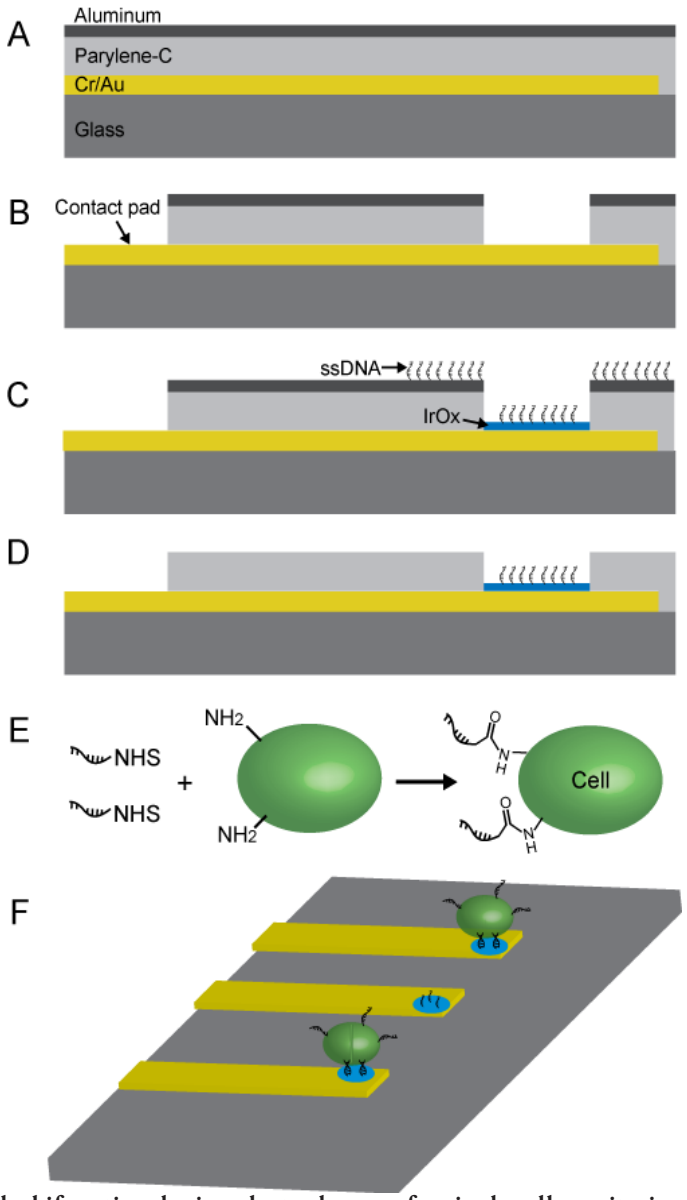

Figure 4. Fabrication of the bifunctional microelectrode array for single cell monitoring. (A) Gold electrodes are patterned on a glass wafer using photolithography and liftoff. A 7 um insulating layer of Parylene-c is then deposited onto the electrodes, and covered with a 100 nm layer of evaporated aluminum. (B) Photoresist is patterned on the aluminum layer, which is then etched and used as an etch mask for the Parylene insulation. (C) The sensor layer of iridium oxide is deposited on the electrode surface and then treated with an aldehyde silane for amine-modified capture DNA attachment. (D) Finally, the aluminum layer is dissolved in strong base, leaving only the capture DNA on the sensor surface. Cells bearing the surface-bound complementary strand are introduced and captured directly and specifically on the sensor. (E) Cells are treated with single stranded DNA (5'-CCCTAGAGT-GAGTCGTATGA-3') bearing a terminal *N*-hydroxysuccinimidyl (NHS) ester functional group, which binds to primary amines on the cell surface. This DNA barcode labeling functionalizes the cell for DNA-directed capture in the device. (F) Schematic of the microfluidic device. The electrodes are enclosed by a PDMS channel, forming the microfluidic device.

CONCLUSION

In conclusion, our bifunctional microelectrode array provides the ability to capture cells selectively and measure their electrical and metabolic activity. Using DNA-barcode capture, both adherent and naturally non-adherent cells can be studied on the same device. The array format allows us to discriminate between cells in a mixture, revealing the variation in single cell properties that make up the ensemble average. This controlled single-cell electrochemical measurement opens the door to the nanoscale cell interface which could enable multiplex, subcellular analysis of cellular activity.

MATERIALS AND METHODS

Electrode sensor fabrication.

Electrodes (40 nm thick Au with a 20 nm Cr adhesion layer) were patterned on 1.1 mm thick glass wafers using standard photolithographic liftoff, as previously described (Fig. 4).[24] A 7 mm thick layer of Parylene-c was deposited on the wafer using a Specialty Coating Systems Labcoter 2 Parylene deposition system, and measured with an AlphaStep IQ profilometer. A 100 nm layer of aluminum was evaporated on the device, and then lithographically etched using Air Products aluminum etchant with surfactant for 30 s at 60 °C (Fig. 4A, B). The etch mask for the aluminum layer was a photolithographically patterned 1 mm thick film of Shipley 1818 photoresist. The aluminum layer was then used as a mask to etch the underlying Parylene using oxygen plasma (60 sccm O_2, 100 W, 60 min).

After removing the Parylene insulation from the sensor area, the sensors were electro-deposited with a layer of iridium oxide following the protocol of Yamanaka *et al*.[25] Briefly, the iridium deposition solution was prepared as follows. 37.5 g of $IrCl_4$ was added to 75 mL of de-ionized water and stirred for 90 min. Next, 125 mg of oxalic acid was added, and the solution was stirred for 3 h. Finally, the solution pH was adjusted to 11 using aqueous K_2CO_3. The solution was initially light yellow, turning light blue, and finally dark blue over the course of several weeks. The deposition solution was stable for at least six months after preparation. Iridium oxide deposition was performed using a CHI 660 potentiostat in voltage cycling mode. 240 cycles of +0.5 V (0.25 s) and –0.5 V (0.25 s) were used, in a three electrode configuration using a saturated calomel reference and a platinum counter electrode.

After deposition, the devices were plasma cleaned for 1 min and modified with trimethoxysilylpropanal by vapor deposition at 60 °C for 60 min. Amine-modified ssDNA (80 μM in phosphate buffered saline) was then deposited onto the devices and bound using reductive amination as described in chapter 1 (Fig. 4C). Following DNA deposition, the protective aluminum layer was dissolved[26] by treatment with 0.1 M NaOH at room temperature with stirring for 20 min, leaving the capture DNA only

on the sensor surface (Fig. 4D).

Microfluidic device preparation.

Poly(dimethylsiloxane) (PDMS) channels were prepared using Dow Corning Sylgard 184 with SU-8 or polystyrene molds. Channels were 5 mm wide, 15 mm long, and 600 mm in height. A fluidic inlet compatible with 20 gage Teflon tubing was punched using an 18 gage blunt-tipped needle, and a 5 mm diameter outlet reservoir was punched on the other end. PDMS channels were cleaned with a UV/ozone system for 10 min, and then applied to the device. The channels were filled with DI water for 1 h to allow hydration of the iridium oxide layer, then the pH response of the electrodes was calibrated using standard pH 4, 5, 7 and 10 buffers. The channel was maintained at 37 °C using a heated aluminum stage with a MinCO polyimide heater and Cole-Parmer DigiSense PID temperature controller.

Cell preparation and labeling.

Jurkat cells were cultured in RPMI-1640 media with 10% fetal bovine serum (FBS) and 1% penicillin-streptomycin solution. Cultured cells were maintained at 37 °C in 5% CO_2, and split 1:10 every 2-3 days. Cell acidification experiments were conducted in custom low-buffered media bases on Dulbecco's Modified Eagle's Medium, containing 25 mM D-glucose, 5.3 mM KCl, and 110.34 mM NaCl, plus 1% FBS. Finally, the media was pH adjusted to 7.45 using 0.1 M NaOH. Primary T cells were the generous gift of Nina Hartman (Jay Groves lab, UC Berkeley Chemistry). Cells were isolated from mice and prepared as previously described.[27]

Cell-surface labeling with ssDNA was achieved using an NHS-DNA conjugate that covalently modifies primary amines on the cell surface (Figure 4E), as described in chapter 1.[28] Briefly, cells were incubated in a 10 μM NHS-DNA solution in PBS at room temperature for 30 min, then washed three times to remove any unbound DNA. Barcode-specific cell capture was tested with spotted DNA microarray slides as previously reported.[2]

Metabolic monitoring.

Cells were suspended at a concentration of 10^6 /ml, and the suspension was flowed into the microfluidic device. Cell suspensions were flowed into the channel using 1 mL syringes with Teflon tubing. Where Jurkat and primary T cells were monitored simultaneously they were labeled with CellTracker Green and Red dyes, respectively, as previously described and mixed in an equal ratio. Following a 5 min incubation to allow DNA-based cell capture, the unbound cells were rinsed away (5 ml/min for 3 min) with the low-buffered media. After rinsing, the pH response was monitored electrochemically for 10 min. After this recording, cells were released from the electrodes by heating the device to 55 °C and applying a strong rinse (200 μL/min) with the low-buffered media. Once rinsed and allowed to return to 37 °C, the device

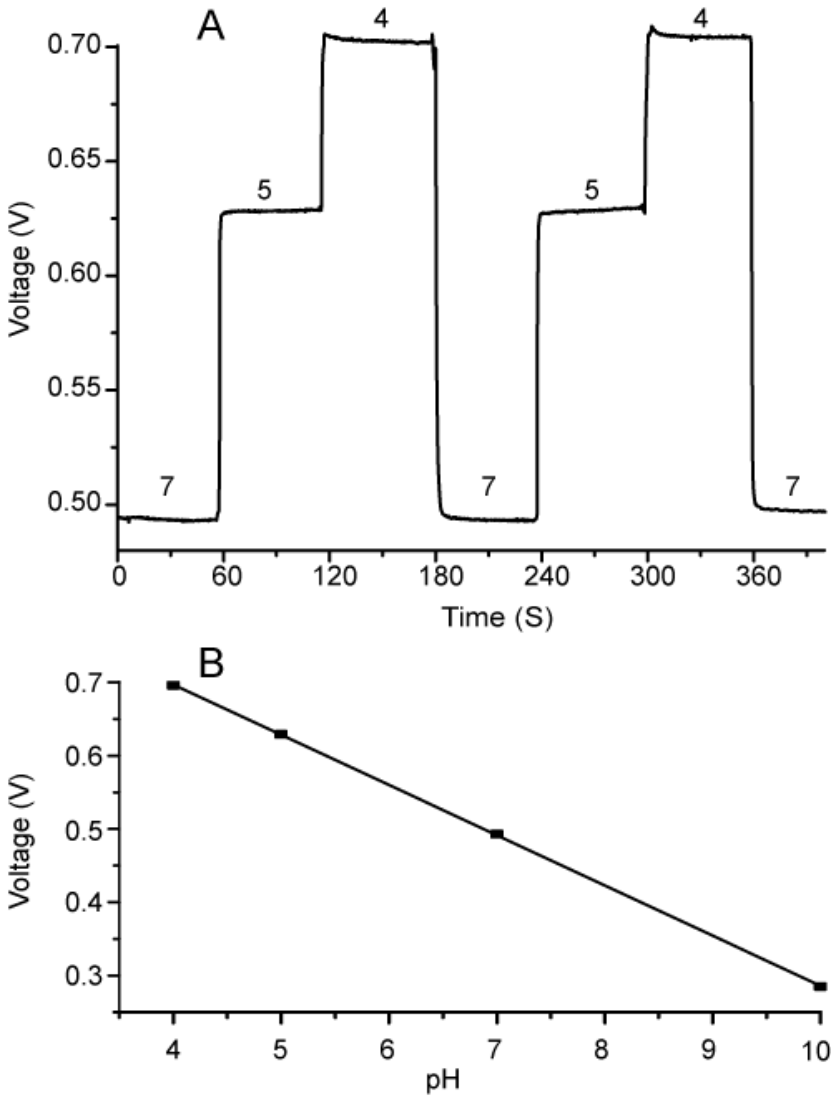

Figure 5. Calibration data for the bifunctional microelectrode array. (A) Typical calibration recording for one DNA-modified iridium oxide sensor using standard pH 4, 5 and 7 buffers. Voltage is measured relative to an Ag/AgCl reference electrode. (B) Plot of the voltage vs. pH standard measurement with a slope of -68.5 mV/pH unit and R2=0.99995.

could be reloaded with cells. This allowed for multiple measurements to be taken with a single cell preparation.

Voltage measurements were recorded between the iridium oxide electrode and a distant FLEXREF Ag/AgCl reference electrode from World Precision Instruments. An identical iridium oxide electrode outside the cell area was used to compensate for any sensor drift. The sensor electrodes were connected to a National Instruments PCI-6031E data acquisition card with 16 bit analog to digital conversion. The digitized signals were monitored using a custom Labview VI, sampling in multiplex at 3 hz. Voltage signals were processed with a 1% Loess filter using Peak Fit software to reduce noise.

Before metabolic analysis, the electrodes were characterized using standard pH buffers (Fig. 5). These DNA-modified electrodes were found to retain their pH sensitivity, with performance comparable to unmodified iridium oxide sensors. The electrode response was stable and fast, responding to a 1 pH unit change in under 500 ms. The pH response of the electrodes was typically -68.5 mV per pH unit, with a linear response over the range of pH 4 to 10. The typical range for cell acidification measurements is approximately 6.5 to 7.5, so this sensor is well suited for these types of measurements. The magnitude of the observed response is in line with the -60 to -80 mV/pH range of other hydrated iridium oxide sensors previously demonstrated.[29-31] The reaction at the electrode that provides the pH sensitivity has been described by Olthuis *et al*.[32] The -60 to -80 mV/pH sensitivity range is dependent on the oxidation state of the iridium oxide film, as deposited by various electrochemical techniques.

References

1. J. El-Ali, P. K. Sorger and K. F. Jensen, *Nature*, 2006, **442**, 403-411.
2. E. S. Douglas, R. A. Chandra, C. R. Bertozzi, R. A. Mathies and M. B. Francis, *Lab Chip*, 2007, **7**, 1442-1448.
3. R. A. Chandra, E. S. Douglas, R. A. Mathies, C. R. Bertozzi and M. B. Francis, *Angew. Chem.-Int. Edit.*, 2006, **45**, 896-901.
4. N. M. D. Toriello, E. S.; Thaitrong, N.; Hsaio, S.C.; Bertozzi, C.R.; Francis, M.B.; Mathies, R. A., *Submitted*, 2008.
5. F. Hafner, *Biosens. Bioelectron.*, 2000, **15**, 149-158.
6. P. Montcourrier, I. Silver, R. Farnoud, I. Bird and H. Rochefort, *Clin. Exp. Metastasis*, 1997, **15**, 382-392.
7. D. Di Carlo, N. Aghdam and L. P. Lee, *Anal. Chem.*, 2006, **78**, 4925-4930.
8. J. Voldman, *Annu. Rev. Biomed. Eng.*, 2006, **8**, 425-454.
9. S. Nagrath, L. V. Sequist, S. Maheswaran, D. W. Bell, D. Irimia, L. Ulkus, M. R. Smith, E. L. Kwak, S. Digumarthy, A. Muzikansky, P. Ryan, U. J. Balis, R. G. Tompkins, D. A. Haber and M. Toner, *Nature*, 2007, **450**, 1235-U1210.
10. D. S. Chen and M. M. Davis, *Curr. Opin. Chem. Biol.*, 2006, **10**, 28-34.
11. A. M. P. Turner, N. Dowell, S. W. P. Turner, L. Kam, M. Isaacson, J. N. Turner, H. G. Craighead and W. Shain, *J. Biomed. Mater. Res.*, 2000, **51**, 430-441.
12. A. F. Dias, G. Dernick, V. Valero, M. G. Yong, C. D. James, H. G. Craighead and M. Lindau, *Nanotechnology*, 2002, **13**, 285-289.
13. H. M. McConnell, J. C. Owicki, J. W. Parce, D. L. Miller, G. T. Baxter, H.

G. Wada and S. Pitchford, *Science*, 1992, **257**, 1906-1912.

14. K. Wille, L. A. Paige and A. J. Higgins, *Recept. Channels*, 2003, **9**, 125-131.

15. I. A. Ges, I. A. Dzhura and F. J. Baudenbacher, *Biomed. Microdevices*, 2008, **10**, 347-354.

16. N. M. Toriello, E. S. Douglas and R. A. Mathies, *Anal. Chem.*, 2005, **77**, 6935-6941.

17. K. Yamanaka, *Jpn. J. Appl. Phys.*, 1989, **28**, 632-637.

18. B. L. Jackson and J. T. Groves, *Langmuir*, 2007, **23**, 2052-2057.

19. A. L. DeMond, K. D. Mossman, T. Starr, M. L. Dustin and J. T. Groves, *Biophysical J.*, 2008, **94**, 3286-3292.

20. S. C. Hsiao, B. J. Shum, H. Onoe, E. S. Douglas, Z. Gartner, R. A. Mathies, C. R. Bertozzi and M. B. Francis, *Submitted*, 2008.

21. H. A. Elsen, K. Slowinska, E. Hull and M. Majda, *Anal. Chem.*, 2006, **78**, 6356-6363.

22. S. A. M. Marzouk, R. P. Buck, L. A. Dunlap, T. A. Johnson and W. E. Cascio, *Anal. Biochem.*, 2002, **308**, 52-60.

23. S. A. M. Marzouk, S. Ufer, R. P. Buck, T. A. Johnson, L. A. Dunlap and W. E. Cascio, *Anal. Chem.*, 1998, **70**, 5054-5061.

24. W. Olthuis, M. A. M. Robben, P. Bergveld, M. Bos and W. E. Vanderlinden, *Sens. Actuators B-Chem.*, 1990, **2**, 247-256.

25. L. J. Mandel, *Current Topics in Membranes and Transport*, 1986, **27**, 261-291.

26. R. Gebhardt, P. Bellemann and D. Mecke, *Exp. Cell Res.*, 1978, **112**, 431-441.

27. K. L. Tsai, S. M. Wang, C. C. Chen, T. H. Fong and M. L. Wu, *J. Physiol.-London*, 1997, **502**, 161-174.

28. M. F. Renschler, H. G. Wada, K. S. Fok and R. Levy, *Cancer Res.*, 1995, **55**, 5642-5647.

29. M. Castellarnau, N. Zine, J. Bausells, C. Madrid, A. Juarez, J. Samitier and A. Errachid, *Sens. Actuators B-Chem.*, 2007, **120**, 615-620.

30. S. E. Eklund, D. Taylor, E. Kozlov, A. Prokop and D. E. Cliffel, *Anal. Chem.*, 2004, **76**, 519-527.

31. S. A. Thayer, M. Sturek and R. J. Miller, *Pflugers Arch.*, 1988, **412**, 216-223.

32. B. Hoang and A. Chiba, *Dev. Biol.*, 2001, **229**, 55-70.

\Chapter 4: DNA-coated AFM cantilevers for the investigation of cell adhesion and the patterning of live cells

INTRODUCTION

The forces governing cell-cell adhesion are vitally important to many biological processes, including cell differentiation, tissue growth,[1,2] tumorigenesis,[1,3] and proper functioning of the vertebrate immune response.[4,5] Typically, the strengths of these interactions are characterized through the attachment of single living cells to probes that are capable of force measurement. For example, individual cells have been grasped by suction using micropipettes[6,7] to quantify the strength of lymphocyte interactions. However, this manipulation process can easily damage the cell membrane, and it does not adequately decouple the adhesion forces of interest from technique artifacts. More recently, optical tweezers[8,9] have been applied to capture single cells and measure these forces with added accuracy, but this technique is limited to applying forces in the piconewton range.[10] Alternatively, atomic force microscopy (AFM),[11] which is capable of quantifying forces on the piconewton to nanonewton range, has been used to measure the mechanical properties of live single cells[12] and study adhesion forces at the single cell level.[13-18] In these studies, the AFM cantilevers were first coated with lectins, including wheatgerm agglutinin (WGA)[18] and concanavalin A (ConA),[13] that bind to carbohydrate moieties on the cell surface. Several fundamental adhesion measurements have been achieved using this method[14,16,17]. However, both WGA[19] and ConA[17,20,21] have been reported to have a degree of cytotoxicity that can influence the cellular properties being evaluated, and as reported these methods rely on non-specific protein absorption onto the AFM cantilever. While these studies highlight the utility of AFM for the measurement of cell receptor-ligand interactions, an expanded set of cantilever attachment methods will be needed to realize the full potential of this technique, especially in the context of time-dependent cell-cell interactions.

To address this, we report herein the application of a DNA-mediated cell adhesion platform for the efficient attachment of live cells to AFM cantilevers (Figure 1). We have found that cell viability is largely unaffected by the DNA anchoring technique, and as this method appears not to activate cell signalling pathways, it enables longer timescale measurements. We have also characterized the adhesion force between the cell and the cantilever and compared this with two protein-based immobilization strategies. Finally, by applying shorter DNA strands (13 bases) on a cantilever and longer strands (20 bases) on the surface of a glass slide, we were able to pick up free cells and transfer them to the substrate at exact positions. This “Dip-Pen” live cell patterning demonstrates the tunability and reusability of the DNA-mediated cell adhesion method, which could prove useful for the construction of complex mixtures of cells with well-defined spatial characteristics.

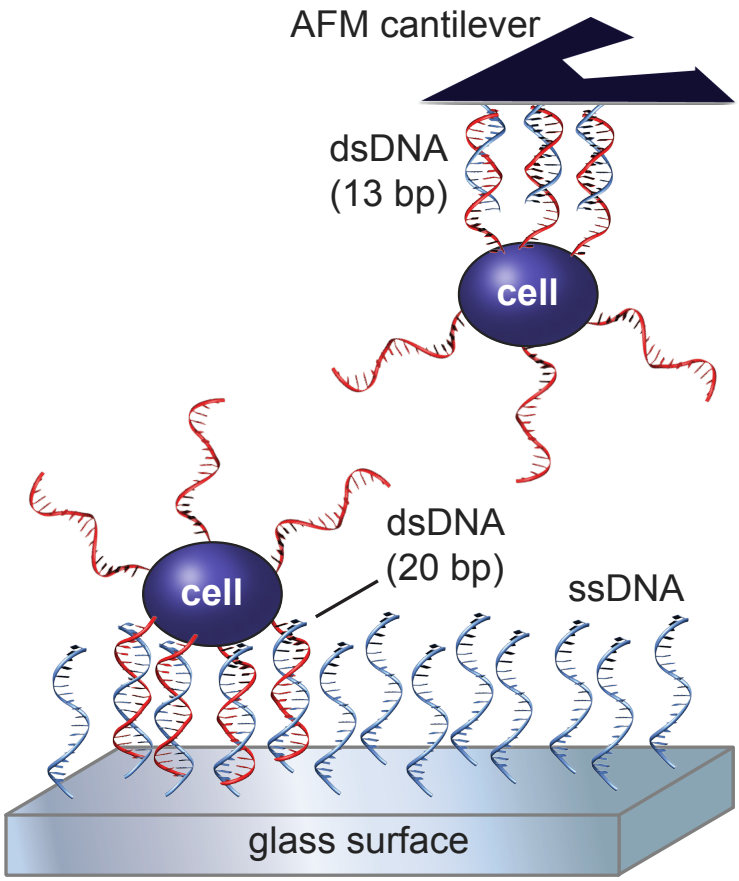

Figure 1. The model of DNA mediated cell adhesion. Cells were attached to AFM cantilever modified with shorter (13bp) DNA strands. Cells could be transfered to glass slided modified with longer (20bp) DNA strands.

RESULTS

Attachment of biomolecules to cantilevers and glass slides

Three different biomolecules, including DNA, concanavalin A, and antibodies, were attached to the cantilevers to anchor mammalian cells. For all attachment methods, the thin layer of silicon oxide on the working surface of the silicon nitride AFM cantilever was first cleaned using oxygen plasma to maximize the number of hydroxyl functional groups. Trimethoxysilylpropanal was then coupled to the cantilever by chemical vapor deposition (CVD) to yield a surface covered with aldehydes (Figure 2a). The surfaces produced using these steps were characterized by contact angle measurement (Figure 3). In more than 50 separate experiments, this two-step modification process has provided a reproducible way to introduce aldehyde functional groups onto cantilever surfaces.

Amine functionalized DNA was attached to the aldehyde groups through

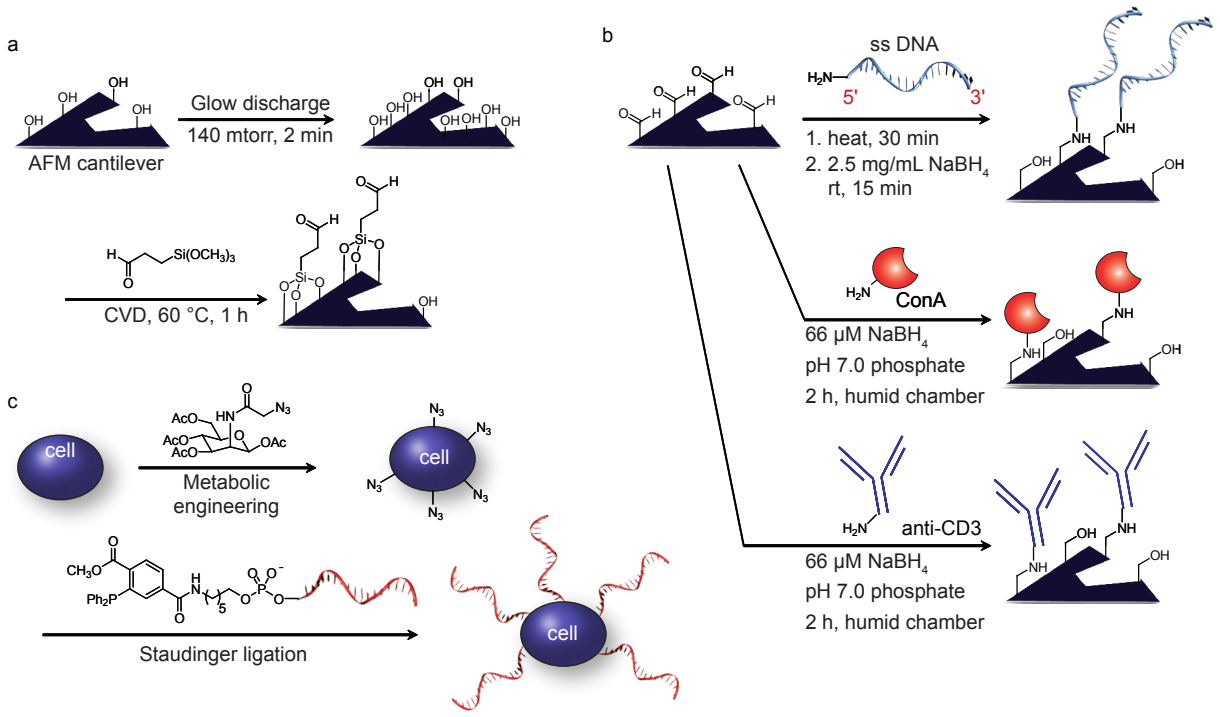

Figure 2. Covalent attachment of biomolecules to cantilevers and cell surfaces. (a) After surface oxidation using an oxygen plasma, aldehyde functional groups were introduced onto silicon nitride cantilevers using chemical vapor deposition (CVD). (b) Solutions of anti-CD3 IgG or ConA containing sodium borohydride were introduced onto aldehyde-coated cantilever surfaces in a humid chamber. DNA modification was achieved by immersing cantilevers in an amine functionalized ssDNA solution at 100 °C for 30 min, followed by exposure to a sodium borohydride solution. (c) Metabolic engineering was used to introduce azide groups onto cell surfaces via treatment with peracetylated-*N*-azidoacetylmannosamine (Ac_4ManNAz). Phosphine functionalized ssDNAs were synthesized and covalently attached to the exterior of cells via the Staudinger ligation.

reductive amination (Figure 2b).[22,23] First, the aldehyde-coated cantilever was immersed in an amine functionalized single-strand DNA (ssDNA) solution and then heated to drive imine formation. After cooling to room temperature, an aqueous solution of sodium borohydride was used to reduce the imines to non-hydrolyzable amine linkages. This step also served to reduce any unreacted aldehyde functional groups to yield alcohols. By coupling 5'-amine functionalized DNA strands bearing fluorescein at the 3'-end, the presence of the strands could be verified by fluorescence imaging.

In previous efforts, proteins have been attached to AFM tips through non-specific adsorption and through glutaraldehyde crosslinking to amine groups introduced on the tip surface.[24] To afford more well-defined linkages (and thus realize more homogeneous cell attachment), we chose instead to use the simple reductive amination strategy that was used for the amino-DNA strands. Surface lysine residues on ConA and anti-human CD3 antibodies (anti-CD3) were reacted with the aldehyde functional groups on the cantilever surfaces (Figure 2b),[25] but a lower concentration of reducing agent was used to minimize the reduction of disulfide bonds that are

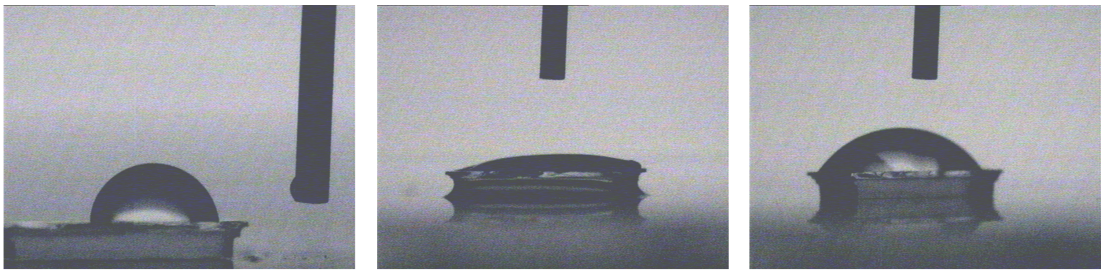

Unmodified Si_3N_4 Lever | Glow Discharged | CVD (Aldehyde)

	Before Modification	Glow Discharged	CVD (Aldehyde)
Cantilevers	80.8 ± 3.5 °	14.7 ± 3.7 °	52.4 ± 3.5 °
		Unmodified SiO_2	Aldehyde Coated
Glass Slides		0.3 ± 0.4 °	50.0 ± 3.7 °

Figure 3. Contact angle measurements of silicon nitride cantilever surfaces. From left to right, the three pictures depict contact angle measurements of the cantilevers before modification, after glow discharge, and after CVD modification. The table lists the contact angles of the coated cantilevers and analogous glass slides.

required to maintain protein tertiary structure. Various concentrations of sodium cyanoborohydride and sodium borohydride were evaluated at pH 8.4 and 7.0, with the conditions of 66 μM $NaBH_4$ at pH 7 yielding optimal coupling efficiency as judged by a cell binding assay (see below). As described above for DNA, FITC-labeled ConA and anti-CD3 samples were used in some experiments to verify biomolecule attachment using fluorescence microscopy. Even after immersing the FITC-labeled DNA, ConA, and antibody coated surfaces in water for seven days, the fluorescence intensity was unchanged. This indicated that the linkage anchoring these molecules to the surface was stable toward hydrolysis.

Comparison of different cell attachment technology

Because the work in this chapter was done in parallel with the NHS-DNA cell adhesion technique described in chapter 1, we applied the previous method to introduced ssDNAs on glycoproteins embedded in the plasma membrane.[26] Peracetylated *N*-a-azidoacetylmannosamine (Ac_4ManNAz) was added to cells, which then metabolized and displayed the azide on their surfaces (Figure 2c).[27] Triarylphosphine-modified ssDNA was prepared through the reaction of 5'-amine-modified ssDNA with a phosphine pentafluorophenyl (PFP) ester. This reagent was then used to label the cell-surface azides through a Staudinger ligation,[28] yielding stable amide linkages. Flow cytometry experiments have previously verified the ability

of phosphine-DNA conjugates to undergo ligation to azide-modified cell surfaces.[26]

To facilitate cell binding efficiency assays, reductive amination procedures analogous to those described above were also used to coat commercially available aldehyde-coated glass slides with the same set of biomolecules. The efficiency of cell capture was evaluated by exposing DNA-coated Jurkat cells to glass slides coated with complementary sequences of DNA. Similarly, unmodified cells were added to glass surfaces coated with either ConA or anti-CD3 antibodies. Comparison of the cell capture efficiencies of these three cell-adhesion methods was achieved by counting the number of cells per unit area on the coated surfaces (Figure 4b). All three surfaces were able to achieve efficient cell binding, with the DNA-based system showing the highest coverage for cell capture (cell density = 1200 cells/mm^2). Cells did not adhere to slides lacking the biomolecules. The DNA-conjugated cells appeared morphologically unchanged when observed after 48 hours of binding, whereas the ConA- and anti-

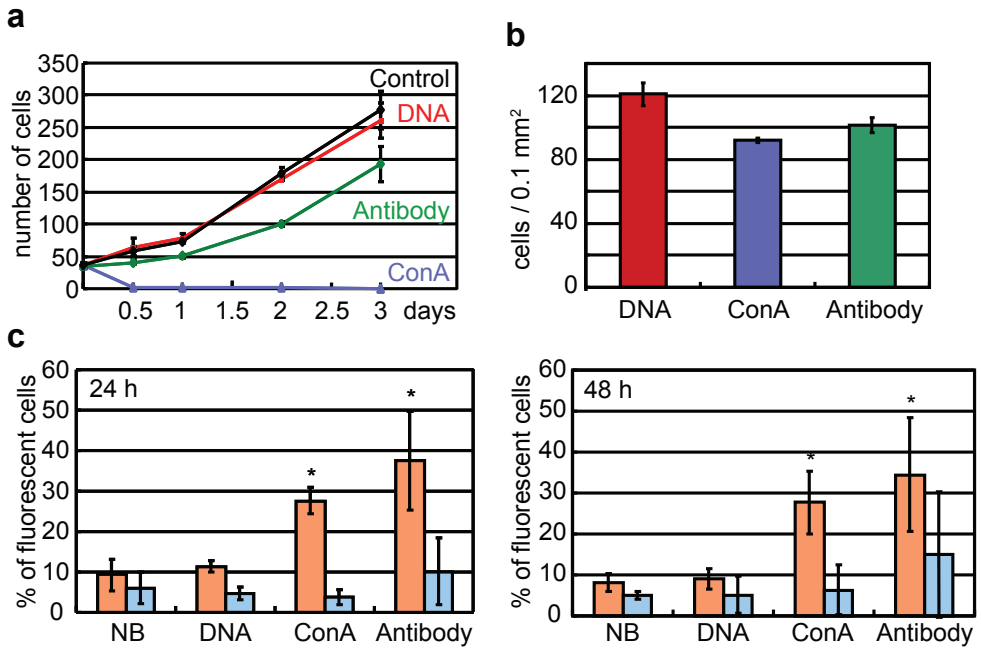

Figure 4. Comparison of biomolecule based adhesion methods. (a) Bulk cell growth rates were first determined in the presence of the adhesion molecules. A suspension of Jurkat cells was combined with ConA or anti-CD3 IgG, and a solution of DNA coated cells was combined with the complementary DNA strands. At various time points the total number of cells was counted. The control sample was grown in the absence of any adhesion molecules. (b) To evaluate cell capture efficiency, solutions of 20 μM FITC-labeled ssDNA, 20 μM FITC-labeled ConA, and 6 μM FITC-labeled anti-CD3 IgG were applied to aldhyde-coated glass slides and the biomolecules were attached via reductive amination. Solutions containing 1x10^7 Jurkat cell/mL were then introduced onto the resulting slides. The samples were incubated for 10 min at room temperature, and then washed with two portions of PBS before evaluation. (c) To evaluate cell viability, cells were immobilized on DNA, ConA, and anti-CD3 IgG coated aldehyde slides. After immobilization for 24 h and 48 h, the cells was incubated with a solution of annexin V-FITC (orange bars) and PI (blue bars). The cells were evaluated within 1 h by fluorescence microscopy. *ConA and antibody immobilized cells that were partially stained by annexin were counted as cells undergoing apoptosis. NB represents control samples that were not bound to the surfaces.

CD3-immobilized cells exhibited significant changes during this time period (Figure 5).

The effects of the adhesion molecules on the viability of the cells were assessed using two different methods. First, suspensions of unmodified Jurkat cells were supplemented with ConA or anti-CD3 antibodies, and the solutions of DNA-coated cells were supplemented with the complementary sequence. Figure 4a shows the growth curves of the resulting cells over a three day period. The growth curve of DNA modified cells was the same as that of unmodified cells, but the anti-CD3 treated cells showed delayed growth. ConA coated cells aggregated and were no longer alive after 12 hours.

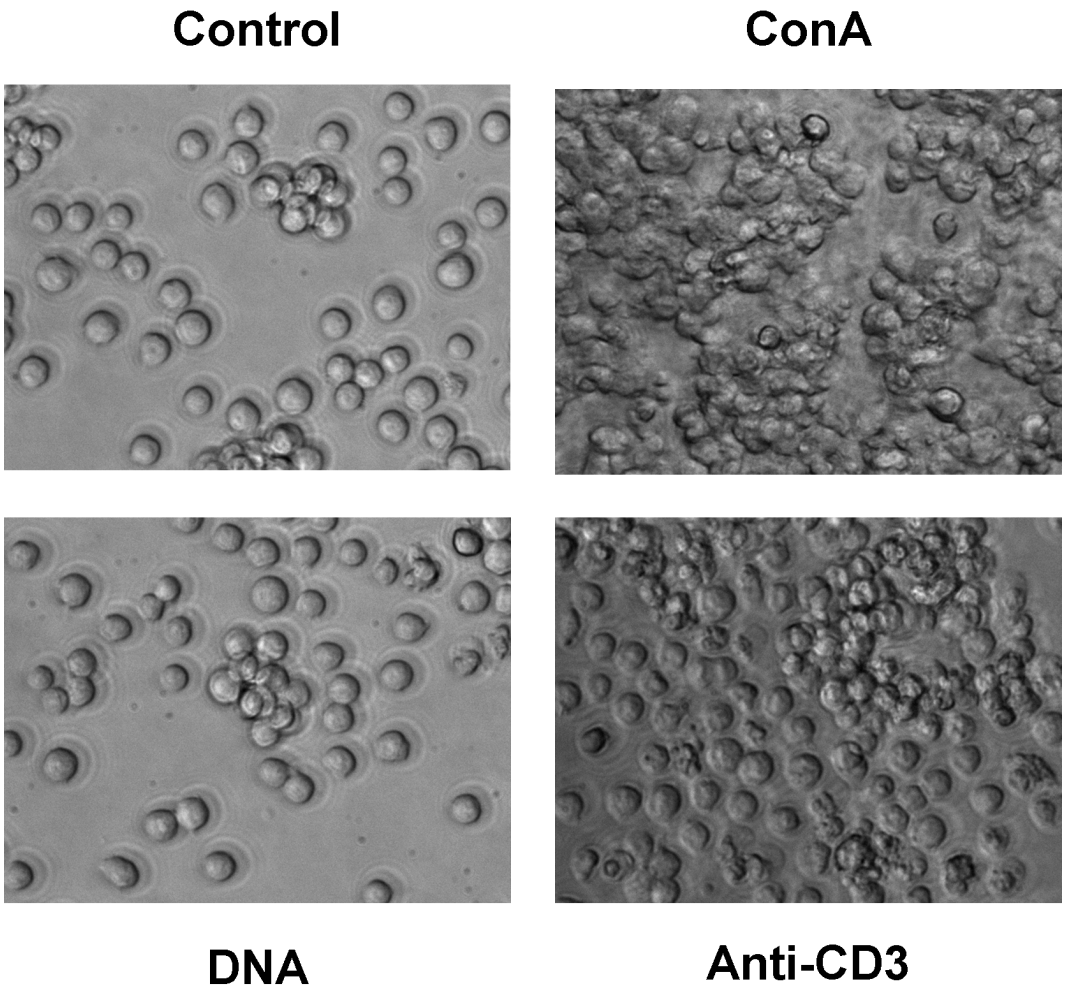

Figure 5. Cell morphology changes induced by soluble biomolecules. Jurkat cells were grown in normal media (Control), DNA-modified Jurkat cells were grown in the presence of 10 μM DNA, and unmodified Jurkat cells were grown in the presence of 10 μM ConA or 1 mg/mL Anti-CD3. The resulting cells were examined under a light microscope after a period of 12 h. The appearance of the cells was largely unchanged in the presence of DNA, but cells grown in the presence of ConA and Anti-CD3 exhibited aggregation and other morphological changes.

The viability of surface-immobilized cells was also investigated using fluorescent staining agents. Cells were immobilized on DNA, ConA, and anti-CD3 coated slides as described above. After immobilization for 24 h and 48 h, the cells were incubated with FITC-labeled annexin V and propidium iodide (PI) solutions.[29] It has been shown that cells actively undergoing apoptosis stain positively with annexin V but not with propidium iodide (PI), whereas dead or necrotic cells stain with both reagents. For the DNA-immobilized cells, the low percentage of apoptotic and necrotic cells was similar to that of unmodified cells (Figure 4c). However, the ConA and Anti-CD3 immobilized cells show significantly higher numbers of apoptotic cells compared to the control samples.

Cell adhesion force measurement

The strength of the interaction between the cell and the cantilever fundamentally limits the range of forces that can be measured when other surfaces are brought into contact with the receptors. Our assay to measure the strength of this interaction was designed such that cell-cantilever adhesions were fewer in number, and therefore weaker overall, than DNA-based adhesions between a cell and the complementarily functionalized glass slide. Due to this arrangement the cell-cantilever interaction would be expected to rupture first, yielding the strength of the interaction that a relatively low concentration of biomolecules can achieve. Rupture of the cell-cantilever interaction before the cell-surface interaction was verified by visual observation during experiments. The force of de-adhesion was measured for

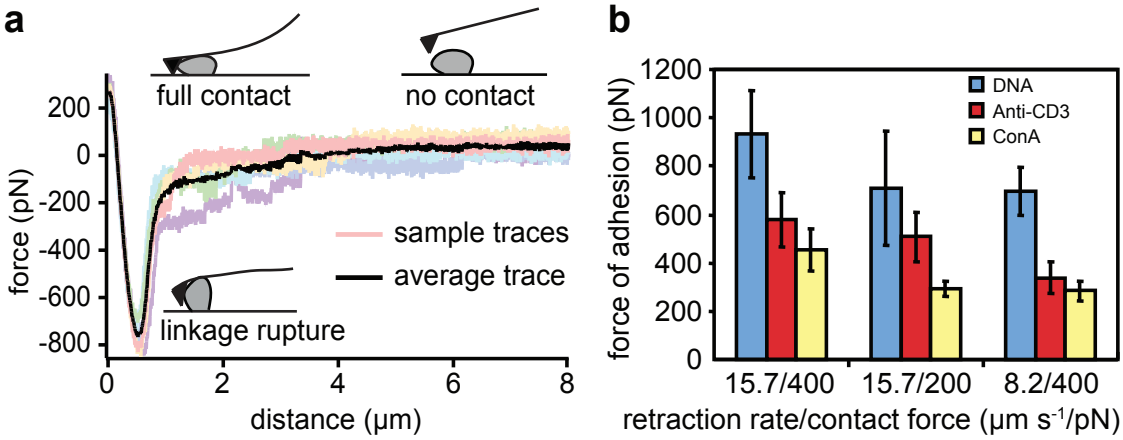

Figure 6. AFM measurement of de-adhesion force. (a) Six sample traces for a single cell are shown in lighter colors, with the average trace shown in black. At zero distance, the cell is in full contact with the cantilever that is applying a positive force. As distance increases, the cantilever is pulled away from the glass slide surface, causing the cell-cantilever linkage to rupture and result in the zero-force, no-contact region. The force of de-adhesion was calculated as the difference between the curve minimum and the horizontal no-contact region. (b) Adhesion forces were measured under different retraction rates (15.7 μm/s and 8.2 μm/s) and contact forces (400 pN and 200 pN) for the DNA, ConA, and antibody systems. Data were obtained by measuring six de-adhesion events on more than four different cells.

each attachment method using two different retraction rates and two different contact forces (Figure 6a). The measured force of de-adhesion increased with contact force and retraction rate across all attachment methods, as predicted by the Bell model.[30] The ConA attachment method yielded zero force attachment events in 12% of the de-adhesion measurements. Such events were not observed in the DNA and antibody cases. A significant spread of forces was observed for all three attachment methods; however under all experimental parameters, the DNA method displayed the strongest average adhesion, followed by antibody attachment, then ConA (Figure 6b). As a control experiment, we have also demonstrated that the capture efficiency of ConA and Anti-CD3 is not affected by the presence of DNA strands introduced on the cell surface (Figure 7). It should be noted that de-adhesion forces determined for each attachment strategy will depend on the details of the preparation conditions, and therefore should not be taken as absolute measurements. Nonetheless, the trends demonstrate that under typical preparation conditions the DNA hybridization method will lead to the most robust attachment.

Direct Patterning of cells on a surface

The strength of the cell-cantilever interaction can be tuned by varying the number of interacting strands and the length of the complementary regions. The reversibility of DNA hybridization also allows the tips to be used many times. Both of these advantages allowed us to use AFM tips to arrange cells one at a time into patterns.

To do this, a 5 μM solution of a shorter DNA strand (13 bases) was applied

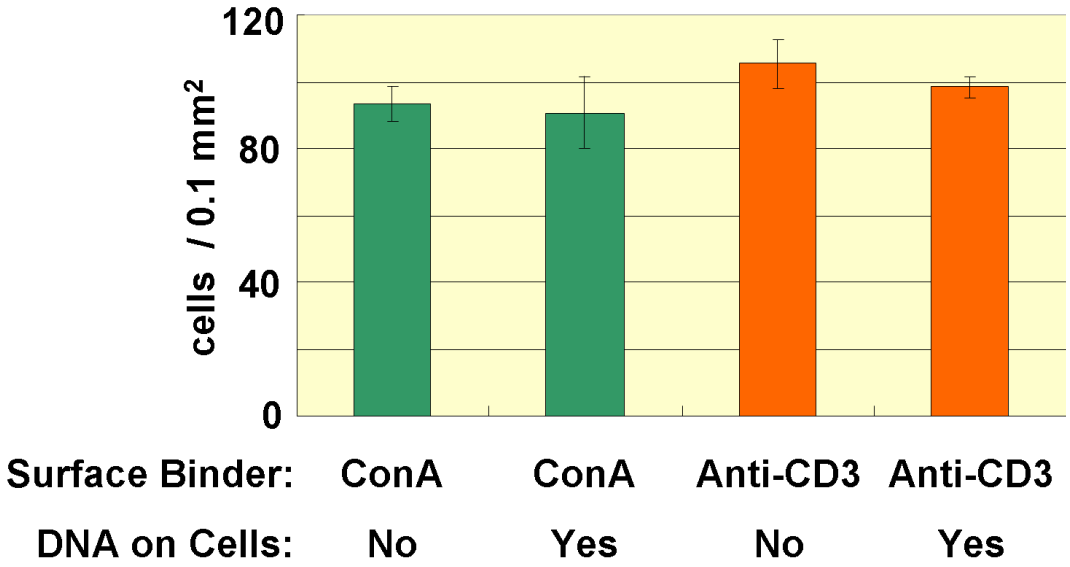

Figure 7. Cell capture efficiency of DNA-modified cells and unmodified cells on ConA and Anti-CD3 coated surfaces. No statistical differences in binding were observed, as indicated by a T-test. This suggests that the attachment of DNA molecules to the cell surface does not block receptor access.

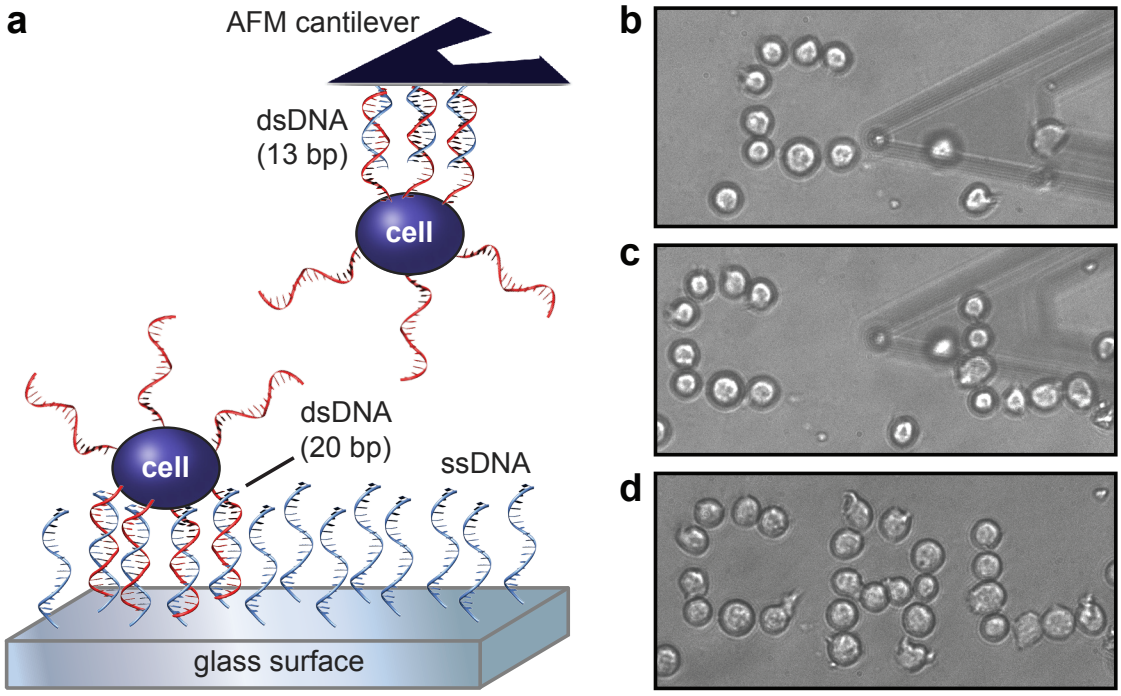

Figure 8. Dip-Pen patterning of live cells. (a) By attaching a shorter DNA strand (13 bases) to a cantilever and a longer strand (20 bases) to the glass slide, a single living cell can be transported by the AFM and directly printed at a desired location on the glass slide. This process is shown stepwise for the formation of a single pattern of cells in b-d.

to the cantilever and an 80 μM solution of a longer strand (20 bases) was coupled to the glass slide. DNA-coated Jurkat cells were incubated in CO_2 independent media and applied to the non-coated side of glass slide under an AFM. To attach a cell to the modified cantilever, the cantilever was lowered into contact with the cell for 10 seconds with a contact force of 400 pN. The cantilever was then retracted, and cell attachment to the cantilever was confirmed visually. The attached cells were then moved to the DNA coated side with maximum rate of 1 mm/s. The cantilever was lowered into contact with the slide, and the cell was allowed to interact with the substrate for 10 sec with a 400 pN contact force. The cantilever was then retracted, whereupon the cell remained attached to the glass slide. By applying this printing method, cells can be given an (x,y) coordinate to position them precisely on a 2D substrate (Figure 8). The cells were found to remain viable after patterning, as shown in Figure 9.

DISCUSSION

In developing this platform, we have demonstrated the covalent attachment of DNA, lectins and antibodies to AFM cantilevers by an efficient reductive amination procedure. This method should provide uniform distributions of DNA molecules.

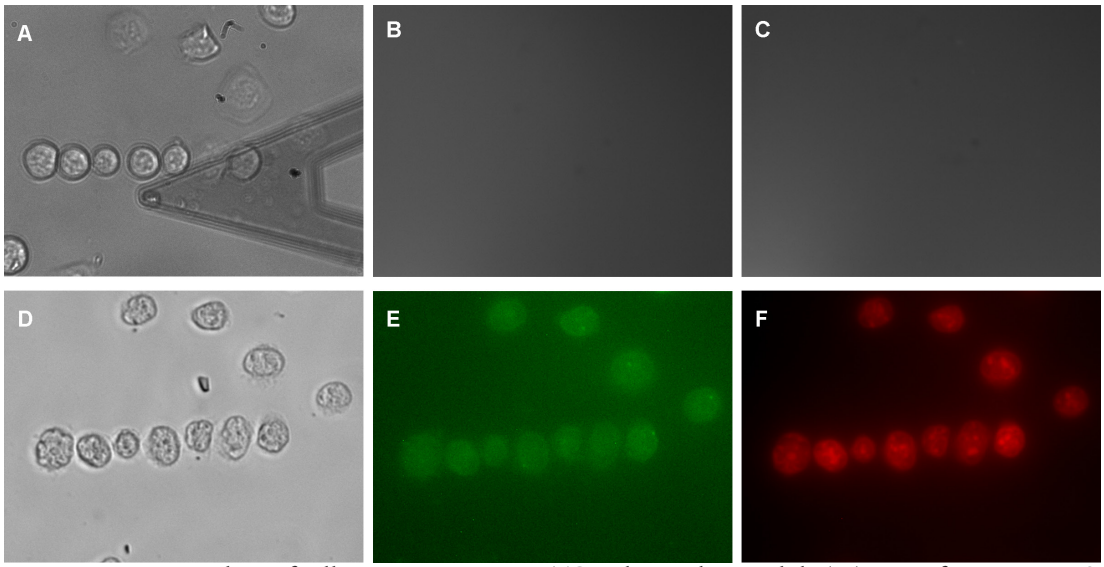

Figure 9. Post-patterning analysis of cells using annexin V-FITC and propidium iodide (PI) assays for apoptosis. Seven cells were positioned by Dip-Pen patterning and then incubated at rt for 3 h before staining. (A) DIC image of the cells after this procedure. (B) Fluorescence image (fluorescein filter set) of the cells after exposure to annexin V-FITC. (C) Fluorescence image (rhodamine filter set) of the cells after PI staining. No signal was observed in either (B) or (C), indicating that the Dip Pen process did not induce apoptosis. (D-F) As positive controls, the apoptosis was induced by incubation with 30% ethanol for 5 min. (E) was taken with a fluorescein filter, and (F) was taken using a rhodamine filter.

Although there are multiple lysine residues on the proteins, we anticipate that they will be attached in a more homogeneous fashion than in cases where non-specific adsorption or crosslinking methods are used. This method is also likely to be quite general, as virtually all proteins possess lysine residues on their surface. In preliminary experiments, this covalent attachment technique has been used to conjugate phytohemagglutinin (PHA) and fibronectin to the cantilever surface with equivalent success.

Although many cell types would be expected to be compatible with this system (and have been explored previously using the DNA-based adhesion method)[26], non-adherent Jurkat cells were chosen for these studies because they do not secrete their own extracellular matrix. Thus, all cell adhesion events arise solely from the biomolecules on their surfaces. According to our viability assays, the DNA-based adhesion method has a lesser effect on cell proliferation, and DNA based cell adhesion does not appreciably affect cell viability. The aggregation and physiological changes of the free cells after adding the ConA are likely due to crosslinking by the four carbohydrate binding sites of the protein, as would be expected by its mitogenic nature[31]. The morphology changes and the early apoptosis of Anti-CD3 immobilized cells are also likely due to receptor dimerization[32]. In other studies, both ConA and Anti-CD3 have been shown to bind to CD3 receptors on the cell surface and activate the immune response of human T cells[33]. In contrast, the DNA molecules appear only to hybridize with their complementary partners, and do not activate any signalling pathways that would disturb the physiology of the cells.

All three attachment methods proved to be reusable for six de-adhesion events on multiple cells, even though the ConA attachment method did display zero-force events in 12% of the measurements. For a given cell, all six de-adhesion measurements were consistent, but somewhat different values were obtained between individual cells. This is likely due to differences in the cell-cantilever contact surface area and ligand orientation. For applications in which cantilever-bound cells are brought into contact with other surfaces of interest, the linkages binding the cell to the cantilever must be stronger than those of the cell with the target surface to allow measurement. While all three attachment methods yielded adhesion forces in the same general range, the consistently stronger behavior of the DNA-based system over a range of experimental parameters suggests that this method of attachment will be superior for measuring larger adhesion forces.

The use of AFM to form accurate and programmable patterns of individual cells provides a useful tool that can be used to understand the influence of neighboring interactions on cell differentiation and regulation. These factors are inherently involved in embryonic development and tissue engineering. In a previous report, we have shown that complex patterns can be prepared through the self-assembly of DNA-coated cells on surfaces printed with complementary oligonucleotides[34]. The AFM dip-pen method described here provides a useful complement to this technique that can achieve the higher resolution that would be needed to create and interrogate clusters consisting of multiple cell types. In a very recent report[35], it was shown that individual DNA strands could be moved from one location to another on a printed substrate, allowing small molecule dyes to be printed in a similar fashion.

In summary, we have described the development of a new tool for the study of cell-cell interactions by AFM. The key advantage of this platform is the modularity and tunability of the biomolecule attachment and the use of well-defined chemical linkages. Of the three biomolecule-based attachment strategies that were used, the DNA method proved superior in terms of viability, strength, and reusability. Precise control over the spatial and temporal positioning of single cells enables this DNA-mediated AFM cell manipulator to be used for direct cell patterning and adhesion force measurement studies that cannot be carried out in bulk solution. Further experiments will involve using this method to elucidate fundamental adhesion mechanisms involved in cancer metastasis and immunology, as well as other biologically relevant phenomena.

CONCLUSION

In summary, we have described the development of a versatile DNA-based adhesion method for the study of cell-cell interactions by AFM. The key advantages of this platform include the reusability of the tip, the tunability of the interaction strength, and the use of well-defined chemical linkages. Of the three biomolecule-based attachment strategies that were used, the DNA method proved superior in terms of cell viability after attachment. The use of AFM to form accurate and

programmable patterns of individual cells provides a useful tool that can be used to understand the influence of neighboring interactions on cell differentiation and regulation. In a previous report, we have shown that complex patterns can be prepared through the self-assembly of DNA-coated cells on surfaces printed with complementary oligonucleotides. The AFM dip-pen method described here provides a useful complement to this technique that can achieve the higher resolution that would be needed to create and interrogate clusters consisting of multiple cell types. We are currently using this method to elucidate fundamental adhesion mechanisms involved in cancer metastasis, immune synapse formation, and cell-cell communication.

MATERIALS AND METHODS

General Experimental Procedures

All cell culture reagents were obtained from Gibco/Invitrogen Corp (Carlsbad, CA) unless otherwise noted. Cell culture was conducted using standard techniques. Jurkat cells were grown in T-25 culture flasks (Corning, USA) in RPMI Medium 1640 supplemented with 10% (v/v) fetal bovine serum (FBS, HyClone) and 1% penicillin/streptomycin (P/S, Sigma).

All oligonucleotides were obtained from Integrated DNA Technologies (Coralville, IA). Concanavalin A and FITC-labeled concanavalin A were purchased from Sigma (St. Louis, MO). Anti-human CD3 IgG (UCHT1) and FITC-anti-human CD3 IgG (UCHT1) were obtained from eBioscience (San Diego, CA).

Fluorescence micrographs were acquired with an Axiovert 200M inverted microscope (ZEISS) with fluorescence filter sets for DAPI/Hoechst, fluoroscein/fluo-3, and rhodamine. Ultraviolet absorption of the different oligonucleotides was determined at 260 nm on a UVIKON 933 double beam UV/Vis spectrophotometer (Kontron Instruments, United Kingdom).

Introduction of aldehyde functionality onto AFM cantilevers.

To enhance reflection of the laser used to quantify force, we used silicon nitride cantilevers coated with gold on one side (opposite the attached cell) for the protein attachment experiments. Non-gold-coated silicon nitride cantilevers were used for DNA attachment because the heating step involved in the modification process caused bending when the metal layer was present. A silicon nitride AFM probe (gold coated probes: MLCT-AUNM; unmodified probes: MLCT-NONM, Veeco Instruments, Sunnyvale, CA) was washed with acetone and placed into a glow discharge plasma panel for 2 min under 140 mtorr and 18 Watt to introduce a uniform layer of SiOx groups onto the silicon nitride surface. A small container charged with 0.4 mL of trimethoxysilylpropanal (TMSP, United Chemical Technologies) was placed on a 60 ^{o}C heat block in a bell jar desiccator that was subsequently purged with N_2 for 1 min.

The freshly cleaned AFM probe was placed in the jar, which was then evacuated and sealed to the atmosphere for 1 h. The heat block and the TMSP were then removed, and the desiccator was purged with N_2 gas for another 1 min. The resulting probe was stored in this environment until use.

Covalent attachment of DNA, lectins, and antibodies to cantilevers.

For DNA-mediated cell adhesion studies, a complementary oligonucleotide sequence pair (A/A') was designed. The sequence identities were as follows:

A: 5'-TCA TAC GAC TCA CTC TAG GG-3'

A': 5'-CCC TAG AGT GAG TCG TAT GA-3'

An aldehyde-coated cantilever (MLCT-NONM) was immersed into a 20 μM solution of 5'-amine functionalized ssDNA in 3X saline/sodium citrate buffer (45 mM sodium citrate, 450 mM NaCl, pH 7.0) for 15 min, heated in an oven at 100 °C for 30 min, and then washed with 0.2% SDS solution and distilled water (1 min each). The resulting cantilever was soaked in a fresh solution of 0.1 g of $NaBH_4$ in 10 mL of ethanol and 30 mL of PBS solution for 15 min, and then it was washed with 0.2% SDS solution and water (1 min each). The cantilever was dried under N_2 and stored in a low moisture environment until use. The ssDNA coated cantilever was characterized by coupling 3'-FITC-labeled 5'-amino ssDNA (A strand) to the aldehyde-coated cantilever surface, followed by imaging with a fluorescence microscope.

Concanavalin A and anti-CD3 IgG monoclonal antibodies were also coupled to an aldehyde-coated cantilever (MLCT-AUNM) surface by a reductive animation procedure. An aldehyde-coated cantilever was exposed to a 20μM (Con A) or 1 mg/mL (Anti-CD3) solution of the protein in pH 7.0 PBS buffer solution containing 66 μM $NaBH_4$ in a humid chamber for 2 h. The cantilever was then washed with excess PBS and water, and stored in pure PBS solution at 4 °C until use.

Cell-surface DNA modification.

A modified version of a previously published protocol was used.[26] To prepare the DNA-Staudinger ligation reagent, a solution of 5'-amine functionalized ssDNA (0.69 mg in 27.6 μL of water) was reacted with phosphine-PFP (1.7 mg in 96.6μL of DMF) and *N*,*N*-diisopropylethylamine (27.6 μL) at rt for 20 h. Both phosphine-PFP and *N*,*N*-diisopropylethylamine were obtained from Sigma (St. Louis, MO). The solution was then diluted with 697 μL of water, eluted through a NAP 5 SEC column (GE Biosciences), and purified by semi-prep HPLC using an Agilent 1100 system (Agilent Technologies, USA). Analyte detection for all HPLC analyses was achieved using an in-line diode array detector (DAD). Preparative reversed-phase HPLC was accomplished using an Agilent Eclipse XDB-C18 column (Agilent Technologies, USA) and an acetonitrile/aqueous 0.1 M triethylammonium acetate (TEAA, buffered at pH 7) gradient. The eluent was lyophilized, and the residue was redissolved in degassed phosphate-buffered saline (PBS, pH 7.4) and quantified by UV-Vis spectroscopy. The

phosphine-DNA solution was stored at -20 °C under an atmosphere of N_2 until use.

Acetylated ManNAz (Ac_4ManNAz) was synthesized according to previously published procedures . A 10 mM ethanolic stock solution of the sugar was sterilized using 0.2 μm mesh Acrodisc® 13 mm filters (Pall Life Sciences, USA). The appropriate volume of Ac_4ManNAz stock solution was pipetted using sterile technique into a culture flask and the solvent was allowed to evaporate. Jurkat cells were grown in culture media that was 25 μM in Ac_4ManNAz for 3 d under the conditions described in General Experimental Methods section. The cells were then centrifuged, washed twice with 5 mL of PBS containing 1% FBS, and reacted with 125 μM phosphine-DNA in 1% FBS/PBS (total volume of 100 μL) for 1 h at 37 °C. The cells were then rinsed with two 5 mL portions of 1% FBS/PBS solution at rt, and then used in cell-adhesion assays within 1 h after preparation.

Cell capture efficiency.

Solutions of 20 μM FITC-labeled ssDNA, 20μM FITC-labeled ConA, and 1 mg/mL FITC-labeled anti-CD3 IgG were spotted onto aldehyde-coated glass slides (SCHOTT Nexterion, Louisville, KY), and the resulting imines were reduced with $NaBH_4$ using the same protocols described above for modification of cantilever surfaces. All spots were imaged with a fluorescence microscope to confirm the presence of the desired biomolecules. Jurkat cells coated with ssDNA (A' strand) were prepared and diluted to a concentration of $1x10^7$ cells/mL. The cells were then applied to a glass slide coated with complementary ssDNA (A strand) for 10 min at rt. The slide was then washed twice with PBS. For the ConA and anti-CD3 IgG systems, unmodified Jurkat cell solutions were concentrated to $1x10^7$ cells/mL and applied directly to the appropriately coated glass slides. Cells were incubated on the slides at rt for 10 min, and then the slides were rinsed twice with PBS. Following the rinses, each slide was imaged and photographed under a fluorescence microscope. Each experiment was repeated in triplicate, and the number of bound cells was counted and plotted for an area corresponding to 0.1 mm^2.

Force measurements.

A $3x10^6$ cells/mL solution of Jurkat cells coated with ssDNA (A' strand) in CO_2 independent media was first applied to a glass slide modified with a 80 μM solution of ssDNA (A strand). A cantilever modified with a 20 μM ssDNA (A strand), 20 μM ConA, or 1 mg/mL anti-CD3 IgG solution was prepared as described above and mounted onto the fluid cell. Jurkat cells 20-25 μm in diameter were chosen for de-adhesion force measurements to control for cell-cantilever contact area. The cantilever was then lowered to the point of contact with the cell. The cell was sandwiched between the cantilever and the glass slide for 10 sec at 200 pN or 400 pN of contact force. The glass slide substrate and cantilever were then separated at a rate of 15.7 μm/s or 8.2 μm/s, causing the cell-cantilever adhesion to rupture and thereby allowing the force of de-adhesion to be measured. Visual observation confirmed that the rupture

event occurred between the cell and the cantilever.

Direct Cell Patterning

Glass slides were prepared by coating one half with an 80 μM solution of ssDNA (A strand), leaving the other half unexposed. Treatment with $NaBH_4$ solution was then carried out as described above to reduce all of the aldehydes and imines on the slides. A silicon nitride cantilever was modified with a 5 μM solution of a 13 base pair ssDNA strand as described above. This strand was a truncated version of the full A strand sequence, with the exact sequence of 5'-TCA TAC GAC TCA C-3'. A 50,000 cells/mL solution of ssDNA (A' strand) coated Jurkat cells was then applied to the unmodified side of the glass slide. The cantilever was lowered into contact with cells and held in place for 10 s with 400 pN of force to allow DNA hybridization. The cell was then lifted from the glass slide with the cantilever. After moving the cantilever to the side of the slide that was coated with 20-mer ssDNA, the cell was lowered into contact with the substrate for 10 s with a 400 pN of pushing force, as monitored by a photodiode detector. The cantilever was then retracted. The transferred cell was then observed and photographed under the microscope.

REFERENCES

1. Radisky, D.C. & Bissell, M.J. Respect thy neighbor! *Science* **303**, 775-777 (2004).

2. Park, C.C. et al. B1 Integrin Inhibitory Antibody Induces Apoptosis of Breast Cancer Cells, Inhibits Growth, and Distinguishes Malignant from Normal Phenotype in Three Dimensional Cultures and In vivo. *Cancer Research* **66**, 1526-1535 (2006).

3. Stetlerstevenson, W.G., Aznavoorian, S. & Liotta, L.A. Tumor-Cell Interactions with the Extracellular-Matrix During Invasion and Metastasis. *Annual Review of Cell Biology* **9**, 541-573 (1993).

4. Shakhar, G. et al. Stable T cell-dendritic cell interactions precede the development of both tolerance and immunity in vivo. *Nature Immunology* **6**, 707-714 (2005).

5. Hugues, S., Boissonnas, A., Amigorena, S. & Fetler, L. The dynamics of dendritic cell-T cell interactions in priming and tolerance. *Current Opinion in Immunology* **18**, 491-495 (2006).

6. Shao, J.Y. & Hochmuth, R.M. Micropipette suction for measuring piconewton forces of adhesion and tether formation from neutrophil membranes. *Biophysical Journal* **71**, 2892-2901 (1996).

7. Chu, Y.S. et al. Force measurements in E-cadherin-mediated cell doublets reveal rapid adhesion strengthened by actin cytoskeleton remodeling through Rac and Cdc42. *Journal of Cell Biology* **167**, 1183-1194 (2004).

8. Dufresne, E.R. & Grier, D.G. Optical tweezer arrays and optical substrates created with diffractive optics. *Review of Scientific Instruments* **69**, 1974-1977 (1998).

9. Thoumine, O., Kocian, P., Kottelat, A. & Meister, J.J. Short-term binding of fibroblasts to fibronectin: optical tweezers experiments and probabilistic analysis. *European Biophysics Journal with Biophysics Letters* **29**, 398-408 (2000).

10. Clausen-Schaumann, H., Seitz, M., Krautbauer, R. & Gaub, H.E. Force spectroscopy with single bio-molecules. *Current Opinion in Chemical Biology* **4**, 524-530 (2000).

11. Binnig, G., Quate, C.F. & Gerber, C. Atomic Force Microscope. *Physical Review Letters* **56**, 930-933 (1986).

12. Radmacher, M. in Atomic Force Microscopy in Cell Biology, Vol. 68 67-902002).

13. Zhang, X.H., Wojcikiewicz, E. & Moy, V.T. Force spectroscopy of the leukocyte function-associated antigen-1/intercellular adhesion molecule-1 interaction. *Biophysical Journal* **83**, 2270-2279 (2002).

14. Zhang, X.H., Wojcikiewicz, E.P. & Moy, V.T. Dynamic adhesion of T lymphocytes to endothelial cells revealed by atomic force microscopy. *Experimental Biology and Medicine* **231**, 1306-1312 (2006).

15. Puech, P.H., Poole, K., Knebel, D. & Muller, D.J. A new technical approach to quantify cell-cell adhesion forces by AFM. *Ultramicroscopy* **106**, 637-644 (2006).

16. Zhang, X.H. et al. Atomic force microscopy measurement of leukocyte-endothelial interaction. *American Journal of Physiology-Heart and Circulatory Physiology* **286**, H359-H367 (2004).

17. Franz, C.M., Taubenberger, A., Puech, P. & Muller, D.J. Studying Integrin-Mediated Cell Adhesion at the Single-Molecule Level Using AFM Force Spectroscopy. *Science STKE* **2007**, 15 (2007).

18. Benoit, M., Gabriel, D., Gerisch, G. & Gaub, H.E. Discrete interactions in cell adhesion measured by single-molecule force spectroscopy. *Nature Cell Biology* **2**, 313-317 (2000).

19. Ohba, H., Bakalova, R. & Muraki, M. Cytoagglutination and cytotoxicity of Wheat Germ Agglutinin isolectins against normal lymphocytes and cultured leukemic cell lines - relationship between structure and biological activity.

Biochimica Et Biophysica Acta-General Subjects **1619**, 144-150 (2003).

20. Ballerstadt, R., Evans, C., McNichols, R. & Gowda, A. Concanavalin A for in vivo glucose sensing: A biotoxicity review. *Biosensors & Bioelectronics* **22**, 275-284 (2006).

21. Palacios, R. Concanavalin a Triggers Lymphocytes-T by Directly Interacting with Their Receptors for Activation. *Journal of Immunology* **128**, 337-342 (1982).

22. Schena, M., Shalon, D., Davis, R.W. & Brown, P.O. Quantitative Monitoring of Gene-Expression Patterns with a Complementary-DNA Microarray. *Science* **270**, 467-470 (1995).

23. Zammatteo, N. et al. Comparison between different strategies of covalent attachment of DNA to glass surfaces to build DNA microarrays. *Analytical Biochemistry* **280**, 143-150 (2000).

24. Piramowicz, M.D., Czuba, P., Targosz, M., Burda, K. & Szymonski, M. Dynamic force measurements of avidin-biotin and streptavdin-biotin interactions using AFM. *Acta Biochimica Polonica* **53**, 93-100 (2006).

25. Zheng, G.F., Patolsky, F., Cui, Y., Wang, W.U. & Lieber, C.M. Multiplexed electrical detection of cancer markers with nanowire sensor arrays. *Nature Biotechnology* **23**, 1294-1301 (2005).

26. Chandra, R.A., Douglas, E.S., Mathies, R.A., Bertozzi, C.R. & Francis, M.B. Programmable cell adhesion encoded by DNA hybridization. *Angewandte Chemie-International Edition* **45**, 896-901 (2006).

27. Dube, D.H. & Bertozzi, C.R. Metabolic oligosaccharide engineering as a tool for glycobiology. *Current Opinion in Chemical Biology* **7**, 616-625 (2003).

28. Saxon, E. & Bertozzi, C.R. Cell surface engineering by a modified Staudinger reaction. *Science* **287**, 2007-2010 (2000).

29. Chen, X., Kis, A., Zettl, A. & Bertozzi, C.R. A cell nanoinjector based on carbon nanotubes. *Proceedings of the National Academy of Sciences of the United States of America* **104**, 8218-8222 (2007).

30. Bell, G.I. Models for Specific Adhesion of Cells to Cells. *Science* **200**, 618-627 (1978).

31. Macdermott, R.P., Nash, G.S., Bertovich, M.J., Merkel, N.S. & Weinrieb, I.J. Human B-Cell Mitogenic Responsiveness to Lectins - Requirement for T-Cells. *Cellular Immunology* **38**, 198-202 (1978).

32. Freywald, A., Sharfe, N., Miller, C.D., Rashotte, C. & Roifman, C.M. EphA receptors inhibit Anti-CD3-Induced apoptosis in thymocytes. *Journal of Immunology* **176**, 4066-4074 (2006).

33. Phillips, J.H. & Lanier, L.L. Lectin-Dependent and Anti-Cd3 Induced Cytotoxicity Are Preferentially Mediated by Peripheral-Blood Cytotoxic Lymphocytes-T Expressing Leu-7 Antigen. *Journal of Immunology* **136**, 1579-1585 (1986).

34. Douglas, E.S., Chandra, R.A., Bertozzi, C.R., Mathies, R.A. & Francis, M.B. Self-assembled cellular microarrays patterned using DNA barcodes. *Lab on a Chip* **7**, 1442-1448 (2007).

35. Kufer, S.K., Puchner, E.M., Gumpp, H., Liedl, T. & Gaub, H.E. Single-molecule cut-and-paste surface assembly. *Science* **319**, 594-596 (2008).

Chapter 5: Unfolding a specific membrance protein embedded in a live cell surface

INTRODUCTION

The atomic force microscope (AFM) enables us not only to image biological samples immobilized on a solid surface, but also to measure hitherto unobservable mechanical properties of nanometer scale biomolecules and structures.[1–3] Earlier work to measure the binding force between ligand–receptor or antigen–antibody pairs provided new insights into the mechanics of biological interactions.[4,5] By applying similar experimental setups, one can also record the force required to mechanically unfold single protein molecules and to determine the threshold forces for the complete breakdown of their three dimensional structures.[6–7] Since we are primarily interested in the mechanical manipulation of membrane proteins, the AFM applications described in the previous chapter are of particular interest. In this chapter, we first develop a bioorthogonal system to form a crosslink between an AFM cantilever and a specific protein receptor (Figure 1). We then set out to measure the forces associated with the removal of a single embedded protein from the membrane environment.

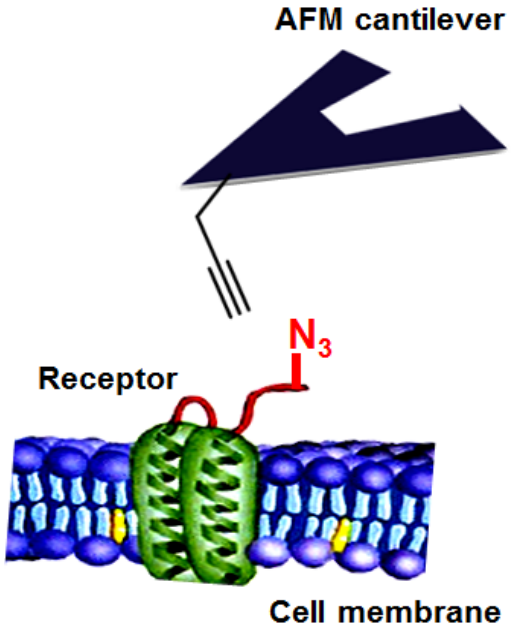

Figure 1. Schematic of a bioorthogonal system for attaching specific proteins to AFM cantilevers. The resulting configuration can allow the force of removing a single protein from a membrane to be measured.

RESULTS AND DISCUSSION

Lipoic acid ligase labeling of PDGFR on a live cell surface.

To introduce a chemically unique functional group for AFM probe attachment, we first adapted the Ting lab's lipoic acid ligation method[8] to label platelet derived growth factor receptor (PDGFR). The expression construct was created by fusing lipoic acid reactive pepetide (LAP) to the N-terminus of cyano fluorescence protein (CFP), which was in turn fused to the extracellular side of the transmembrane (TM) helix of the PDGF receptor. This protein was then espressed in live HeLa cells, which were used for all of the describe experiments. To verify the presence of the site-specifically introduced azido tag, we used several membrane-impermeant conjugates of difluorocyclooctyne (DIFO)[9] that were coupled to activated esters of Alexa Fluor 488 (Figure 2).

To perform live cell labeling, HeLa cells expressing the LAP-CFP-TM fusion protein were treated first with lipoic acid ligase (LplA), the azide, and ATP for 1 h at 32 °C, Figure 2. The introduced azide was then selectively modified with the DIFO fluorophore conjugates by reaction at 25 °C for 20 min. Figure 2 shows the specific labeling of transfected (CFP-positive) cells. This demonstrated the azide-dependent and site-specific nature of the ligation.

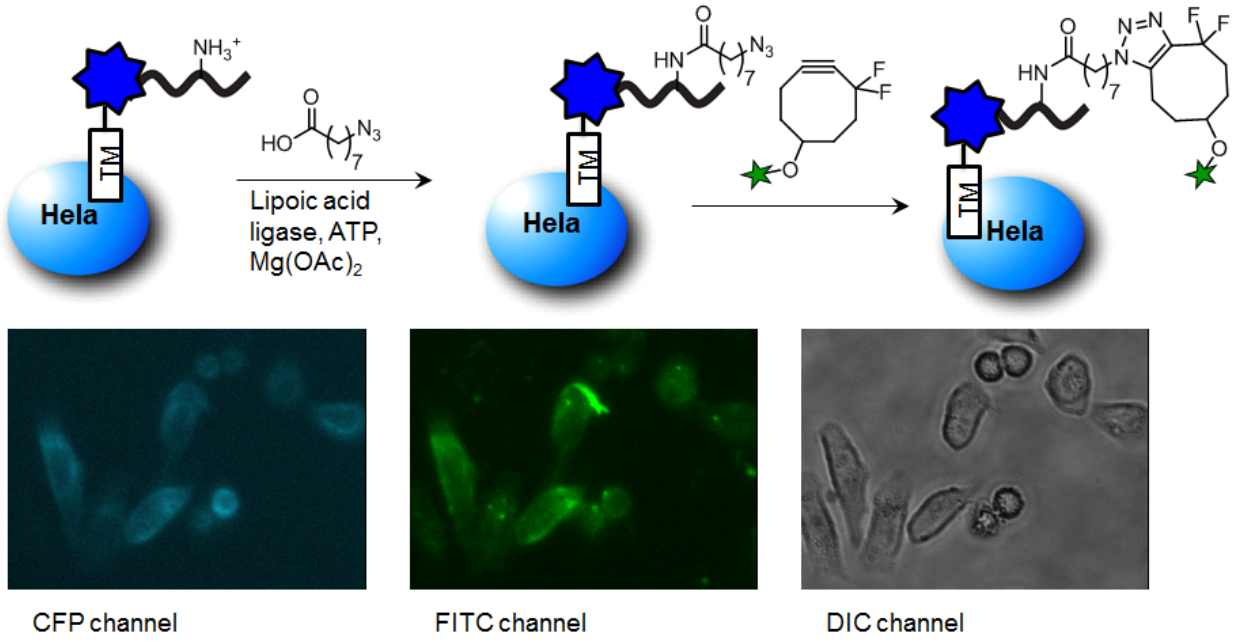

Figure 2. Lipoic ligation for PDGFR-CFP. The scheme shows PDGFR-CFP is first conjugated to an azido tag by lipoic ligase and then labelled with DIFO-488. The CFP fluorescence image shows expression of PDGFR-CFP on HeLa cells. The FITC fluorescence image shows azido tag can be labeled with DIFO-488. The DIC image shows morphology of HeLa cells.

Conjugation of alkyne functional groups to AFM tips

A linear alkyne was next attached to AFM cantilevers for use in bioorthogonal "Click"-type reactions. In order to maximize the number of hydroxyl functional groups, a thin layer of silicon oxide was introduced on the AFM cantilever tips. To do this, the silicon nitride surface was first cleaned using oxygen plasma.[10, 11] Alkynyl trimethoxyl silane was then coupled to the cantilever by chemical vapor deposition (CVD) as described in previous chapters, resulting in an alkyne functionalized surface (**Figure 3**) that was characterized by contact angle measurement.[10, 11] The contact angle changes from 10 degrees to 65 degrees. The alkyne groups on the cantilever surface were reacted with FITC-labeled azides to confirm their presence using fluorescence microscopy (**Figure 4**).

Force measurements

Figure 5 shows typical force curves obtained on a glass surface (Figure 5a) and on the surface of a live HeLa cell (Figure 5b) using an unmodified silicon nitride tip and a vertical scan rate of 100 nm/s. In the curve shown in Figure 5a, the transition to the vertical deflection of the cantilever was characterized by an abrupt change in the slope. In contrast, Figure 5b shows that a gradual upward deflection occured. This difference is the result of the cantilever's responses to a hard and a soft surface, respectively. In Figure 5a, there was no indentation observed on either the tip or the sample, while in Figure 5b, the sample was deformed under the vertical stress inflicted by the tip.

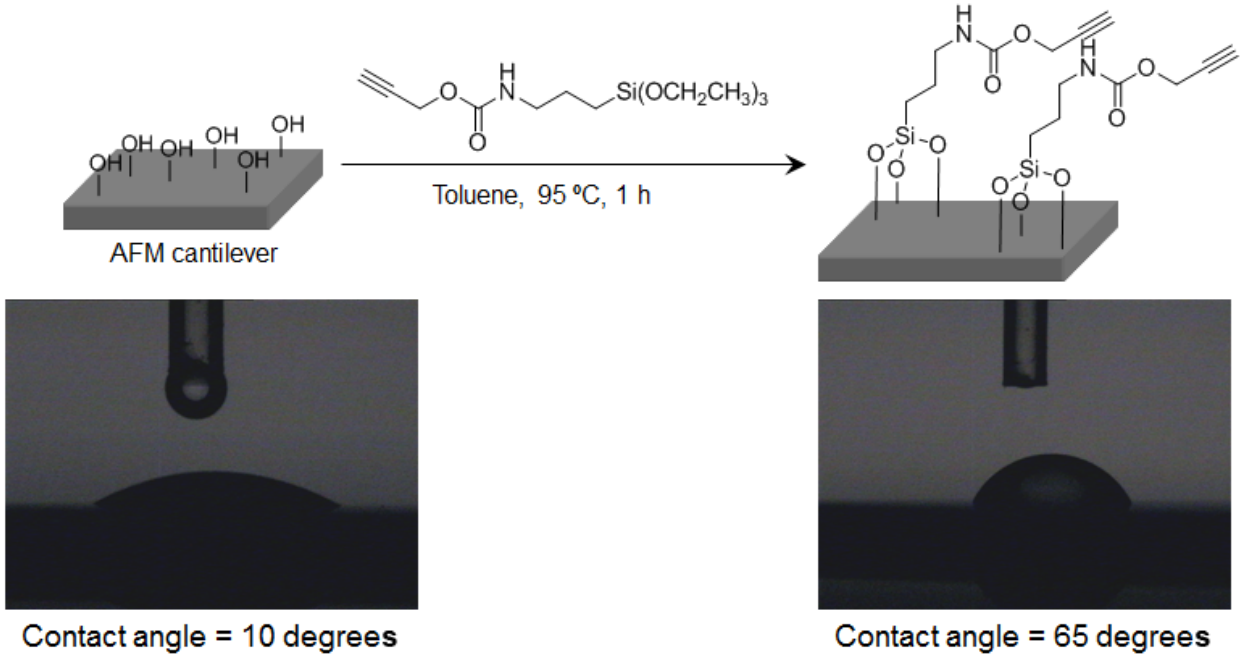

Figure 3. Silanization of AFM cantilevers using an alkynyl triethoxysliane. The contact angle of surfaces increased from 10 degrees to 65 degrees after silanization.

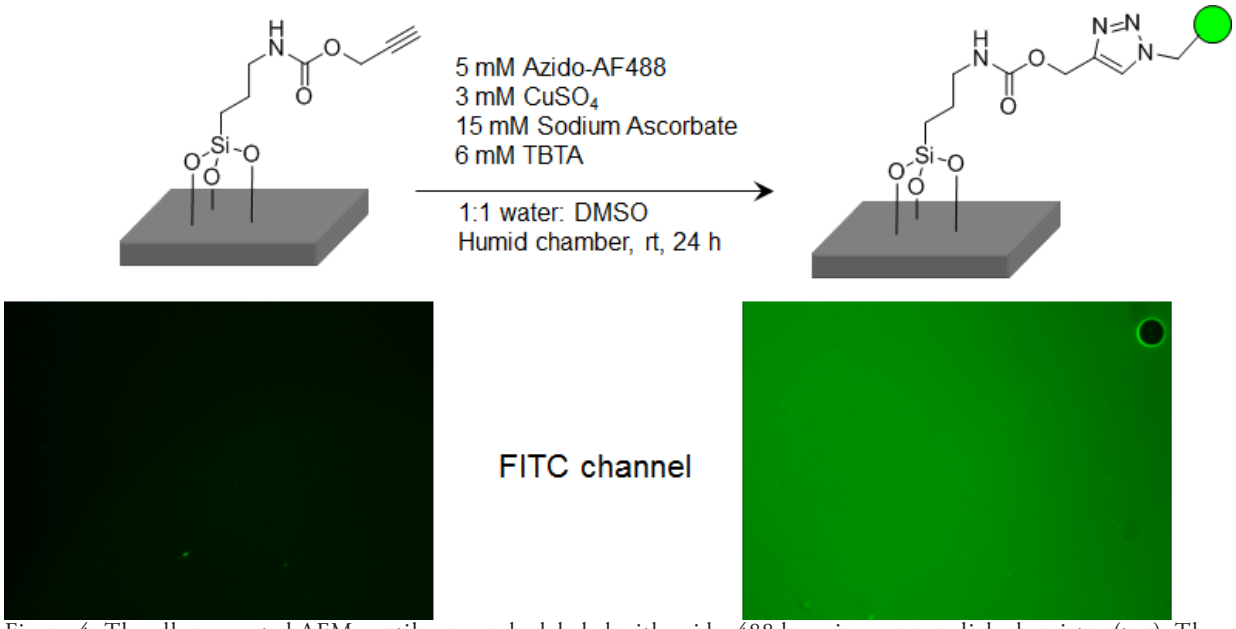

Figure 4. The alkyne coated AFM cantilever can be labeled with azido-488 by using copper click chemistry (top). The subsequent FITC fluorescence images show increased fluorescence intensity following the reaction (bottom).

The nearly perfect reversibility of the curve in Figure 5b indicated that the cell deformation was elastic, and that no irreversible deformation or adhesive interactions occured between the tip and the cell surface during the contact time as long as the vertical scan speed was 100–300 nm/s. The gradual change in force curvature during contact with the cell surface on both the approach and return can be used to extract information regarding surface softness based on the classical Hertz model of indentation.[12,13] The graph shown in Figure 5c represents a typical force curve obtained on the surface of an azide-displaying cell using a alkyne modified tip and 50 uM copper bromide. Although the approach portion of the curve was similar to that shown in Figure 5b, its return was characterized by a prolonged downward deflection, which ended abruptly after a sample extension of approximate 60 pN (Figure 5c circled area). This curve suggests that an adhesive interaction was established between the tip and the sample surface during their contact (approximately 1 s). The cantilever was pulled down by approximate 7 nm. The tensile force at the final point of separation bewteen the tip and the cell surface was calculated to be approximately 60 pN using the force constant of the cantilever (approximately 0.06 nN/nm). When unmodified silicon nitride tips were used on live cells, 90% of the force curves (N = 50) showed no indication of adhesive interactions. The remaining 10% exhibited weak interaction forces of less than approximate 50 pN.

To verify that the relatively strong separation force observed in Figure 5c corresponded to the extraction of membrane proteins through covalent bond formation, multiple cantilevers were used to obtain a statistically relevant force curve comparison set. A single modified tip was used to collect approx 50 force curves from a 15 μm × 15 μm region of the same cell. The operation was then repeated, changing the tip and the cell. The upper right region of Figure 6 shows the number

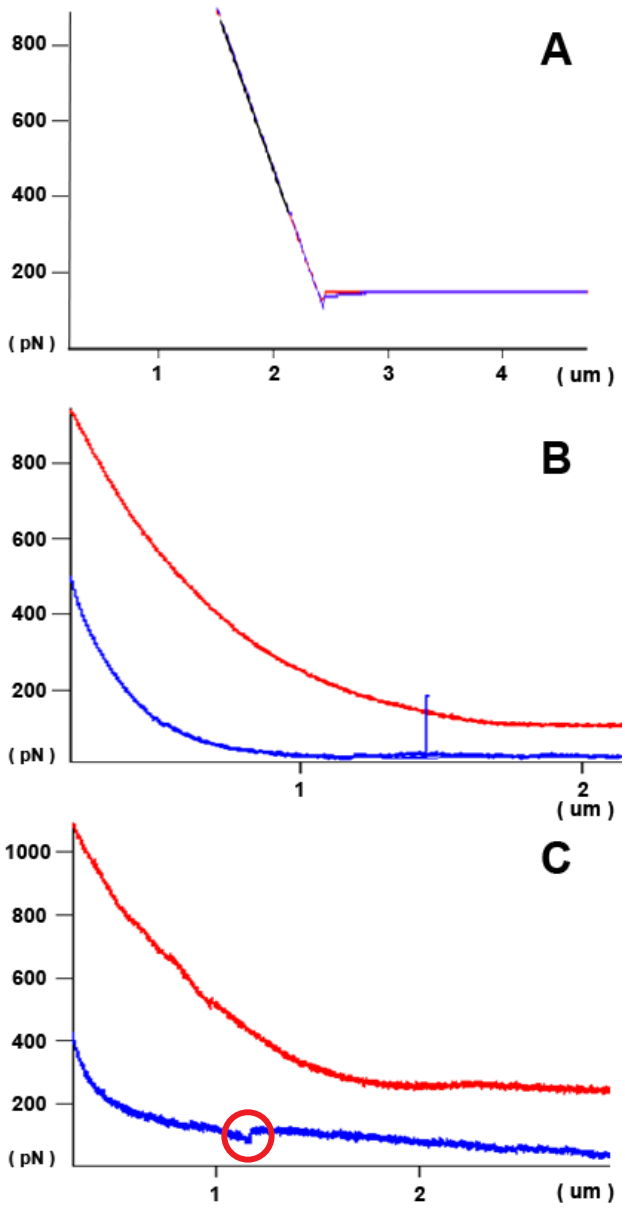

Figure 5. (A) A representative force curves resulting form an AFM tip approaching a glass surface (red), and then being withdrawn (blue) (B) A force curve resulting from an unmodified AFM tip approaching a living HeLa cell. (C) A representative force curve of a alkyne labeled AFM tip approaching a Hela cell surface with expressing azido PDGFR.

of interactions of a given strength when an alkyne-coated tip was contacted with an azide-labeled HeLa cell in the presence of copper bromide. Controls experiments, in which one or more components were omitted, are also shown. In the positive experiment histogram, the force values clustered between 40 and 80 pN, with a

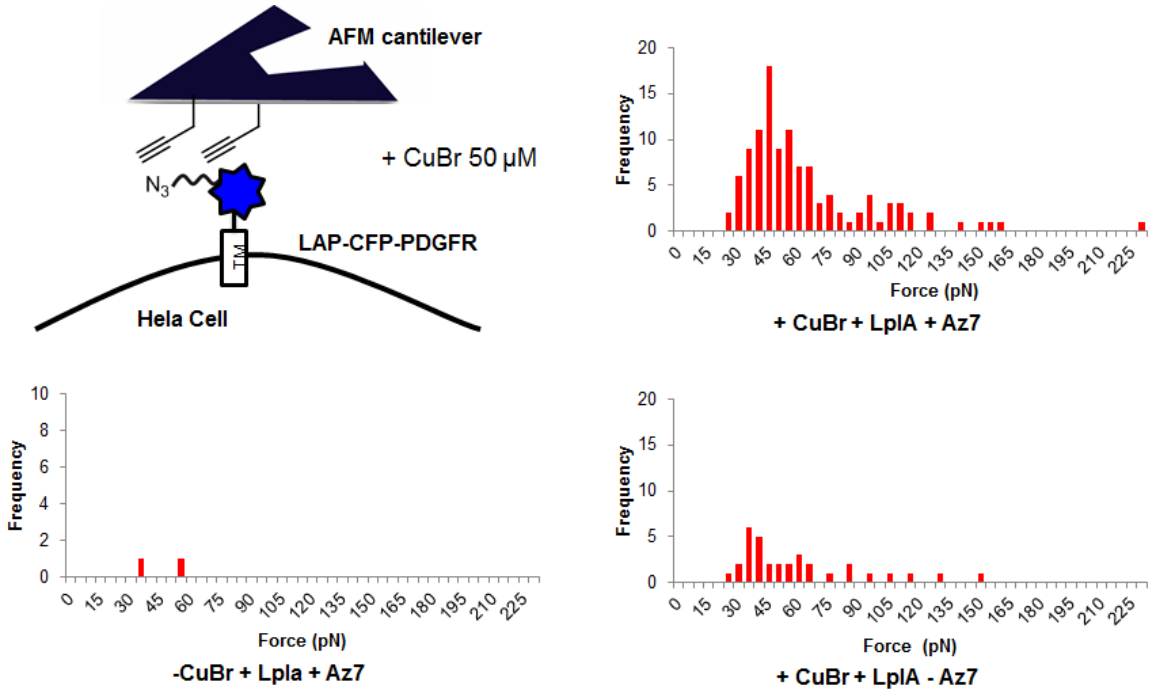

Figure 6. Force curves were obtained by contacting an alkyne coated AFM tip to the surface of a Hela cell with azido PDGFR expressed in its plasma membrane. Following this, the AFM tip was slowly withdrawn. Force curves analogous to those in Figure 5C were obtained and analyzed. The data are presented as a series of histograms.

peak at 50–60 pN. We therefore consider a force in the range of 40–60 pN to be the minimim required to extract or, according to Bell, "uproot" intrinsic membrane proteins from the cell membrane.[14]

Grandbois et al.[15] have reported a theoretical prediction that the weakest bond in a crosslinking system such as ours would be the Si-C bond, and concluded from their experimental results that covalent bond rupture occurs at 2.0 ± 0.3 nN (with a distribution mostly between 1.0 and 2.0 nN) at a loading rate of 10 nN/s. In a similar loading rate range, we most often obtained 40 - 100 pN for the final rupture force, which was significantly lower than that measured for a covalent linkage. Thus, we attribute our observed force measurements to the removal of the protein from the membrane, rather than the fission of a covalent bond in the linking groups.

We have tried attaching cycloocytynes, such as DIFO[9] to the AFM tips for the purpose of forming covalent bonds with cell surface receptors. However, the force measurements done by using cyclooctyne-coated AFM tips had more background adhesion. We hypothesized that cycloocytynes had more hydrophobic interaction with cell lipid membrane and generated more background adhesion. After testing different alkynes and cycloalkynes, we decided to use low concentration copper catalzed click reaction, which provided low backgroud adhesion. Cells are stained with Annexin and PI before and after the force measurement. The results (not shown here) showed cells were alive after AFM force measurements.

CONCLUSION

By using a bioorthogonal chemical reaction to attach a functionalized AFM tip to an enzymatically modified protein, the force required to extract PDGFR from a live cell surface was measured to be approximately 60 pN. The transmembrane domain of PDGFR is considered to be a single alpha-helix with an approximate diameter of 1.0–1.3 nm. Evans and Ludwig reported that the force required for extracting a single lipid molecule from a lipid membrane was in the range of 20–25 pN when the loading rate was between 5 and 3000 pN/s.[16,17]

The work described here verifies the use of covalently modified AFM tips as a practical means to extract specific membrane proteins from live cells for subsequent biochemical analyses. Through the automation of these measurements for the generation of large data sets, the force values associated with the molecular level of many mambrane-absed events may be elucidated in future experiments.

MATERIALS AND METHODS

Cell line

All cell culture reagents were obtained from Gibco/Invitrogen Corp (Carlsbad, CA) unless otherwise noted. Cell culture was conducted using standard techniques. Hela were grown in T-7 culture flasks (Corning, USA) in DMEM media supplemented with 10% (v/v) fetal bovine serum (FBS, HyClone) and 1% penicillin/streptomycin (P/S, Sigma).

Labeling of cell surface LAP-CFP-TM with DIFO-488

Hela cells were transfected with the LAP-CFP-TM plasmid using Lipofectamine 2000 according to the manufacturer's protocol. After 36-48 hours at 37 °C, the cells were washed twice with fresh growth media (DMEM supplemented with 10 % FBS and 1 % penicillin/streptomycin). Enzymatic ligation of azido heptoic acid was performed in complete growth media with 10 μM LplA, 350 μM azido heptoic acid , 1 mM ATP, and 5 mM magnesium acetate for 15 minutes at 32 °C. Cells were then rinsed three times with growth media, and incubated for 15 minutes at 32 °C with 250 μM DIFO-488. The cells were washed once with growth media at room temperature and twice with ice-cold DPBS, pH 7.4 (to reduce endocytosis), and imaged in the same buffer on a Zeiss Axiovert inverted epifluorescence microscope using a 20x lens.

Introduction of aldehyde functionality onto AFM cantilevers.

A silicon nitride AFM probe (gold coated probes: MLCT-AUNM; unmodified probes: MLCT-NONM, Veeco Instruments, Sunnyvale, CA) was washed with acetone and placed into a glow discharge plasma panel for 2 min under 140 mtorr and 18 Watt to introduce a uniform layer of SiOx groups onto the silicon nitride surface. A small container charged with 0.4 mL of alkynyl trimethoxysilane (from Frechet Lab) was placed on a 60 °C heat block in a bell jar desiccator that was subsequently purged with N_2 for 1 min. The freshly cleaned AFM probe was placed in the jar, which was then evacuated and sealed to the atmosphere for 1 h. The heat block and the silane were then removed, and the desiccator was purged with N_2 gas for another 1 min. The resulting probe was stored in this environment until use.

Force measurements.

Transfected or normal Hela cells were washed with 1%FBS in PBS twice, and incubate in 1%FBS/PBS in 5 cm petri dish and used for AFM force measurement immediately. 50 uM copper bromide was added into petri dish. The alkyne coated cantilever was then lowered to the point of contact with the cell. The tip contacts cells for 1 sec at 100 pN of contact force. The cell and cantilever were then separated at a rate of 200 nm/s, causing the cell-cantilever adhesion to rupture and thereby allowing the force of de-adhesion to be measured. Visual observation confirmed that the rupture event occurred between the cell and the cantilever.

REFERENCES

1. N.J. Tao, S.M. Lindsay, S. Lees, Biophys. J. 63 (1992) 1165–1169.
2. M. Radmacher, M. Fritz, C.M. Kacher, J.P. Cleveland, P.K. Hansma, Biophys. J. 70 (1996) 556–567.
3. A. Ikai, Surf. Sci. Rep. 26 (1996) 261–332.
4. E.L. Florin, V.T. Moy, H.E. Gaub, Science 264 (1994) 415.
5. U. Dammer, M. Hegner, D. Anselmetti, P. Wagner, M. Dreier, W. Huber, H.-J. Gu¨ntherodt, Biophys. J. 70 (1996) 2437.
6. M. Rief, J. Pascual, M. Saraste, H.E. Gaub, J. Mol. Biol. 286 (1999) 553.
7. F. Oesterhelt, D. Oesterhelt, M. Pfeiffer, A. Engel, H.H. Gaub, D.J. Muller, Science 288 (2000) 143.
8. Redirecting lipoic acid ligase for cell surface protein labeling with small-molecule probes. Nature Biotechnology 2007, 25, 1483-1487. M. Fernández-Suárez, H. Baruah, L. Martínez-Hernández, K. T. Xie, J. M. Baskin, C. R. Bertozzi, and A. Y. Ting.

9. Proc Natl Acad Sci U S A. 2007 Oct 23;104(43):16793-7. Epub 2007 Oct 17. Copper-free click chemistry for dynamic in vivo imaging. Baskin JM, Prescher JA, Laughlin ST, Agard NJ, Chang PV, Miller IA, Lo A, Codelli JA, Bertozzi CR.

10. Douglas, E. S., Chandra, R. A., Bertozzi, C. R., Mathies, R. A., and Francis, M. B. (2007) Lab on a Chip 7(11), 1442-1448

11. Hsiao, S. C., Crow, A. K., Lam, W. A., Bertozzi, C. R., Fletcher, D. A., Francis, M. B. (2008) Angewandte Chemie-International Edition 120(44), 8601-8605

12. Tao, N. J., Lindsay, S. M., and Lees, S. (1992) Measuring the microelastic properties of biological material. Biophys. J.63, 1165–1169.

13. Sneddon, I. N. (1965) The relation between load and penetration in the axisymmetric Boussinesq problem for a punch of arbitrary profile. Int. J. Eng. Sci.3, 47–57.

14. Bell, G. I. (1978) Models for the specific adhesion of cells to cells. Science 200, 618–627.

15. Grandbois, M., Beyer, M., Rief, M., ClausenSchaumann, H., and Gaub, H. E. (1999) How strong is a covalent bond? Science283, 1727–1730.

16. Evans, E. (2001) Probing the relation between force-lifetime and chemvistry in single molecule bonds. Annu. Rev. Biophys. Biomol. Struct. 30 105–128.

17. Evans, E. and Ludwig, F. (2000) Dynamic strengths of molecular anchoring and material cohesion in fluid biomembranes. J. Phys. Condens. Matter12, A315–A320.